STRUCTURAL BEHAVIOR OF CABLE-STAYED SUSPENSION BRIDGE STRUCTURE

EGON KIVI

TUT
PRESS

Department of Structural Design

Faculty of Civil Engineering

TALLINN UNIVERSITY OF TECHNOLOGY

Dissertation was accepted for the commencement of the degree of Doctor of Philosophy in Engineering Sciences on 22 September 2009

Supervisor: Professor Valdek Kulbach, Department of Structural Design, Faculty of Civil Engineering, Tallinn University of Technology.

Opponents: Professor Alexandr Shimanovsky, OJSC "V. Shimanovsky UkrRDIsteelconstruction"
Professor Siim Idnurm, Department of Transportation, Faculty of Civil Engineering, Tallinn University of Technology.

Commencement: 3 November 2009

Declaration: Hereby I declare that this doctoral thesis, my original investigation and achievement, submitted for the doctoral degree at Tallinn University of Technology has not been submitted for any degree or examination.

Egon Kivi

VANT-RIPPSILLA KONSTRUKTIIVSE KÄITUMISE ANALÜÜS

EGON KIVI

TTÜ
KIRJASTUS

Acknowledgements

I would like to express my deepest gratitude to my supervisor Professor Valdek Kulbach.

I am extremely thankful to Evald Kalda who carried through all the actual modelling in laboratory of Tallinn University of Technology.

I thank Juhan Idnurm for his helping hand in using discrete calculation method.

I am grateful to Mare-Anne Laane for revising main language of the thesis.

Contents

Abstract

The purpose of this thesis is to investigate the structural design and modelling of cable structures with a hybrid cable-stayed suspension structure as an example. The thesis covers the choice and estimation of the essential structural parameters as far as up-due-date methods used for the final design of cable structures. A significant part of this thesis consists of theoretical and experimental work with a structure model: detailing, testing and analysis of the results of the model and analysis of the results. The structural model provided an opportunity to estimate and ensure the methods and solutions chosen.

The aim of the theoretical analysis was to choose bridge geometry, stiffness and loading parameters. Taking into account this essential research, drawings for the model were made. During the research different models were under investigation and solution was verified step-by-step with theoretical and experimental work.

Analysis of the self-anchored structure includes studies of the stability problems of the stiffening girder.

A question arose with the plan of realisation of the fixed-link Saaremaa. The solution examined in this thesis is also one possible bridge for a navigable part of the fixed-link. At first approach, a traditional suspension bridge with loaded anchor cables was under investigation; span lengths for this structure were 200+480+200m. Taking into account economic aspects, span lengths were reduced to 120+300+120m.

The combined suspension cable-stayed structure was chosen as a slightly less investigated area of suspension structures. Investigation of combined structures also provides wide knowledge even if for fixed-link traditional suspension or a cable-stayed structure is to be chosen.

For theoretical and experimental work, a hybrid structure was chosen as a slightly less investigated area of suspension structures. A hybrid cable-stayed and a suspension bridge were chosen as a favourable solution for a fixed link, taking into account local geological conditions and distinctions in traffic load distribution. Characteristic of the structure is the narrow bridge deck and few traffic lanes This causes a specific relation between the traffic load and self-weight. Taking into account this specific relation, a self-anchored hybrid cable-stayed suspension bridge with unloaded anchor cables and a scheme with a suspension bridge's span length and height relations was chosen for investigation. Self-anchoring requires an untraditional construction process.

For experimental research, a model of the structure was erected. Theoretical research is also based on this model, to expand theoretical results and to ensure work as a whole.

One of the essential aims of the experimental testing was to verify the general stability of the stiffening girder.

Kokkuvõte

Käesolevas töös on analüüsitud kombineeritud vant-rippsilda nii kasutus- kui ka kandepiirseisundi korrmustulemite määramiseks. Töö üheks võimalikuks väljundiks on Saaremaa püsiühenduse laevatatava ava sillakonstruktsiooni projekteerimine.

Aluseks mudelkatsetele ja arvutustele on kombineeritud vant-rippsild avadega 120+300+120 meetrit.

Töös on Eurocode üldjuhiste, Briti Standardi ja Soome Standardi Rahvusliku Lisa alusel hinnatud nii maksimaalset võimalikku, kui ka tõenäolist reaalses projekteerimises kasutatavat liikluskoormust. Tulemusena rõhutatakse eriliselt eeluuringute olulisust. Illustreerimaks antud väidet võib tuua, et Eurocode üldjuhiste ja Soome Standaridi Rahvusliku Lisa kohaste liikluskoormuste vahe koormustulemite arvutamiseks on 1,8 kordne.

Lähtekonstruktsiooni alusel püstitati sillakonstruktsiooni mudel mõõtkavas 1:100. Mudelit katsetati erinevate koormuse jaotuse ja väärtuste juures ning mõõdeti nii jäikurtala vertikaalpaigutisi kui ka püloonide ja ankrutugede horisontaalpaigutisi.

Mudeli katsetamise tulemusena tehtud mõõtmiste ja nende võrdlusel arvutuslikega võib väita, et erilist tähelepanu mudeli ehituse ajal tuleb pöörata sõlmede korrektsele lahendusele. Sõlmede mastaap on mudeli omast erinev ja erinevuste ning mitte korrektselt töötavate sõlmede mõju väärtus ja suund on tihti mitte ennustatavad. Eelistada tuleks hõõrdele töötavaid sõlmi ja trosside tagasipöörete ja ühepoolseid poldiga kinnitusi tuleks vältida.

Võrdlustulemused arvutustulemustega aga olid adekvaatsed, vertikaalpaigutise puhul oli erinevus maksimaalsel juhul 15%. Horisontaalpaigutiste puhul oli kokkulangevus halvem kuid üleüldine käitumine oli kirjeldatud korrektselt.

Valitud arvutusmeetodid olid sobilikud.

Mudelkatsetuste üheks oluliseks eesmärgiks oli jäikurtala stabiilsuse kaole vastava kandevõime hindamine. Mudeli jäikurtala ei kaotanud kandevõimet ühelgi katsetatud koormusjuhtumitest. Samuti ei olnud täheldatavaid märke stabiilsuse kaole eelneva deformeerunud kuju näol. Arvutustulemused toetasid saadud tulemust igati. Arvutused näitasid, et vertikaalset summarset koormust võiks suureneda 4,2 korda enne kui nõtkumine muutuks tõeneäoliseks.

Erinevate arvutusmeetodite võrdlus näitas selget efekti lineaarse ja mittelineaarsete lähenemiste vahel aga erinevate mittelineaarsete laheneduste erinevuste vahemik oli 6%. Erinevate mittelineaarsete arvutusmeetodite eeliseid ja puuduseid tuleks analüüsida täiendavalt, arvestades ka nende arvutuste mahukust ja arvutusvigade võimalikkust.

Arvutuslikus osas on määratud erinevate antud konstruktsioonitüübi geomeetriat ja jäikust mõjutavate parameetrite nagu pülooni suhteline kõrgus, äärmise ava suhtelise pikkuse, vantide asukoha ja vantide ning rippkonstruktsiooni omavahelise jäikuse mõju.

Arvutustel põhinevana esitati koondatud koormuse mõju paigutistele ja sisejõudude jaotusele ja väärtusele.

1. Introduction

1.1. Background and scope

Saaremaa County has about 40,000 inhabitants and covers a territory of some 2900 m². Kuresaare, the capital city of Saaremaa, has about 16,000 inhabitants. Saaremaa has six sea harbours and a number of smaller harbours. The majority of the passenger and goods traffic goes through the eastern harbour, Kuivastu, on the island Muhu. Saaremaa has one deep harbour in the village of Ninase on the north-western coast of the island. The deep harbour, ice-free all the year round, together with the fixed link to the mainland, would give Saaremaa a good transit corridor for goods transport and development of international tourism.

In March 1997 the Saare County Government together with the Estonian Road Administration organized in Kuresaare a conference to discuss feasibility problems of erection of the fixed link. On the basis of the conference resolution the Saare County Governor set up a commission for examination of social, environmental, traffic and technical problems connected with realization of the project. In June 1998 an Estonian-Finnish working group was set up to compile a report on the feasibility study concerning the Saaremaa fixed link. Under the management of INTERREG II A a decision was adopted to give financial support to the Finnish group of specialists. The Technical Centre of the Estonian Road Administration published the results of the feasibility study in 2000. In 1999 Norwegian authorities and specialists joined the group to investigate the problems for realization of the project.

For the bridge location, of mainly five possible sites under examination (Figure 1.2), two (nos. 4 and 5) were eliminated due to environmental conditions. The shortest of the traces passes the Suur Strait on the northern coast of the islet of Viire. The possible level for the foundation ranges from 2 to 30 metres above the water level. The strait consists of a very shallow western part between the island of Muhu and the islet of Viire and the eastern mainstream channel. The geological structure of the Silurian period is very complex. The central part of the strait is longitudinally cleaved by a major furrow; the bedrock is situated 30–40 m below the sea level. During the period of retreat of the continental glacier, a 10 m layer of till was left on the bottom of the furrow; outside the furrow the layer of till is much thinner (1–4 m). Erection of the bridge will be associated with serious environmental problems. The region of the fixed link is surrounded by nature conservation areas, including a number of nature reserves. Aspects of the biosphere (vegetation, birds, animals, and fish) may be problematic. The environmental impacts occur during construction as well as the period of exploitation of the overpass. The region may be also problematic for the community of marbled seals and their survival. The natural landscapes should be preserved from disruption. The most serious problems for the chosen track seem to be connected with migration of birds.

Total length of the water sheet on the chosen trace is about 6 100 meters. The maximum depth for the foundation bed in cases of 100-m distances between the

bridge piers is about 20 meters and in the case of a 500-m distance about 25 meters from the surface of the water. Thickness of the layer of the weak soil on average is 1 to 2 meters, so the pile foundation is not very suitable, and a direct foundation should be preferred.

The total for of the bridge deck for the preliminary design was taken as 13 meters. This corresponds to the second class of bridges, as determined by Estonian design codes. The total width, 13 meters, consists of the bridge road (two traffic lines of 3.7m) and two safety tracks of 2.75 m; the latter may be used not only as overpasses for pedestrians and cyclists, but also for location of vehicles, forced to stop on the bridge. On two traffic tracks, three lines of vehicles may be located simultaneously; therefore, for calculation, the traffic load of three lines of vehicles was foreseen.

Due to the clearance in the height of 35 meters for a navigable span, the maximum level of the bridge deck was taken to be +40.00 m from the surface of water. The longitudinal slope of the bridge deck was chosen on the ground condition of fluent transition from the mainland's highway to the navigable part of the bridge; the maximum local slope on the transition area was 4%.

The bridge consists of a central navigable part, two approach bridges and two embankment sections with a total length of 2 300 meters. The embankment between the island of Muhu and the islet of Viire is to be supplied with culverts to ensure sufficient water exchange. For the navigable part of the overpass, a central span of 300 meters was foreseen.

For approach bridges, girder structures are usual. Steel, reinforced concrete and composite structures are in use. The most widely used bearing structures for today's bridges are continuous girders of variable depth. Very often box girders are preferred. In cases of an open cross-section, two main girders are usual. When needed, additional longitudinal beams, supported by transfer beams, may be needed. The span of approach bridges is usually chosen on the basis of minimising of the final cost of the superstructure and substructure. In every case the longer spans improve environmental conditions.

Figure 1.1 Location of Saaremaa.
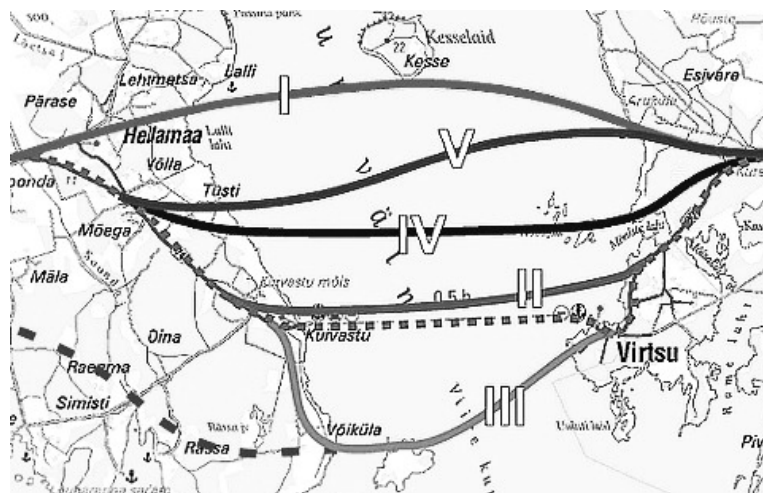
Figure 1.2 Possible traces for fixed-link Saaremaa – Reproduction from [32].

The usual contemporary reinforced concrete bridge model is connected with cantilevered element-by-element positioning of girders and step-by-step adding of the following tension cables. Usually the box cross sections with vertical walls are preferred. The options with inclined walls may appear more spectacular, but erection of these with variable depth is complicated. One example of a contemporary reinforced concrete, constructed in environmental conditions similar to the Suur Strait, is the West Bridge of fixed link of the Great Belt with spans of 110.5 m.

For the steel superstructure, continuous flow-line box girders of constant depth with orthotropic deck plate are normal. A good example is the East Bridge with a span of 193 m. Structures were mounted by floating cranes. Because of the to very slender girders, special vibration damping equipment was used. Composite structures for continuous girders are usually of variable depth; they consist of steel girders with more developed lower flanges and reinforced concrete deck plate cast in situ. As the main option for approach spans of the fixed-link

11

Saaremaa, the composite structures of variable depth with spans 80, 100 and 120 m, depending upon the foundation level, were chosen.

Problems with the foundation of the bridge are similar to those for the region of the Great Belt. On the same basis the pile foundation was abandoned. The open caisson structures with reinforced bottoms and walls and concrete fillings were chosen. The pyramidal transition box elements were used for connection between piers and foundations. The box elements of foundations and piers may be mounted by means of floating cranes. For preparation of the foundation level, the seabed can be excavated by a bucket dredger. A layer of filter stone is to be strewn under the foundation.

1.2.   General data of the link and the bridge

The overpass from the Estonian mainland to the island of Muhu has an overall length of about 6,100 metres; it consists of the central part of 120 + 300 + 120 m, the composite continuous girder structures of approach bridges with a total length of 3460 m and the causeways of about 2100 m. Our main attention has been paid to the structures for the central span with the cable-supported structures.

Figure 1.3 Perspective view of the fixed link.
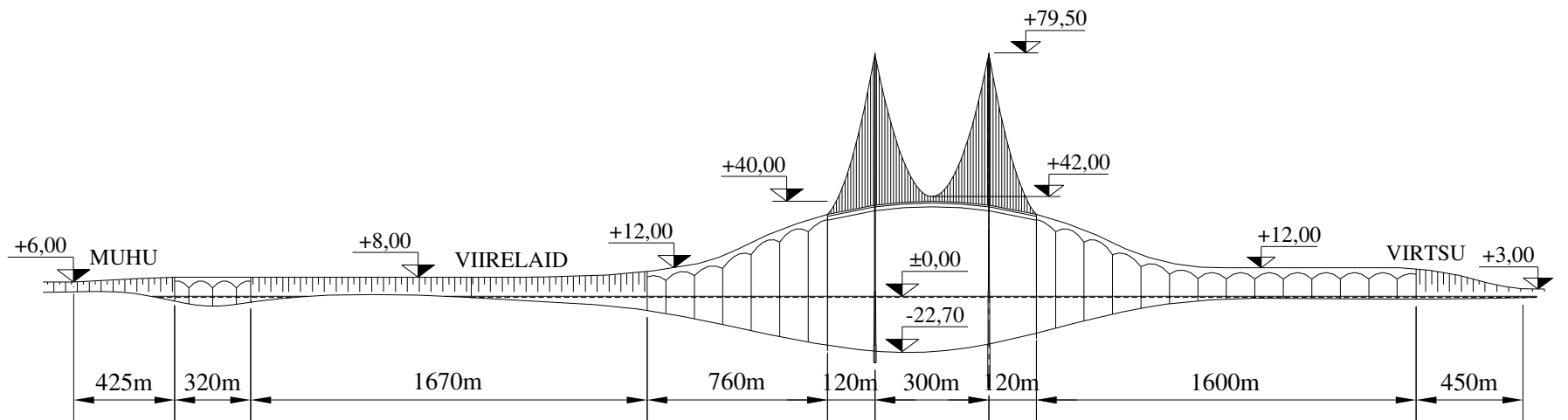
Figure 1.4 Overview of the Saaremaa bridge.

13

Due to the clearance in height of 35 meters for the navigable span, the maximum level of the bridge deck was taken as +40.00 from the sheet of water. The longitudinal slope of the bridge deck was chosen on the basis of the condition of the fluent transition from the mainland highway to the navigable part of the bridge; the maximum local slope on the transition area was 4%.

The total width of the bridge deck for the preliminary design was taken as 13 meters. It corresponds to the second class of bridges, as determined by Estonian designing codes. The total width consists of the bridge road (two traffic lines of 3.75m) and two safety tracks of 2.75 m; the latter may be used not only as overpasses for pedestrians and cyclists, but also for vehicles forced to stop on the bridge.

Due to complicated estimation of bridge behaviour under the action of a fluctuating wind load, the ultimate design is impeded by thorough theoretical analysis and wind-tunnel tests. Due to serious ice action and possible ship collisions, a corresponding risk analysis is required.

Data from [5,7,8,19,32]

1.3. Aims and content of the study

1.3.1. General aims

The most important aim of this thesis is to ensure a general approach for analysing and testing cable structures. The initiative for this thesis is raised with a plan for a fix-link Saaremaa. This thesis deals with the navigable part of the bridge. Studies of a hybrid cable-stayed suspension structure, as the most complicated cable structure, provide information for a cable-stayed structure and suspension structure design. Much information can serve in general use.

1.3.2. Aims engaged with fixed-link

Work for this thesis will provide important information if the planning of the fixed-link goes ahead and the initial task for structural engineers becomes more exact. In the thesis the load values and distributions of the Eurocode, British and Finnish Standard are presented. The experiment used general guidelines of the Eurocode – these load model values are not correct for the final design. Load values are exaggerated in a considerable degree. Load values, distributions and combinations should be determined taking into account local conditions and their future development.

For cable structures there are unfavourable parameters like width of bridge deck and span length which affect structural behaviour. This thesis offers guidelines for future work.

1.3.3. Contents of study

The theoretical part of the thesis presents guidelines for choosing first geometrical and stiffness parameters to the modern methods of analysing cable

structures. Static load models and the main effects of dynamics and wind load are described. Detailed attention has been directed to load model and moving load effects.

The scheme under investigation requires, taking into account the self-anchoring that unlike construction stages should be used.

The theoretical section of the thesis characterises the discrete calculation model of a hybrid cable-stayed-suspension structure. Data of the experimental model; initial structure, scaling, properties of materials, loading and measuring. All presented experimental results are compared with theoretical analysis and the comparison is discussed, and theoretical and experimental methods are submitted.

1.3.4. Build-up of the study

The study follows a chronological pattern of work. Useful information has come from previous work when traditional suspension structures with straight and loaded anchor cables were under investigation. This thesis aspires to present all analyses for one scheme to ensure a reference basis. Any exceptions to the reference basis are specially mentioned.

2. Literature review

2.1. Idea of structural system

Mainly from [21,22]. Additional information for general information can be found in [30, 38, 41, 43]

2.1.1. Structural components

The basic structural components of a suspension bridge system are shown in Figure 2.1.
   1. Stiffening girder/trusses: longitudinal structures which support and distribute moving vehicle loads act as cords for the lateral system and secure the aerodynamic stability of the structure.
   2. Main cables: a group of parallel-wire bundled cables which support stiffening girders/trusses by hanger ropes and transfer loads to towers.
   3. Main towers: intermediate vertical structures which support main cables and transfer bridge loads to foundations.
   4. Anchorages: massive concrete blocks which anchor the main cables and act as end supports of a bridge.

2.1.2. Types of Suspension Bridges

Suspension bridges can be classified by number of spans, continuity of stiffening girders, types of suspenders, and types of cable anchoring.
Stiffening girders are typically classified into two-hinge or continuous types. Two-hinge stiffening girders are commonly used for highway bridges. For combined highway-railway bridges, the continual girder is often adopted to ensure train runability.

Suspenders, or hanger ropes, are either vertical or diagonal. Generally, suspenders of most suspension bridges are vertical. Diagonal hangers have been used to increase the damping of the suspended structures. Occasionally, vertical and diagonal hangers are combined for higher stiffness.

Bridges can be classified into externally anchored or self-anchored types. External anchorage is most common. Self-anchored main cables are fixed to the stiffening girders instead of the anchorage; the axial compression is carried into the girders.

2.1.3. Main towers

In the longitudinal direction, towers are classified into rigid, flexible or locking types. Flexible towers are commonly used in long-span suspension bridges, rigid towers for a multi-span suspension bridge to provide enough stiffness to the bridge, and locking towers occasionally for relatively short span suspension bridges.

In the transverse direction, towers are classified into portal or diagonally braced types. Moreover, the tower shafts can either be vertical or inclined. Typically, the centre axis of inclined shafts coincides with the centre line of the cable at the top of the tower. Careful examination of the tower configuration is important in that towers dominate bridge aesthetics.

2.1.4. Cables

Cables in modern bridges are cold-drawn and galvanised steel wires. The types of parallel wire strands and stranded wire ropes that typically compromise cables are shown in Table 2.2. Generally, strands are bundled into a circle to form one cable. Hanger ropes might be steel bars, steel rods, stranded wire ropes, parallel wire strands or others. Stranded wire rope is most often used in modern suspension bridges.

2.1.5. Stiffening girders

Stiffening girders may be I-girders, trusses, or box girders. In some short-span suspension bridges, the girders have insufficient stiffness themselves and are usually stiffened by storm ropes. In long-span suspension bridges, trusses or box girders are typically adopted. I-girders become disadvantageous due to aerodynamic stability. There are both advantages and disadvantages to trusses and box girders, involving trade-offs in aerodynamic stability, ease of construction, maintenance, and details.

2.1.6. Anchors

In general, the anchorage structure includes the foundation, anchor block, cable anchor frames, and protective housing. Anchorages are classified into gravity or tunnel anchorage systems. Gravity anchorage relies on the mass of the anchorage itself to resist the tension of the main cables. This type is commonplace in many suspension bridges. Tunnel anchorage takes the tension of the main cables directly into the ground.

2.1.7. Combined cable-stayed suspension structural system

The hybrid of a cable-stayed and a suspension bridge has more structural features than an ordinary cable-stayed and a suspension bridge. Its typical features are characterized in terms of comparison as follows.

Comparison with a cable-stayed bridge:
1. Buckling stability improves because the axial force in the girder decreases because of the reduced number of stayed cables (in cases of externally anchored suspension cable).
2. It leads to a longer span because of the above mentioned reason (in cases of externally anchored suspension cable).
3. Its advantages are in cable erection and vibration problems because of short stayed cables length.
4. The height of pylons can be short for the reduced number of stayed cables.

Comparison with a suspension bridge:
1. Aerodynamic stability improves because of the increased rigidity for deformation of the girder, based on the stayed cables.
2. It enables the tension force in the main cables to be reduced because of its decreased share for loads, based on the stayed cables.
3. It enables the diameter of the main cables to be reduced because of the abovementioned reason.
4. It has an advantage in its anchorage because of the same reason.

Detailed attention to combined systems had been paid in [38, 44]
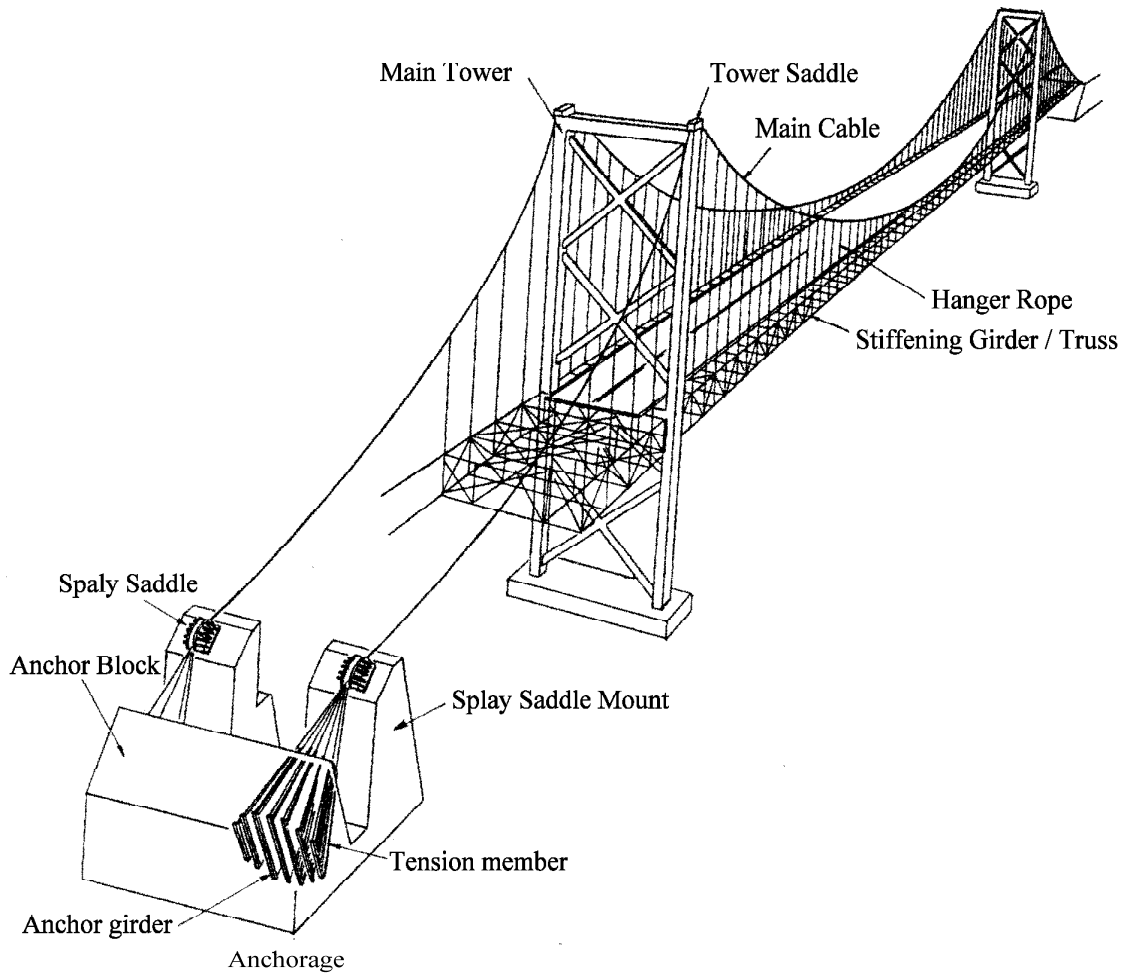
Figure 2.1 Components of a suspension bridge. Reproduction from [21]

Table 2.1 Types of main tower skeletons. Reproduction from [21]

	Truss	Portal	Combined Truss and Portal
Shape			
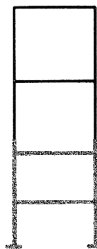
Table 2.2 Suspension Bridge Cable Types Reproduction from [21]

Name	Shape of section	Structure
Parallel Wire Strand		Wires are hexagonally bundled in parallel
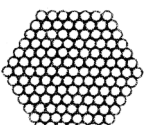
18
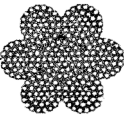
Strand Rope		Six strands made of several wires are closed around a core strand
Spiral Rope		Wires are stranded in several layers in opposite lay directions
Locked Coil Rope		Deformed wires are used for the outside layers of spiral rope
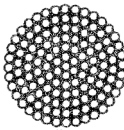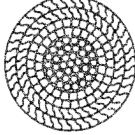
2.2. Main design principles

2.2.1. General

Engineers use structural analysis as a fundamental tool to make design decisions. It is important for engineers to have access to several different analysis tools and understand their development assumptions and limitations. Such an understanding is essential to select the proper analysis toll to archive the design objectives.

Structural analysis methods can be classified on the basis of different formulations of equilibrium, the constitutive and compatibility equations as discussed below.

1. Classification based on equilibrium and compatibility formulations

    First-order analysis: An analysis in which equilibrium is formulated with respect to the unreformed (or original) geometry of the structure. It is based on small strain and small displacement theory.

    Second-order analysis: An analysis in which equilibrium is formulated with respect to the deformed geometry of the structure. A second-order analysis usually accounts P-Δ effect (influence of axial force acting through displacement associated with member chord rotation) and the P-δ effect (influence of axial force acting through displacement associated with the flexural curvature of a member) (see Figure 2.3). It is based on small strain and small member deformation, but moderate rotations and large displacement theory.

    The large deformations analysis: An analysis for which large strain and large deformations are taken into account.

2. Classification based on constitutive formulation

    Elastic analysis: An analysis in which elastic constitutive equations are formulated.

    Inelastic analysis: An analysis in which inelastic constitutive equations are formulated.

    Rigid-plastic analysis: An analysis in which elastic rigid-plastic constitutive equations are formulated.

    Elastic-plastic hinge analysis: An analysis in which material inelasticity is taken into account by using concentrated "zero-length" plastic hinges.

Distributed plasticity analysis: An analysis in which the spread of plasticity through the cross-sections along the length of the members are modelled explicitly.

```
                          ┌──────────────┐
                          │    Start     │
                          └──────┬───────┘
                                 │
                                 ▼
              ┌──────────────────────────────────┐
              │        Initial Conditions         │
              ├──────────────────────────────────┤
              │          Configuration            │
              │           Span legth              │
              │           Cable sag               │
              │       Assumtion of members        │
              │           Dead load               │
              │           Stifness                │
              └──────────────────────────────────┘
```

In-palne Analysis — Live load

Out of plane Analysis — Wind load

Dynamic Analysis (Seismic Analysis) — Earthquake

Design of Members — Cables — Stiffening girder

Analysis of the Towers

Design of Tower Members

Vertification of the Assumed Value of Members — No / Yes

Vertification of the Aerodynamic Stabilty — No / Yes

End

Figure 2.2 General procedure for a suspension bridge design [21].
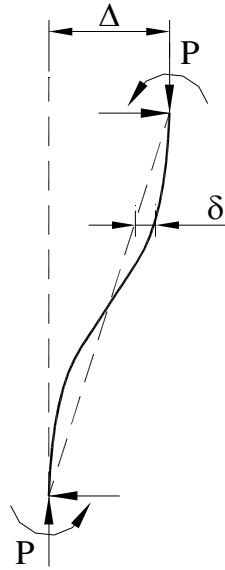
Figure 2.3 Second-order effects.

Table 2.3 Structural Analysis Methods [21]

| Methods | | Features | | |
		Constitutive Relationship	Equilibrium Formulation	Geometric Compatibility
First-order	Elastic	Elastic	Original unreformed geometry	Small strain and small displacement
	Rigid-plastic	Rigid plastic		
	Elastic-plastic hinge	Elastic perfectly plastic		
	Distributed plasticity	Inelastic		
Second-order	Elastic	Elastic	Deformed structural geometry (P-Δ and P-δ)	Small strain and moderate rotation (displacement may be large)
	Rigid-plastic	Rigid plastic		
	Elastic-plastic hinge	Elastic perfectly plastic		
	Distributed plasticity	In elastic		
True large displacement	Elastic	Elastic	Deformed structural geometry	Large strain and large deformation
	Inelastic	Inelastic		

1. Selection of initial configuration: span length and cable sag are determined, and dead load and stiffness are assumed.
2. Analysis of the structural model: In the case of in-plane analysis, the forces on and deformations of members under live load are obtained by using the finite deformation theory or the linear finite deformation theory with the two-dimensional model. In the case of out-of-plane analysis, wind forces on and deformations of members are calculated, based on the linear finite deformation theory with the three-dimensional model.
3. Dynamic response analysis: The responses of earthquakes are calculated by the response spectrum analysis or the time-history analysis.
4. Member design: The cables and girders are designed using the forces obtained from previous analysis.
5. Tower analysis: The tower is analysed using loads and deflection which determined from the global structure analysis previously described.
6. Verification of the assumed values and aerodynamic stability: The initial values assumed for dead load and stiffness are verified to be investigated through analysis and/or wind tunnel tests using dimensions obtained from the dynamic analysis.

2.2.2. Design load

Design load for a suspension bridge must take into consideration the natural conditions of the construction site, the traffic on the bridge, its span length, and its function. It is important in the design of suspension bridges to determine the dead load accurately because the dead load typically dominates the forces on the main components of the bridge. Securing structural safety against strong winds and earthquakes is also an important issue for long-span suspension bridges. In cases of high wind, consideration of the vibrational and aerodynamic characteristics is extremely important. Other design loads include effects due errors in fabrication and erection of members, temperature change, and possible movement of the supports.

2.2.3. Dynamic effects of traffic load

Vehicles, such as trucks and trains, passing a bridge at a certain speed will cause dynamic effects, including global vibration and local hammer effects. Dynamic loads of moving vehicles are considered to have an "impact" on bridge engineering because of relatively short duration. The magnitude of the dynamic response depends on the bridge span, stiffness and surface roughness, and vehicle dynamic characteristics such as moving speed and isolation system. Unlike earthquake loads which can cause vibration in bridge longitudinal, transverse, and vertical directions, moving vehicles mainly excite vertical vibration of the bridge. Impact effect has influence primarily on the superstructure and some of substructure members above the ground because the energy will be dissipated effectively in members underground by the bearing soils.

Although the interaction between moving vehicles and bridges is rather complex, the dynamic effects of moving vehicles on bridges are accounted for by a dynamic load allowance, in addiction to static live load in the current bridge design specifications.

Additional information can be found in [24, 34, 39, 40]

2.2.4. Design of cables

Parallel wire cable has been used exclusively as the main cable in long-span suspension bridges. Parallel wire has the advantage of high strength and high modulus of elasticity compared with stranded wire rope. The design of the parallel wire cable is discussed next, along with structures supplemental to the main cable. Alignment of the main cable must decided first, the sag-span ratios should be determined in order to minimize the construction costs of the bridge. In general, this sag-span ratio is around 1:10. However, the vibration characteristics of the entire suspension bridge change occasionally with changes in the sag-span ratios, so the influence on the aerodynamic stability of the bridge should be also considered. After structural analysis are executed according to the design process shown in overcool design, the sectional area of the main cable is determined based on the maximum cable tension, which usually occurs at the side span face of the tower top.

The tensile strength of cable wire has been about 1570N/mm² in recent years. For a safety factor 2.5 or 2.2 is used

2.2.5. Design of the stiffening girder

The width of the stiffening girder is determined in order to accommodate the carriageway width and shoulders. The depth of the stiffening girder, which affects its flexural and torsion rigidity, is decided so as to ensure aerodynamic stability. After examining alternative stiffening girder configurations, a wind tunnel test is conducted to verify the aerodynamic stability of the girders.

In judging the aerodynamic stability, in particular the flutter, of the bridge design, a bending-torsional frequency ratio of 2.0 or more is recommended. However, it is not always necessary to satisfy this condition if the aerodynamic characteristics of the stiffening girder are satisfactory.

The basic dimensions of a box girder for relatively small suspension bridges are determined only by requirements of fabrication, erection, and maintenance. Aerodynamic stability of the bridge is not generally a serious problem. The longer the centre span becomes, however, the stiffer girder needs to secure aerodynamic stability. The girder height is determined to satisfy the rigidity requirement. Fatigue due to live loads needs to be especially considered for the upper flange of the box girder, because it directly supports the bridge traffic. The diaphragms support the floor system and transmit the reaction force from the floor system to the hanger ropes.

2.2.6. Design against wind effects

The suspension and cable-stayed bridges shown are typical structures susceptible to wind induced problems.

Figure 2.4 shows the wind-resistant design procedure specified. In the design procedure, wind-tunnel testing is required for two purposes: one is to verify the airflow drag, lift, and moment coefficients which strongly influence the static design; and the other is to verify that harmful vibrations would not occur.

Gust response analysis is an analytical method to verify the forced vibration of the structure by wind gusts. The results are used to calculate structural deformations and stress in addition to those caused by mean wind. Divergence, one type of static instability, is analysed by using finite displacement analysis to examine the relationship between the wind force and deformation. Flutter is the most critical phenomenon in the analysis of the dynamic stability of suspension bridges, because of the possibility of collapse. Flutter analysis usually requires the motion equation of the bridge to be solved as a complex eigenvalue problem where unsteady aerodynamic forces from wind-tunnel tests are applied.

In general, the fallowing wind-tunnel tests are conducted to investigate the aerodynamic stability of the stiffening girder.

1. Two-Dimensional Test of Rigid Model with Spring Support: The aerodynamic characteristics of a specific mode can be studied. The scale of the model is generally higher than 1/100.
2. Three-Dimensional Global Model Test: Test is used to examine the coupling effects of different modes.

```
┌─────────────┐
│    Start    │
└─────────────┘
       │
       ▼
┌──────────────────────────────┐
│        Static Design         │
│ Vertification of member forces│
└──────────────────────────────┘
       │
       ▼
┌──────────────────────────────┐
│   Vertification of Air-flow   │
│       Force Coefficient       │
│      (Wind tunel test)        │
│         Drag                  │
│         Lift                  │
│         Moment                │
└──────────────────────────────┘
       │
       ▼
┌──────────────────────────────┐
│    Vertification of Static    │
│           Stabilty            │
│         Deivergence           │
└──────────────────────────────┘
       │
       ▼
┌──────────────────────────────┐
│   Vertification of Dynamic    │
│           Stabilty            │
│       (Wind tunel test)       │
│      Gust responce            │
│      Flutter                  │
│      Vortex-induced oscillation│
└──────────────────────────────┘
       │
       ▼
┌─────────────┐
│     End     │
└─────────────┘
```
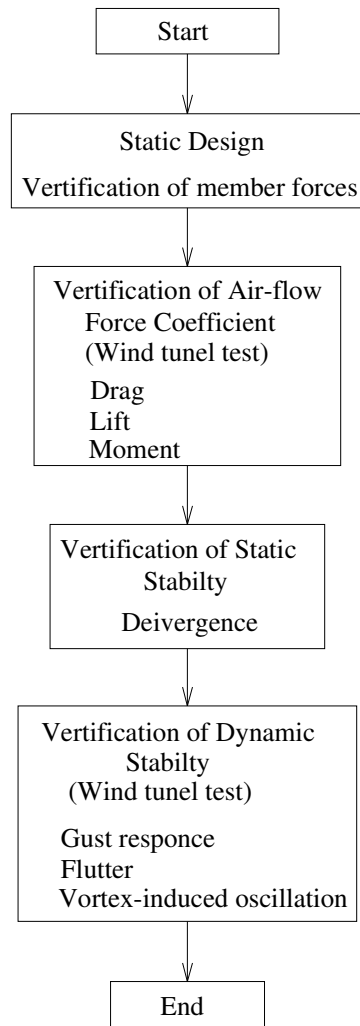
Figure 2.4 Procedure for wind resistant design [21].

3. Road traffic actions

This section describes an approach of a standard load model for the traffic load of a bridge. The Eurocode [34,35] guidelines for specific cases assume that a load for such structures is determined in detail in terms of local conditions and future perspectives taking into account alternate transport possibilities. The analysis and investigation used the most maximum ever load values and distributions. In this thesis load values are extreme; in contrast, in real design load cases will be much more favourable. The estimation of possible load values and distributions follows the guidelines of the British [22] and Finnish [36] Standard. Figure 3.1 presents a uniformly distributed load for each traffic lane. Figure 3.2 shows a decreasing function for longer span lengths for a uniformly distributed load. Table 3.1 and   present a comparison of general rules for the Eurocode and Finnish standard. These graphs and tables illustrate approximate values and distributions in real design. As shown, the uniformly distributed value in the Finnish Standard is three times smaller than in our investigation, span length decreases also the uniformly distributed load value almost for three times for long span lengths. The remaining area of bridge deck is assumed to be load free in the Finnish Standard.
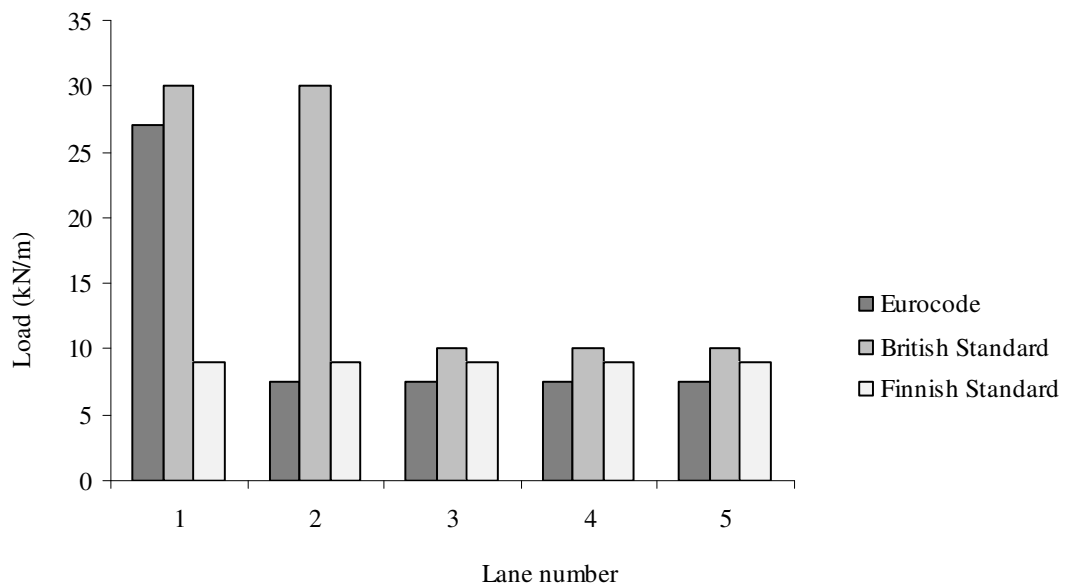
Figure 3.1 Traffic load on lanes [22,34,35,36].
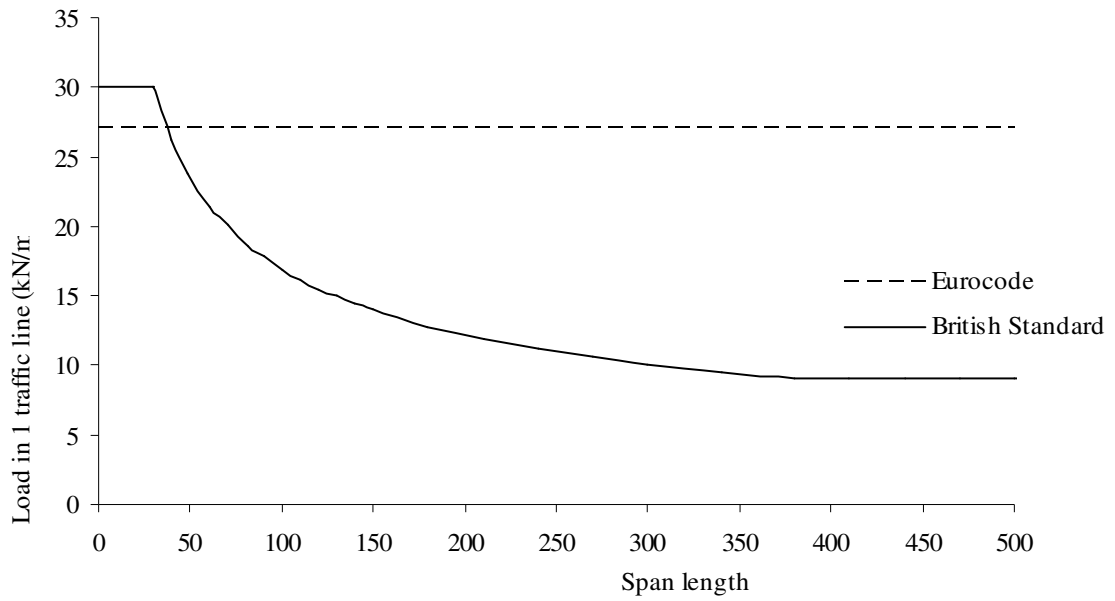
Figure 3.2 Traffic load on the first lane as a function of span length [22,34,35].

Table 3.1 Traffic load in load model 1 [34,35,36]

Location	Eurocode		Finnish Standard	
	Tandem system: Two axle loads $2 \times Q_{ik}$ with wheelbase 1.2 m Q_{ik} [MN]	UDL system q_{ik} [MN/m^2]	Tandem system: Three axle loads $3 \times F_{ik}$ with wheelbases ≥ 2.5 m, ≥ 6 m F_{ik} [MN]	UDL system p_{ik} [MN/m^2]
Lane 1	0.3	0.0090	0.21	0.003
Lane 2	0.2	0.0025	0.21	0.003
Lane 3	0.1	0.0025	0	0.003
Lane ≥ 4	0	0.0025	0	0.003
Remaining area	0	0.0025	0	0
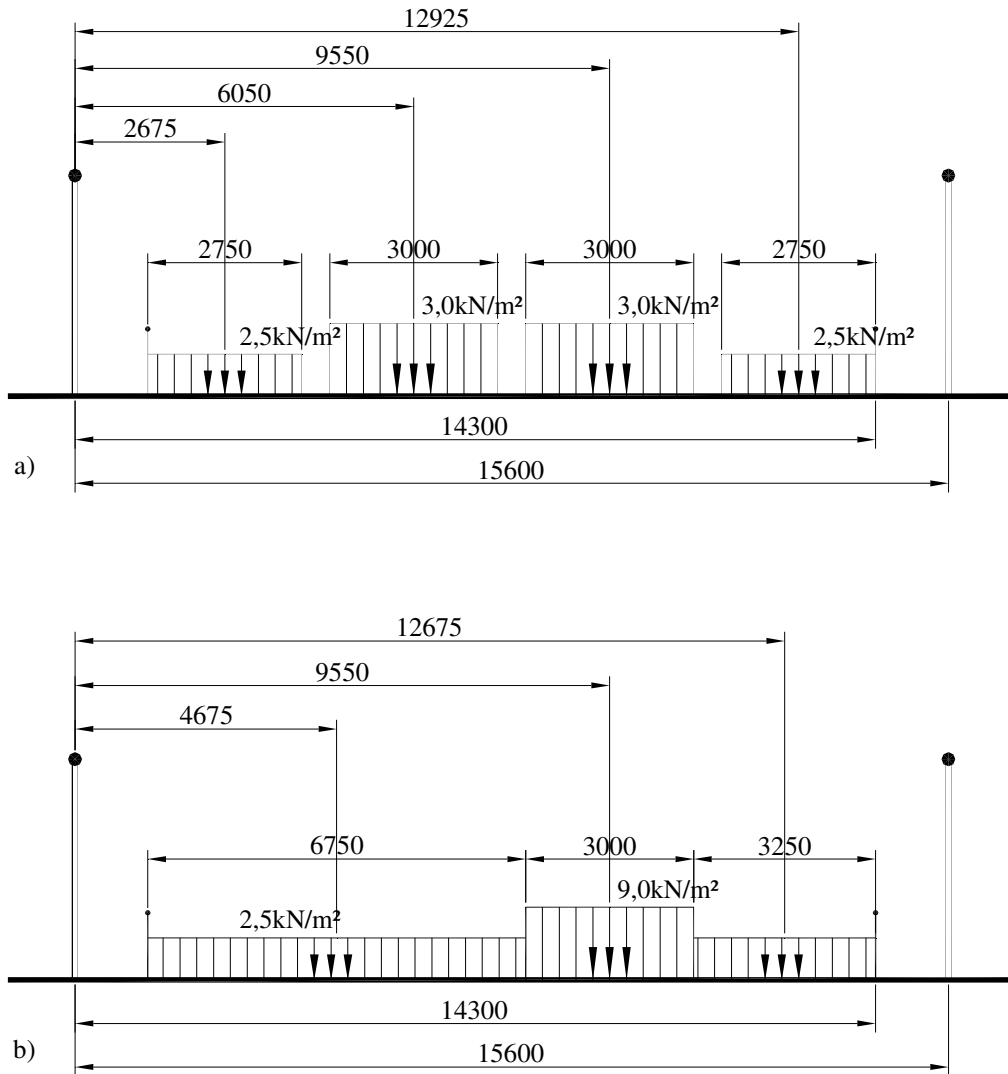
Figure 3.3 Schemes for load calculations for hangers and cable-stays: a) according to Finnish NA [36], b) Eurocode general guidelines [34,35]

4. Description of the bridge model

4.1. Assumed bridge structure

The length of the middle span of the bridge was chosen 300 m and the length of the side spans 120 m. The rise of the main suspension cables in the middle span was chosen 37.5m (1/8 of the span length).
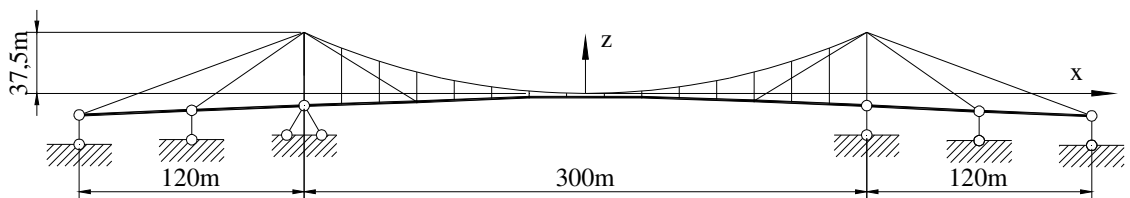
Figure 4.1 Hybrid, cable-stayed and suspension bridge – improved bridge structure.
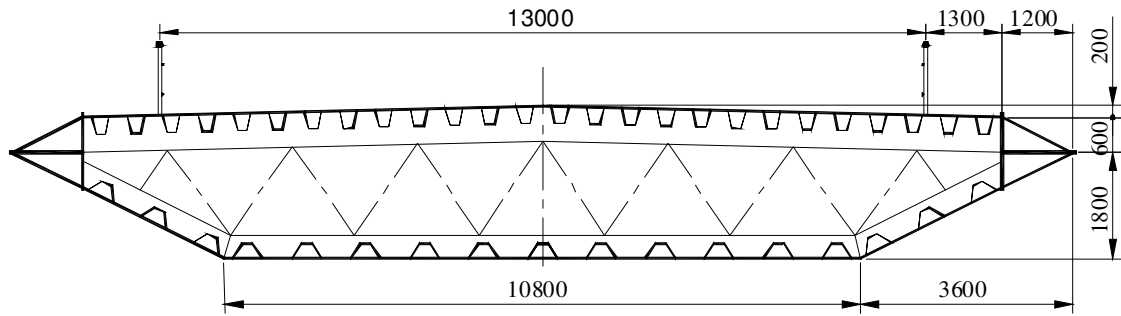
Figure 4.2 Stiffening girder of the bridge.

4.2. Construction stages

For the reason that self-anchoring is assumed, construction stages are different for a hybrid cable-stayed suspension structure in contrast to the traditional suspension structure. In an initial construction stage, the structure works as a cable-stayed structure and the carrying cable will be mounted after assembly of the stiffening girder. Cable stays of the bridge start acting as the stiffening girder is being assembled, but the suspension part of the structure starts acting for the deck cladding and the imposed load. The stiffening girder starts acting in an initial construction stage when the structural scheme is cable-stayed. Temporary supporting and post-tensioning may be considered.

4.3. Description of the model

The model under investigation was erected in the scale of 1:100. The carrying cable of the bridge uses steel cable, for which sectional are is measured and the modulus of elasticity is determined. The carrying cable has a diameter of 2.5 mm, a cross-sectional area of 2.2 mm² and the modulus of the elasticity of 93.6 GPa. Cable-stays have a diameter of 1.0 mm, a cross- sectional area of 0.64 mm², and the modulus of the elasticity of 189 GPa. The stiffening girder was modelled by two steel angles which are engaged with a diagonal network and covered by a steel sheet. The stiffening has a cross- sectional area of 1.52 cm², the moment of inertia of 0.02454 cm^4, and the modulus of elasticity of 210 GPa. Pylons of the model was made by a circular hollow section tube. For the left pylon, the support is fixed and for the right pylon it is pinned. Both pylon supports were solved by steel plates, for the fixed support, a circular tube was welded to the anchor plate and the stiffening plates and for the pinned support, the tube is situated between the steel plates joined by a bolt (see Figure 4.14 and 3.15). Loading of the structure was modelled with a leveller system (see Figure 4.11). For the span length, load was applied to five points and through the leveller system, a load is distributed to the stiffening girder (see Figure 4.17).

4.3.1. Scaling

Table 4.1 Data of the model and actual structure (for estimation)

	Model	Coefficient	Actual
Geometry			
Middle span	3000mm	10^2	300m
Side span	1200mm	10^2	120m
Carrying cable			
Sectional area	4,40mm²	10^4	440,0cm²
Modulus of elasticity	93,6GPa	1	93,6GPa
Cable-Stays			
Sectional area	1,28mm²	10^4	128,0cm²
Modulus of elasticity	187,9GPa	1	187,9GPa
Stiffening girder – timber board	17×2cm		
Sectional area	17,0cm²	10^4	17,0m²
Moment of inertia	34,0cm⁴	10^8	34,0m
Modulus of elasticity	10	1	10
Stiffening girder – steel bars			
Sectional area	158mm²	10^4	1,58m²
Moment of inertia	0,576cm⁴	10^8	0,576m⁴
Modulus of elasticity	210	1	210
Load			
Initial load	0,096	10^2	11,2kN/m
Self-weightDead weight	0,828	10^2	81kN/m
Traffic load	0,828	10^2	56,4(31,74*)kN/m

* - according to Finnish NA [25]

4.3.2. Detailing

The carrying cable of the model is fixed to the pylons by steel plates which are squeezed by two bolts (see Figure 4.12). In the anchor support, the carrying cable is fixed through the stretching unit which is fixed to the additional, perpendicular steel angle on the stiffening girder (see Figure 4.6). For fixing hangers to the carrying cable there are two steel plates; on the bottom of one steel plate is an opening for suspending the hanger. Two steel plates are squeezed by two bolts to carry the cable between them (see Figure 4.16). Hangers are fixed to the stiffening girder by two nuts through the flange of the steel angle with the threaded end of the hanger (see Figure 4.17). Hangers are solid steel bars.

Cables stays are fixed to the pylon similarly to the carrying cable. To the stiffening girder cable stays are fixed to the stiffening girder by a crook around the screw which is fixed to the vertical flange of the stiffening girder's angle (see Figure 4.13). At the one end of each cable stay (side span) there is a stretching unit (see Figure 4.8). The stiffening girder has direct vertical supports at both ends of the bridge in place of the pylons and in the side span in the anchoring node of the cable stays. In all cases a vertical support is provided by steel plates which in plane are hinged in the ends.

4.3.3. Properties of materials

Naturally close attention was paid to the determing of the correct and exact modulus of elasticity for the carrying cables and cable stays. Different cables were tested to achieve minimum residue deformation. For cable-stays testing results and calculations are presented in Table 4.2 and for the carrying cable in Table 4.3.

For the cable stays, maximum load presented in Table 4.2, detailed calculations are

$$F = 3pc \times 28kg \times 9,81\frac{m}{s^2} = 824N$$

$$\sigma = \frac{0,82 \times 10^3}{0,6385 \times 10^{-6}} = 1284 \times 10^6 \, Pa = 1284 MPa$$

$$\Delta l = 241,5 - 231,2 = 10,30mm$$

$$\varepsilon = \frac{10,30}{1500} = 6,87 \times 10^{-3}$$

Figure 4.10 shows the linear trendline for data in Table 4.2.
Unit rise k is 0.1200 and elastic modulus for the cable stay is

$$E = \frac{0,1200}{0,6385} \times 10^3 = 187,9 GPa$$

4.3.4. Testing

As mentioned above, the model was loaded by a leveller system through the stiffening girder. The leveller system is suspended to the stiffening girder with a steel bar over the stiffening girder and anchoring plates at ends of the bar. In the middle span there are five loading points.
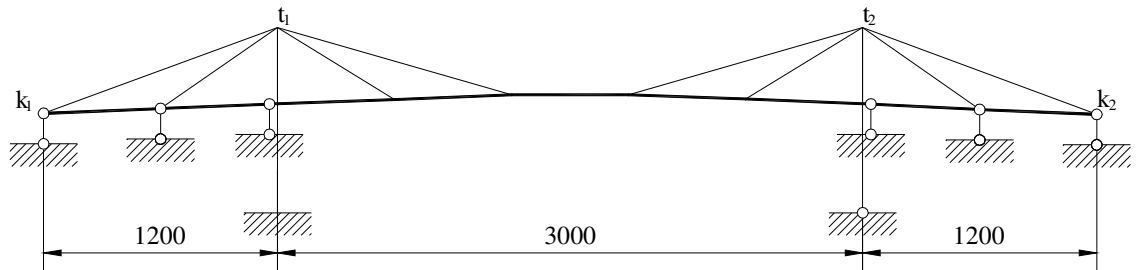
Figure 4.3 Cable-stayed bridge. Bridge structure before installing the suspension cable and hangers.
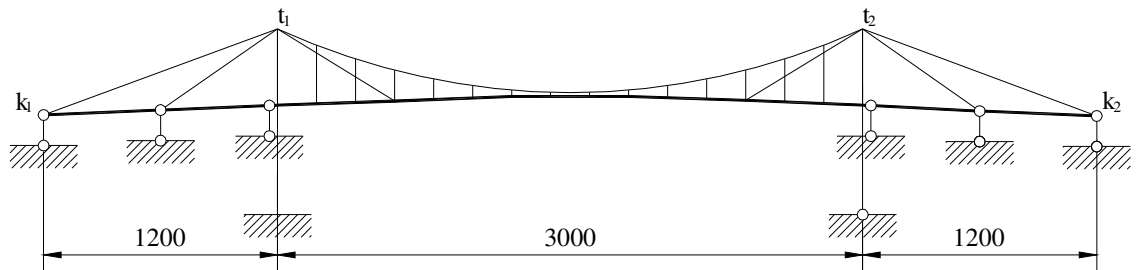
Figure 4.4 Combined, cable-stayed and suspension structure.

Vertical displacements were measured from the origin cable stretched above the whole structure. Measurements were taken with the ruler. Horizontal displacements of pylons were measured by a suspended plummet and the ruler was placed at the support of the pylon to take the measurements. Horizontal displacements were measured by callipers directly from the support. For callipers an additional support structure outside the model was built.

Figure 4.5 Overview of the model.

Figure 4.6 Anchor support of the model.
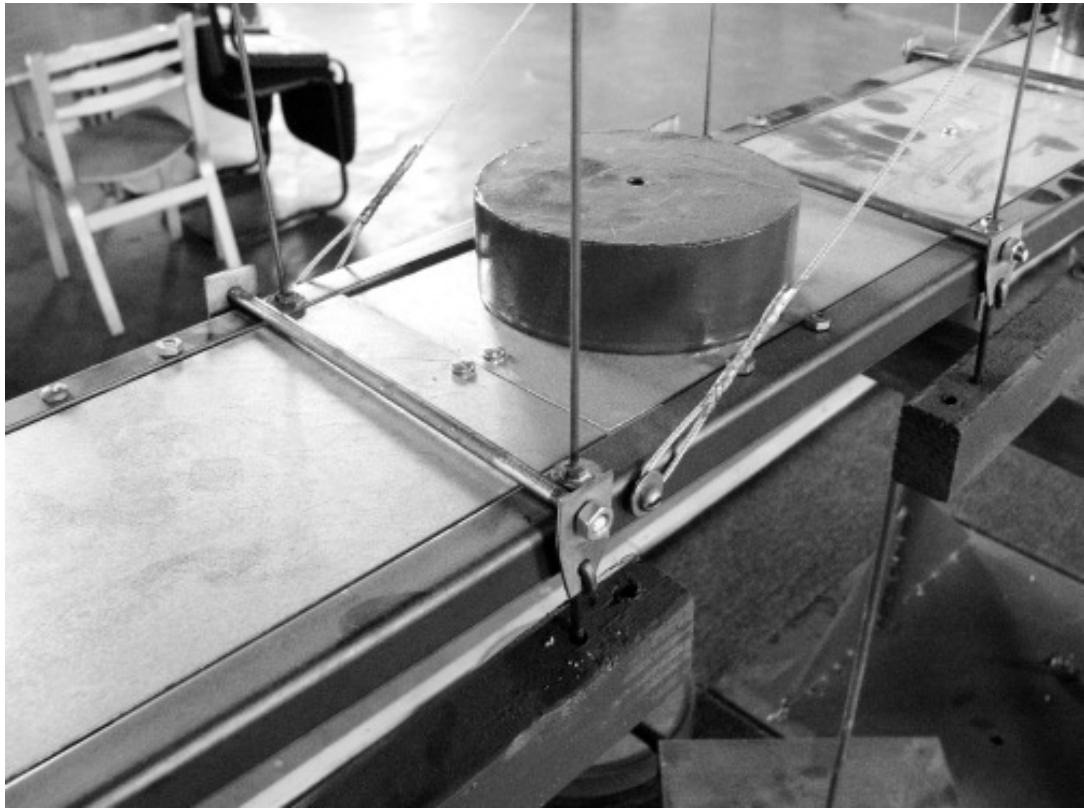
Figure 4.7 Anchoring of the cable-stay in the middle span.

Figure 4.8 Anchoring of the cable-stay in the side span.

Figure 4.9 Measuring of horizontal displacements of the pylons.
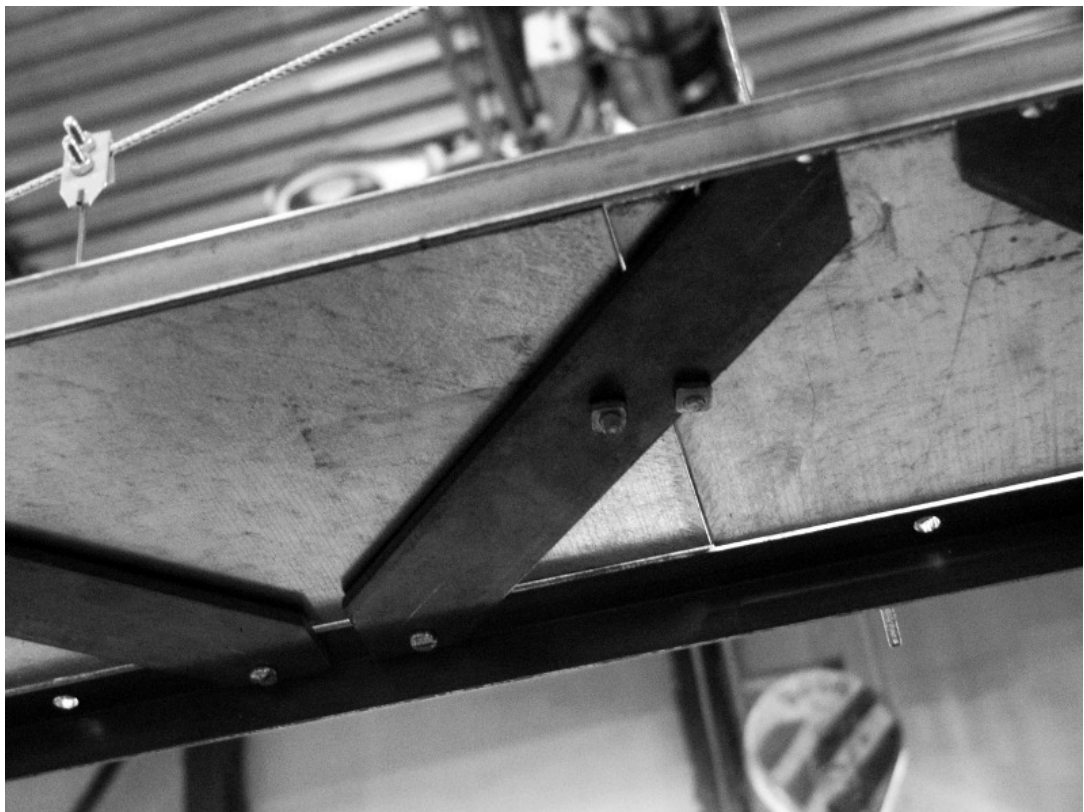
Figure 4.10 Stiffening girder truss.

Figure 4.11 Loading the leveller system.

Figure 4.12 Anchoring the carrying cable and cable-stays at the to of the pylon.
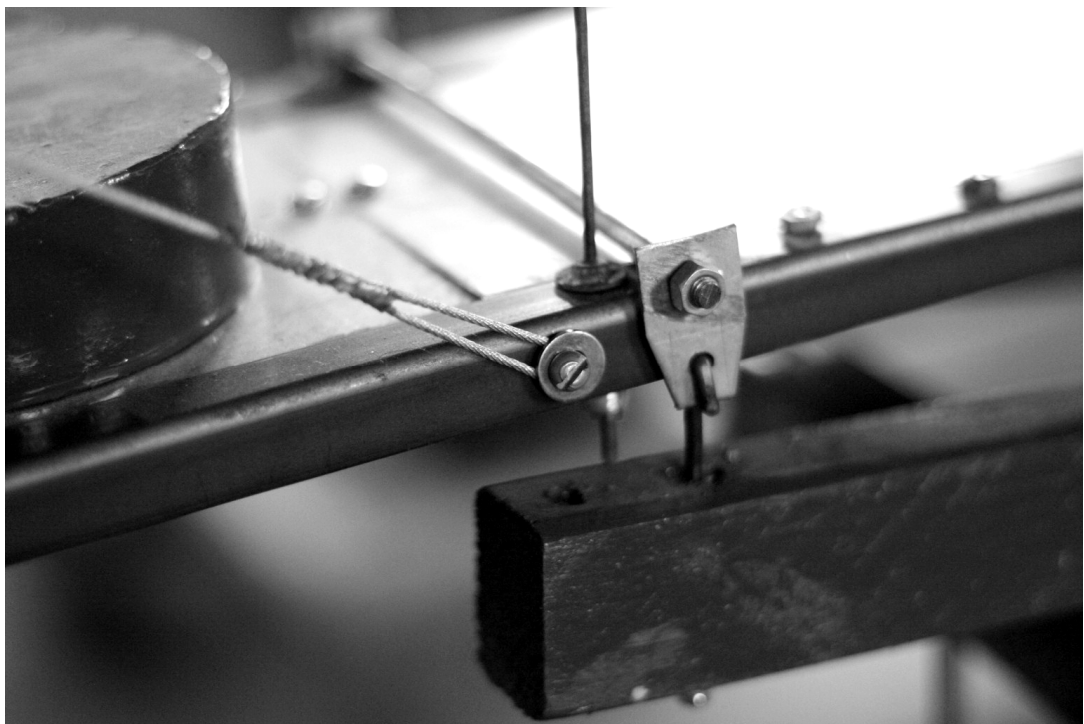
Figure 4.13 Anchoring of the cable-stay and the middle span and the suspending detail of the loading leveller system.
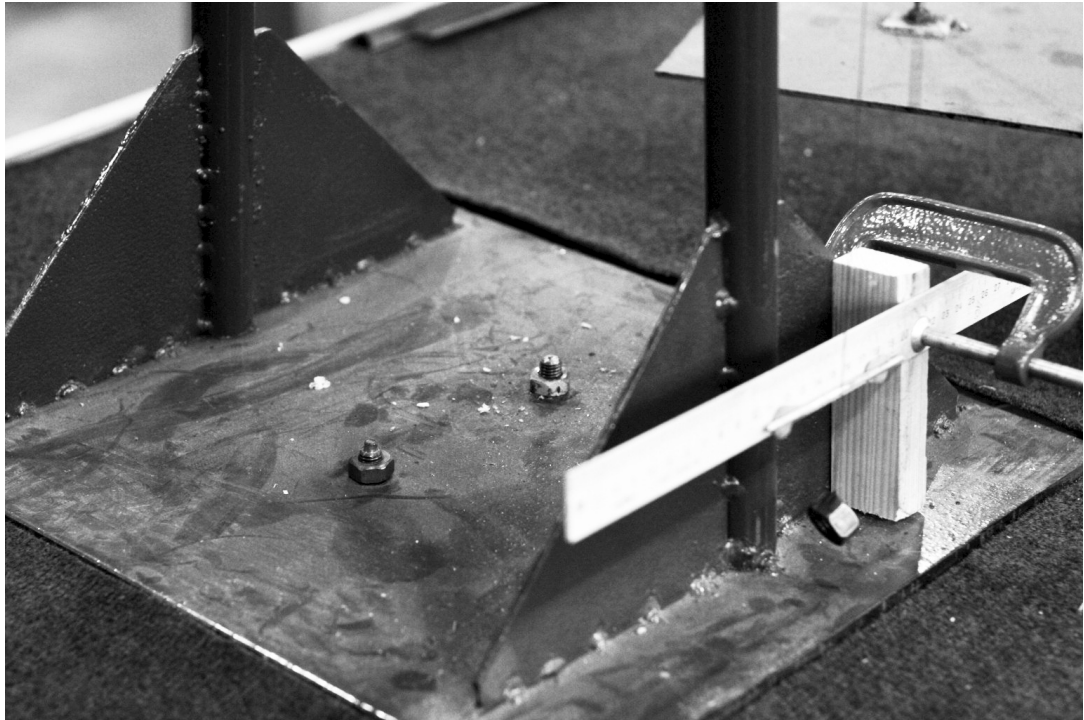
Figure 4.14 Support of the left pylon.
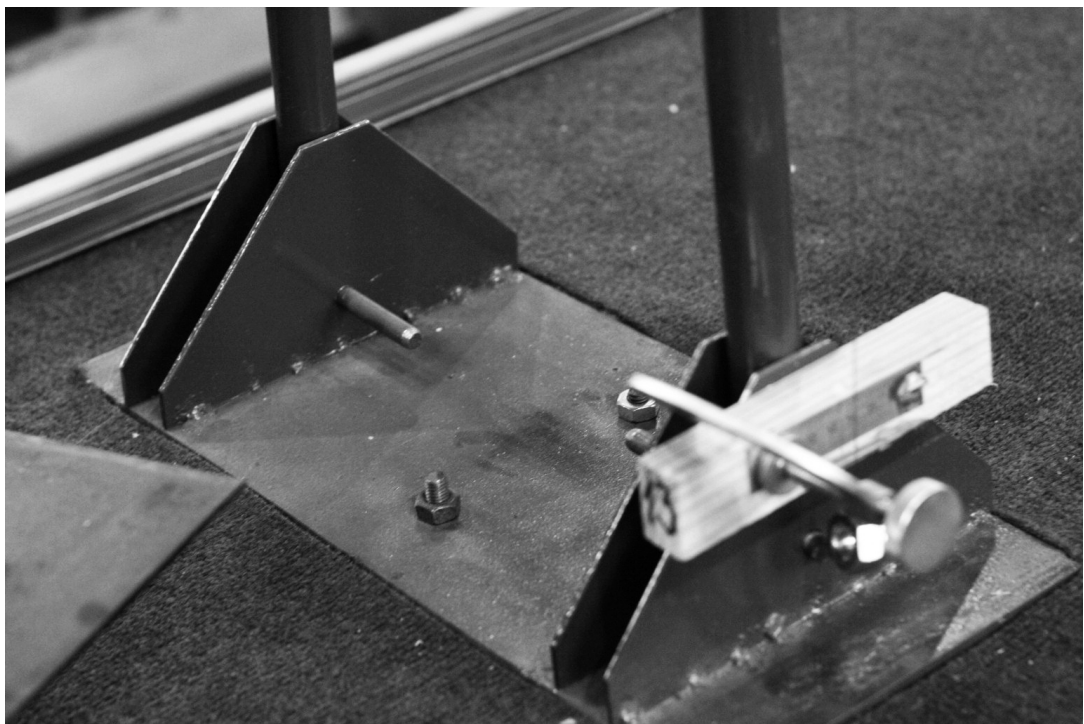
Figure 4.15 Support of the right pylon.
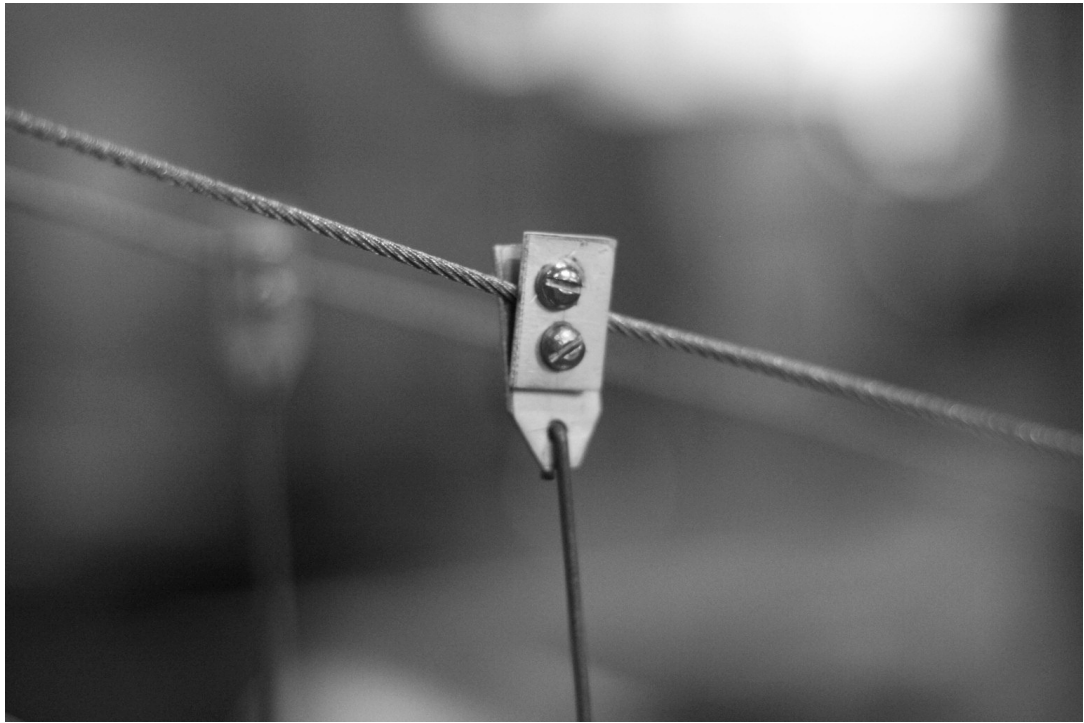
Figure 4.16 Fixing the hangers to the carrying cable.
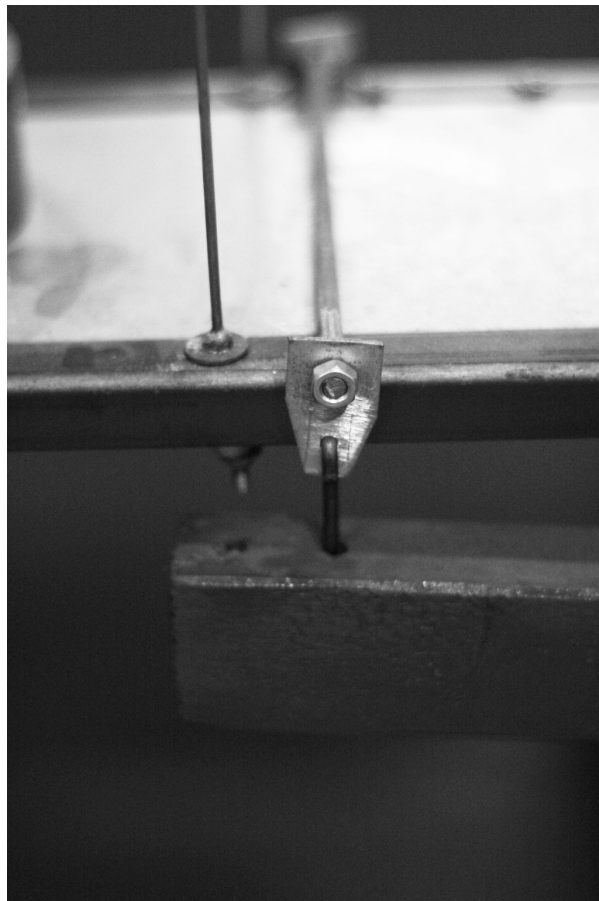
Figure 4.17 Fixing the hangers to the stiffening girder.

Figure 4.18 Supporting the stiffening girder in place of the pylons.

Table 4.2 Experimental data for the drawing the trendline for Ø1.0 cable

L= 1500 mm A= 0.6385 Mm²

F	σ	N		Δl		ε	
kN	MPa	mm		mm		×10⁻³	
		1k.	2k.	1k.	2k.	1k.	2k.
		231.2	231.3				
0.10	157	232.3		1.10		0.73	
0.18	282	233.5	233.6	2.30	2.30	1.53	1.53
0.26	407	234.5		3.30		2.20	
0.34	532	235.5	235.5	4.30	4.20	2.87	2.80
0.42	658	236.5		5.30		3.53	
0.50	783	2373	237.5	6.10	6.20	4.07	4.13
0.58	908	238.3		7.10		4.73	
0.66	1034	239.5	239.5	8.30	8.20	5.53	5.47
0.74	1159	240.5		9.30		6.20	
0.82	1284	241.5	241.5	10.30	10.20	6.87	6.80
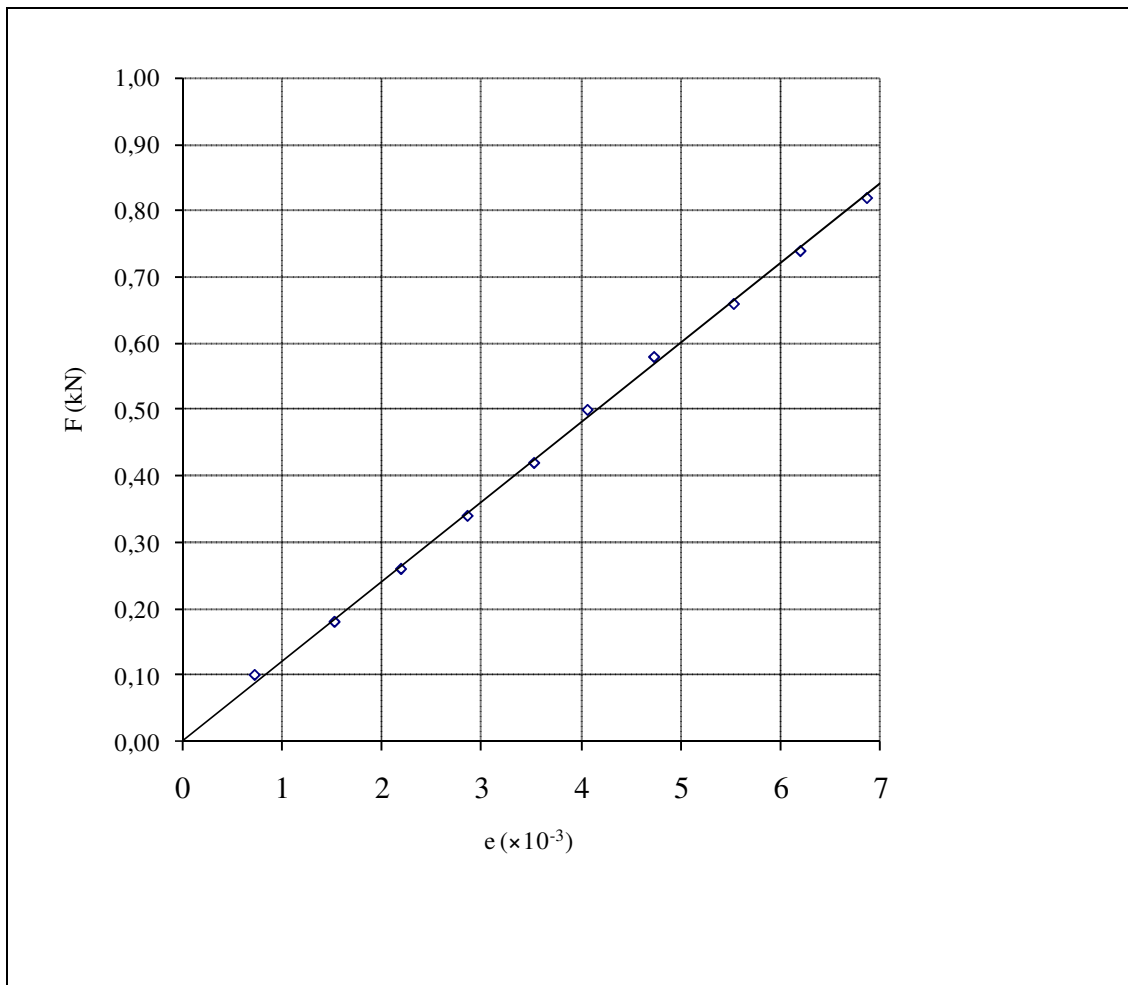
Figure 4.19 Trendline for determining modulus elasticity for cable Ø1.0 mm.

$$E = \frac{k}{A} = \frac{0,1200}{0,6385} \times 10^3 = 187,9\text{GPa}$$

Table 4.3 Experimental data for the drawing the trendline for Ø1.0 cable

| L= | 1500 | mm | | A= | 2,2 | mm² | |

F	σ	N		Δl		ε	
kN	MPa	mm		mm		×10⁻³	
		1k.	2k.	1k.	2k.	1k.	2k.
		241.5	244.0				
0.265	120	244.5		3.00		2.00	
0.530	241	246.4	249.0	4.90	5.00	3.27	3.33
0.795	361	248.0		6.50		4.33	
1.060	482	249.5	252.5	8.00	8.50	5.33	5.67
1.325	602	251.0		9.50		6.33	

1.590	723	252.5	255.7	11.00	11.70	7.33	7.80
1.855	843	254.0		12.50		8.33	
2.120	964	255.7	258.5	14.20	14.50	9.47	9.67
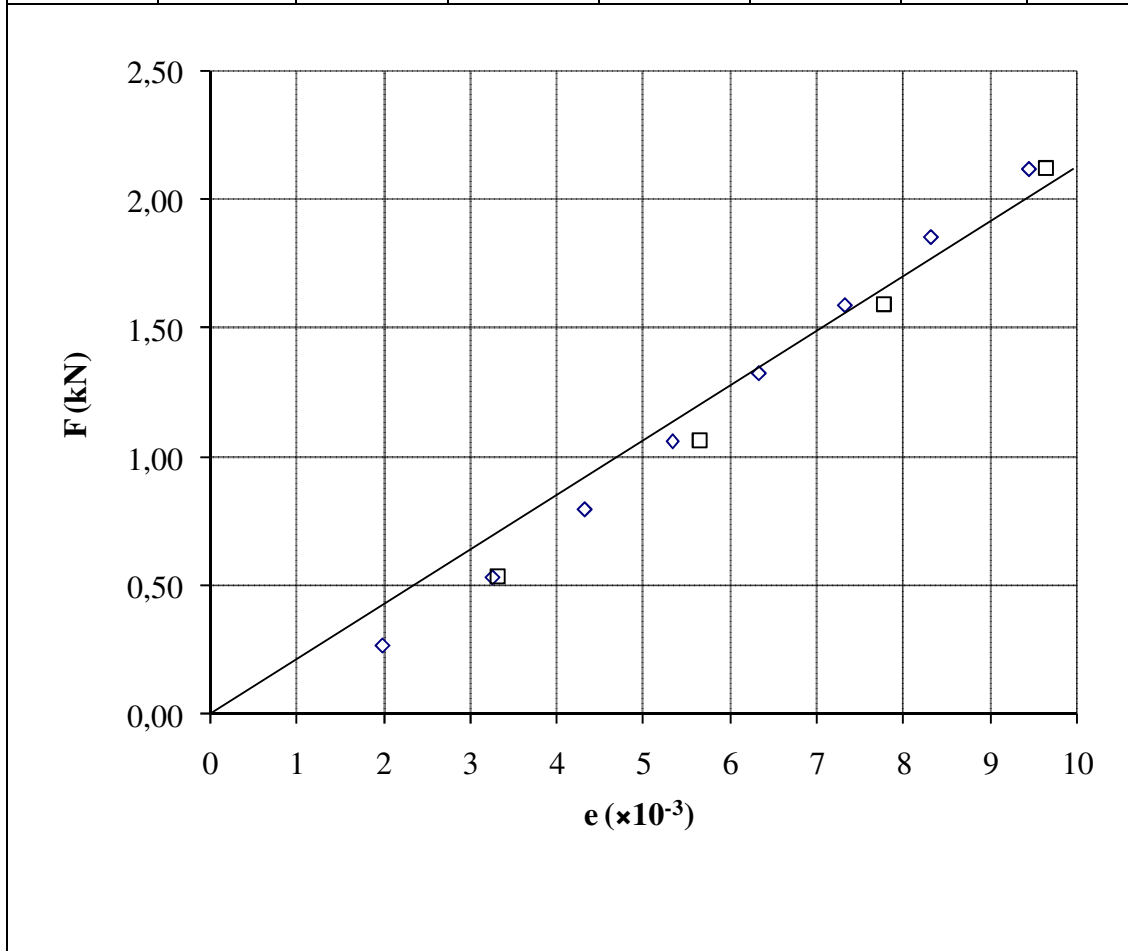
Figure 4.20 Trendline for determining modulus elasticity for cable Ø2.5 mm.

$$E = \frac{k}{A} = \frac{0,2059}{2,2} \times 10^3 = 93,6 \, GPa$$

5. Static analysis

5.1. Theoretical basis for calculating cable structures

Cable structures are structures with a cable as the main load-carrying element. If one of the main dimensions of an element is larger than the two remaining ones, and section rigidity with respect to bending and torsion is small in comparison to tension rigidity, such an element is regarded as a cable.

The basic conclusion drawn from the above definition is that only tensile forces can be applied to cables. However, in some cases small bending or torsional moments and shearing forces can be applied to cables. The most significant advantage of cable structures has its origin in the fact that cables have great admissible tensile stresses. Therefore, a cable section can be used in an optimum way and light, economical and aesthetic structures can be designed. Two main factors are in favour of applying cable elements in the designed structures: firstly - the possibility of entering the initial cable tension, which enables for internal force regulation and makes the results more effective; secondly - simple assemblage (e.g. suspension and assemblage of an entire structure due to its small weight).

The theory of cable structures is based on the following assumptions:
· loads and other external effects are of quasi-static type and constant in time,
· for cables no bending moments and shearing forces are considered,
· cable elements work in the elastic range (Young's modulus E = const),
· any loads can be applied, except for the moment loads,
· large displacements u, but small gradients du/dx are admissible,
· cable section area F is constant (F=const),

5.2. Methods for analysis

5.3. Discrete analysis [6][12]

5.3.1. Initial configuration of cable

An elastic cable loaded by system of concentrated forces obtains the shape of a string polygon. The initial form of cable is determined by conditions of equilibrium of its nodes (points of application of loads). The behaviour of the cable under the action of additional loads depends upon the loads and displacements of the cables nodes.

For the case of planar cable loaded by vertical forces, the condition of equilibrium may be written in the following scalar form

$$H_0\left(\frac{z_{i-1}-z_i}{a_{i-1}}+\frac{z_{i+1}-z_i}{a_i}\right)+F_{0i}=0 \tag{5.1}$$

where H_0 is the horizontal component of the cable's force.

The proper fractions inside the parentheses in Equation (5.1) present tangents of angles of inclination of the corresponding cable sections. Equation may be presented in the form suitable for direct calculation of ordinates z_i

$$z_i=\frac{1}{1+\dfrac{a_i}{a_{i-1}}}\left(z_{i-1}\frac{a_i}{a_{i-1}}+z_{i+1}-\frac{F_{0i}a_i}{H_0}\right) \tag{5.2}$$
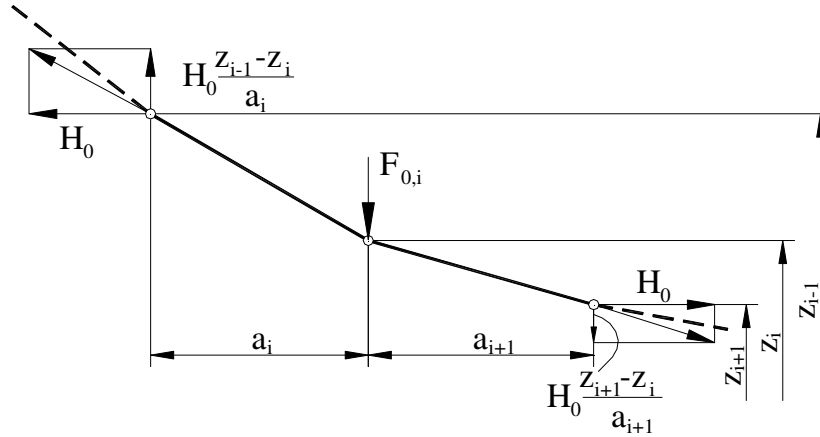
Figure 5.1 A cable section under the action of initial vertical loads [6].

In case the distances between the forces are equal, then by simplifying the expression (5.2) we get,

$$z_i = \frac{1}{2}\left(z_{i-1} + z_{i+1} + \frac{F_{0i}a}{H_0}\right) \tag{5.3}$$

If we know the cable's force H_0 then using Equations (5.2) and (5.3) we can find the ordinates of the string polygon. To find H_0 we can provide an additional equilibrium condition for the support point of the cable.

$$H_0 = V_0 \frac{a_0}{z_2 - z_1} = \frac{a_0 \sum\limits_{i=1}^{n} F_{0i}(1 - x_i)}{l(z_2 - z_1)}, \tag{5.4}$$

where

$$V_0 = \frac{\sum\limits_{i=1}^{n} F_{0i}(1 - x_i)}{l}$$ -vertical support reaction in the cable's support point

l – span of the cable

With support points located at different heights, the cable's force H_0 can be found with the following expression:

$$H_0 = \frac{a_0 \sum\limits_{i=1}^{n} F_{0i}(1 - x_i)}{l(z_2 - z_1) - a_0(z_1 - z_{n+1})} \tag{5.5}$$

The configuration of cable presented in such a way can be defined if we know the three ordinates z_1, z_2, z_{n+1}.

Knowing H_0, we can present the expression (5.1) as

$$\frac{H_0 z_{i-1}}{a_{i-1}} - \frac{H_0 z_i}{a_{i-1}} + \frac{H_0 z_{i+1}}{a_i} - \frac{H_0 z_i}{a_i} + F_{0i} = 0 \tag{5.6}$$

Denoting $\dfrac{H_0}{a_{i-1}} = A$ and $\dfrac{H_0}{a_i} = B$, and regrouping, we can write the expression (5.6) as

$$A z_{i-1} - (A + B)z_i + B z_{i+1} = -F_{0i} \tag{5.7}$$

Thus, knowing H_0, the ordinates of the node points of the entire cable can be found by solving the following equation system:

$$\begin{vmatrix} -(A_1 + B_1) & B_1 & 0.0 & 0 & 0 \\ A_2 & -(A_2 + B_2) & B_2. 0 & 0 & 0 \\ . & . & . . . & . & . \\ . & . & . . . & . & . \\ . & . & . . . & . & . \\ 0 & 0 & 0 .A_{n-1} -(A_{n+1} + B_{n-1}) & B_{n-1} \\ 0 & 0 & 0.0 & A_n & -(A_n + B_n) \end{vmatrix} \times \begin{vmatrix} z_1 \\ z_2 \\ . \\ . \\ . \\ z_{n-1} \\ z_n \end{vmatrix} = - \begin{vmatrix} F_{01} \\ F_{02} \\ . \\ . \\ . \\ F_{0n-1} \\ F_{0n} \end{vmatrix} \tag{5.8}$$

In case of equal distances between forces, the given equation system is symmetrical in relation to the diagonal:

$$\begin{vmatrix} -2A & A & 0 & . & 0 & 0 & 0 \\ A & -2A & A & . & 0 & 0 & 0 \\ . & . & . & . & . & . & . \\ . & . & . & . & . & . & . \\ . & . & . & . & . & . & . \\ 0 & 0 & 0 & . & A & -2A & A \\ 0 & 0 & 0 & . & 0 & A & -2A \end{vmatrix} \times \begin{vmatrix} z_1 \\ z_2 \\ . \\ . \\ . \\ z_{n-1} \\ z_n \end{vmatrix} = - \begin{vmatrix} F_{01} \\ F_{02} \\ . \\ . \\ . \\ F_{0n-1} \\ F_{0n} \end{vmatrix} \qquad (5.9)$$

where $\dfrac{H_0}{a} = A$

5.3.2. Equations for cables in load condition

After loading the cable with a complementary loading ΔFi in equilibrium condition (5.1), the node i takes the form of

$$H\left(\frac{z_{i-1} - z_i}{a_{i-1}} + \frac{z_{i+1} - z_i}{a_i} + \frac{w_{i-1} - w_i}{a_{i-1}} + \frac{w_{i+1} - w_i}{a_i} \right) + F_i = 0 \qquad (5.10)$$

where

w_{i-1}, w_i, w_{i+1} – vertical deformation of corresponding nodes,
H – the force of the cable from the total load,
$F_i = F_{0i} + \Delta F_i$ – the whole concentrated load in node i.

From the expression (5.10), the node's vertical deformation of the node can be derived

$$w_i = \frac{1}{1 + \dfrac{a_i}{a_{i-1}}} \left[w_{i-1} \frac{a_i}{a_{i-1}} + w_{i+1} + \frac{a_i}{a_{i-1}} \left(z_{i-1} - z_i \right) + \left(z_{i+1} - z_i \right) + \frac{F_i a_i}{H} \right]. \qquad (5.11)$$

In the given equation, the unknowns are w_i and H. Thus, to provide equations for all nodal points, there is a need for a complementary equation to determine H.
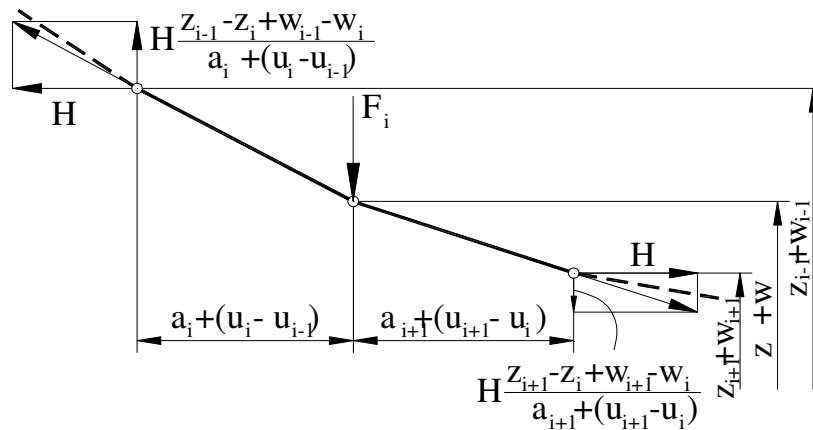
Figure 5.2 A cable section under the action of additional vertical loads [6]
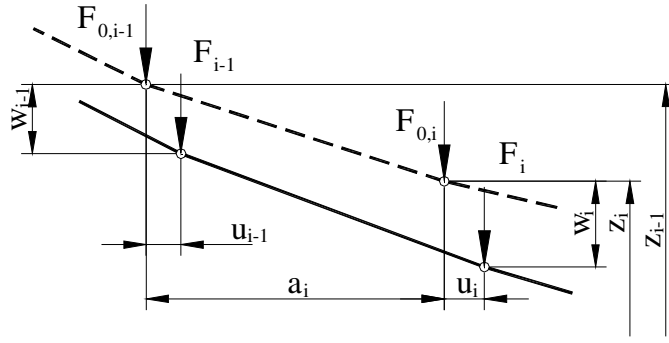
Figure 5.3 Displacements of the end nodes of a cable section [6]

The needed equation can be derived when viewing the elongation of the cable. The elongation of segment of the cable, as represented through the deformations of the nodal points, can be described as follows:

$$\varepsilon_i = \frac{1}{1+\left(\dfrac{z_{i+1}-z_i}{a_i}\right)^2}\left[\frac{u_{i+1}-u_i}{a_i}+\frac{w_{i+1}-w_i}{a_i}\left(\frac{z_{i+1}-z_i}{a_i}+\frac{w_{i+1}-w_i}{2a_i}\right)\right], \quad (5.12)$$

And the linear deformation caused by internal forces through the expression

$$\varepsilon_i = \frac{H-H_0}{EA}\sqrt{1+\left(\frac{z_{i+1}-z_i}{a_i}\right)^2}, \qquad (5.13)$$

where EA is the tension rigidity of the cable.

When equalling (5.12) and (5.13) we get the following equilibrium condition from the elongation of the cable segment.

$$\frac{u_{i+1}-u_i}{a_i}=\frac{H-H_0}{EA}\left[1+\left(\frac{z_{i+1}-z_i}{a_i}\right)^2\right]^{1/2}-\frac{w_{i+1}-z_i}{a_i}\left(\frac{z_{i+1}-z_i}{a_i}+\frac{w_{i+1}-w_i}{2a_i}\right).(5.14)$$

To eliminate horizontal displacements of single nodal points u_i, the expressions of single segments can be added up (5.14), and after the replacement

$$\sum_{i=0}^{n}\left(u_{i+1}-u_i\right)=u_{n+1}-u_1 \qquad (5.15)$$

the expression (5.15) can be presented as

$$\frac{H-H_0}{EA}\left\{\sum_{i=1}^{n}a_i\left[1+\left(\frac{z_{i+1}-z_i}{a_i}\right)^2\right]^{\frac{3}{2}}-\frac{EA}{H-H_0}\left(u_{n+1}-u_1\right)\right\}=$$

$$=\sum_{i=1}^{n}\left(w_{i+1}-w_i\right)\left(\frac{z_{i+1}-z_i}{a_i}+\frac{w_{i+1}-w_i}{2a_i}\right) \qquad (5.16)$$

where u_{n+1} and u_1 are horizontal displacements of the support nodes of the cables.

The resulting system is nonlinear equation system, which provides us all the unknowns sought for. It appears that the cable's internal force H must be determined within the range $H_0 < H < H_1$ where H_1 is the cable's internal force

47

found by help of Equations (5.5)...(5.9), using the total load F_i as the node point load. This makes it possible to simplify the nonlinear system, which otherwise converges with difficulty. Namely, the expression (5.10) can be presented as

$$\frac{H}{a_{i-1}}z_{i-1} - \frac{H}{a_{i-1}}z_i + \frac{H}{a_i}z_{i+1} - \frac{H}{a_i}z_i + \frac{H}{a_{i-1}}w_{i-1} - \frac{H}{a_{i-1}}w_i + \frac{H}{a_i}w_{i+1} - \frac{H}{a_i}w_i + F_i = 0\ (5.17)$$

Re-grouping the expression (4.17) and substituting $\dfrac{H_0}{a_{i-1}} = A$ and $\dfrac{H_0}{a_i} = B$, and

$$\frac{H}{a_{i-1}}z_{i-1} - \frac{H}{a_{i-1}}z_i + \frac{H}{a_i}z_{i+1} - \frac{H}{a_i}z_i + F_i = -C \quad \text{we can present the expression}$$

analogous to the expression (5.8) in matrix form:

$$
\begin{vmatrix}
-(A_1+B_1) & B_1 & 0.\ 0 & 0 & 0 \\
A_2 & -(A_2+B_2) & B_2.\ 0 & 0 & 0 \\
. & . & .\ .\ . & . & . \\
. & . & .\ .\ . & . & . \\
. & . & .\ .\ . & . & . \\
0 & 0 & 0\ A_{n-1}\ -(A_{n+1}+B_{n-1}) & B_{n-1} \\
0 & 0 & 0.\ 0 & A_n & -(A_n+B_n)
\end{vmatrix}
\times
\begin{vmatrix}
z_1 \\ z_2 \\ . \\ . \\ . \\ z_{n-1} \\ z_n
\end{vmatrix}
= -
\begin{vmatrix}
F_{01} \\ F_{02} \\ . \\ . \\ . \\ F_{0n-1} \\ F_{0n}
\end{vmatrix}
\quad (5.18)
$$

In case of equal distances between forces, the given equation system is symmetrical in relation to the diagonal:

$$
\begin{vmatrix}
-2A & A & 0 & .\ 0 & 0 & 0 \\
A & -2A & A & .\ 0 & 0 & 0 \\
. & . & . & .\ .\ . & . & . \\
. & . & . & .\ .\ . & . & . \\
. & . & . & .\ .\ . & . & . \\
0 & 0 & 0 & .\ A & -2A & A \\
0 & 0 & 0 & .\ 0 & A & -2A
\end{vmatrix}
\times
\begin{vmatrix}
z_1 \\ z_2 \\ . \\ . \\ . \\ z_{n-1} \\ z_n
\end{vmatrix}
= -
\begin{vmatrix}
F_{01} \\ F_{02} \\ . \\ . \\ . \\ F_{0n-1} \\ F_{0n}
\end{vmatrix}
\quad (5.19)
$$

To solve the system (5.18) we have to find H and the whole cable is calculated with the following algorithm:
1. We find the values of cable's force $H_A=H_0$ and $H_B=H_1$, where H_1, is calculated like H_0 (5.4) but the load for the cable is the total load from self-weight and traffic.
2. $H=0.5(H_A+H_B)$ is taken for the value of H.
3. The displacements of all nodal points are found from Equations (5.18) or (5.19).
4. Using the displacements found, the value of H is calculated from the expression (5.16), marking it with H_u. If the value is close enough to the basic value of H, it can be said that both the equations (5.18) and the expression (5.16) have been satisfied, and the displacements and internal forces found can be used as the solutions of the system.
5. If $H_u > H$, then the substitution $H_A = H$ is made, otherwise $H_B = H$ and the calculation is continued again from point 2.

5.3.3. Discrete model for girder-stiffened cables

If the cable is combined with a girder, then the whole load is not distributed to the cable only, but part of it will be carried by the girder. In the case of suspension bridges, the dead weight of all elements suspended on the cable during the assembly of the girder is fully distributed to the cable. After connecting of the suspended elements with each other, the remaining dead weight of the deck construction and the complementary varying load apply both to the girder and the cable. Therefore, to solve a system like this (Figure 5.4), the behaviour of the girder and cable must be examined.
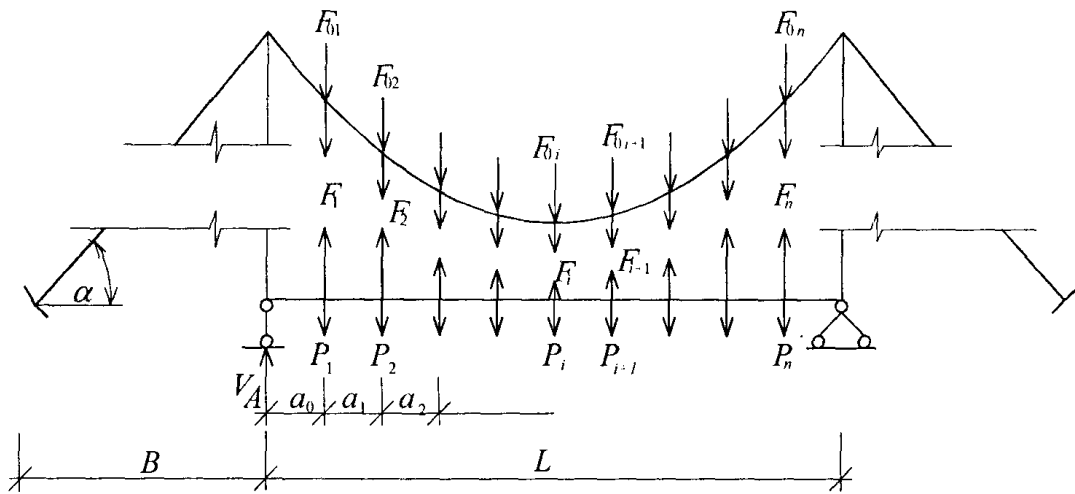
Figure 5.4 Distribution of forces in a cable-stayed bridge with straight anchor cables [12]

The initial load F_{0i} is fully distributed to the cable, and it is used to determine the pre-stress force H_0 for the cable, using the formulas (5.4) or (5.5). The complementary load placed on the girder is, by means of hangers, partially distributed to the cable, so that the displacements of the cable and the girder in the same section are equal or, taking into account the deformations of the hangers, differ by the elongation caused by the contact forces. Thus the girder can be examined as a structure, which is loaded with complementary loading, and contact forces opposite to it. The solution of the system is to find such contact forces, which provide for equal displacements of the girder and the cable.

There are various ways to solve the system described. The girder structure can either be solved analytically or by the use of a discrete element method (FEM). As much calculation is involved in the discrete element method, it is reasonable to compose a separate calculation program to be used of in this method. When using the finite element method to find a girder's displacements and internal forces, it must be built into the created packet, or to use automated data transfer between different packets. As the use of FEM requires of a complementary

equation system to be composed and numerous solutions, to speed up the calculations, it is reasonable, to derive the solution analytically, if possible. If a girder construction is applied, the universal equation of the girder's elastic curve can be used for the relation between the girder's internal forces and displacements.

$$E_b I_b w(x) = E_b I_b w_1 + E_b I_b \varphi_1 x - \sum_{j=1}^{m} M_j \frac{(x-a_j)^2}{2} \times H(x-a_j) +$$

$$+ \sum_{k=1}^{s} F_k \frac{(x-b_k)^3}{6} \times H(x-b_k) + \sum_{l=1}^{l} p_l \frac{(x-c_l)}{24} \times H(x-c_l) - \quad (5.20)$$

$$- \sum_{l=1}^{l} p_l \frac{(x-d_l)^4}{24} \times H(x-d_l)$$

where

$E_b I_b$ - girder's flexural rigidity

w_1 - vertical deformation of girder's node at the beginning
            of the girder

φ_1 - slope of the girder at its beginning

a_j, b_k, c_l, d_l - initial and final coordinates of girder's loading forces
            from the beginning of girder

$H(x)$ - Heaviside function

Through the expression (5.20), it is possible to find the girder's displacements from the converged moments M_j, converged forces F_k and uniformly distributed loadings p_l,. placed on the girder.

When pylons are vertical, the horizontal displacements of the cable's support points in the case of a straight anchor cable can be presented as follows:

$$u_1 = u_{n+1} = \frac{(H - H_0)B}{E_a A_a \cos^3 \alpha} \quad (5.21)$$

where

B - anchor cable span

α - cable's elevation angle

From the Equation (5.20), we can write the following expression for every hanger's fastening, describing the displacement of the corresponding fastening point:

$$w_m = w_1 + \varphi_1 x_m + \sum_{i=2}^{m-1} F \frac{(x_m - x_i)^3}{6 E_b I_b} + V_A \frac{x_m^3}{6 E_b I_b} + \sum_{k=1}^{s} F_k \frac{(x-b_k)^3}{6} \times H(x-b_k) +$$

$$+ \sum_{l=1}^{l} p_l \frac{(x-c_l)^4}{24} \times H(x-c_l) - \sum_{l=1}^{l} p_l \frac{(x-d_l)^4}{24} \times H(x-d_l) \quad (5.22)$$

where

F_i - contact force in the i-th hanger

V_a - vertical support reaction of the beginning of the girder

For the missing support reaction, concerning the equilibrium conditions of the moments related to the end-point of the girder, we can write:

$$\sum_{i=2}^{n} F_i(L-x) + V_a L + M_p = 0 \qquad (5.23)$$

where M_p is the moment of the load placed on the girder as related to the end of the girder.

The unknown quantity φ_1, can be derived from the elastic curve universal equation as related to the end support of the girder, knowing that the displacement at the end of the girder w(L) = 0. Thus there are equations to determine all the unknowns. To solve such a system in its entirety, the following algorithms can be used:

1) If we link the equations of the girder and the cable by the common contact forces in the hangers, the algorithm for the solution of the bridge can be presented as follows:

```
┌────────────────────────┐
│   The cable's initial   │
│  internal force Ho is   │
│  calculated, using the  │
│  expressions (5.4) or   │
│          (5.5)          │
└────────────────────────┘
             │
             ▼
┌────────────────────────┐
│ The initial contact forces are │
│ calculated, provided that the  │
│ cable has approx. 90% of the   │
│ bridge's total load            │
└────────────────────────┘
             │
             ▼
┌────────────────────────┐      ┌────────────────────────┐
│ Using the contact forces, by │ │ New contact forces      │
│ use of the discrete method,   │◄│ are calculated, using   │
│ the cable's nodal points'     │ │ the initial and the     │
│ displacements and the         │ │ found contact forces    │
│ cable's force H are found     │ └────────────────────────┘
└────────────────────────┘                  ▲
             │                               │
             ▼                               │
┌────────────────────────┐                  │
│ Using the found         │                  │
│ displacements, the elastic │               │
│ curve equations (5.22) and (5.23) │        │
│ are solved, new contact forces │          │
│ are found                │                 │
└────────────────────────┘                  │
             │                               │
             ▼                               │
         ╱╲                                  │
        ╱  ╲        no                       │
       ╱ If the contact ╲ ──────────────────┘
       ╲ forces found equal the ╱
        ╲ initial contact forces ╱
         ╲  ╱
          ╲╱
          │ yes
          ▼
┌────────────────────────┐
│ The internal force of the girder │
│ is calculated, the bridge is     │
│ solved                           │
└────────────────────────┘
```

Figure 5.5 Algorithm for girder stiffened suspension structure – linking equations in fastenings on stiffening girder [12]

If the joint displacements in the fastening nodes of the hangers are to be used solve to the equations of the cable and the girder by simultaneous, the solution algorithm is as follows:

```
┌─────────────────────────────┐
│   The initial internal force of │
│   the cable Ho is calculated,   │
│  using the expressions(5.4)or   │
│             (5.5)               │
└─────────────────────────────┘
              │
              ▼
┌─────────────────────────────┐
│  The initial contact forces are │
│  calculated, provided that the  │
│   cable has approx. 90% of the  │
│       bridge's total load       │
└─────────────────────────────┘
              │
              ▼
┌─────────────────────────────┐
│  Using the contact forces, the  │
│  displacements of the cable's   │
│  nodal points are found by the  │
│        discrete method          │
└─────────────────────────────┘
              │
              ▼
┌─────────────────────────────┐        ┌──────────────────────────┐
│  Using the contact forces and the│     │   New displacements of    │
│ girder's loadings, the elastic curve│   │   the average of the      │
│   equations  (5.22) and the      │◄────│  displacements of the     │
│  displacements of the hangers'   │     │  cable and the girder,    │
│ fastening points  (5.23) are solved│   │   and, through the        │
└─────────────────────────────┘        │  displacements, new       │
              │                          │  contact forces and the   │
              ▼                          │  cable's internal force   │
         ╱ If the girder ╲               │   H are calculated        │
        ╱ displacements found╲           └──────────────────────────┘
       ╱ equal the corresponding╲   no              ▲
       ╲ displacements of the   ╱──────────────────┘
        ╲      cable          ╱
         ╲                  ╱
              │ yes
              ▼
┌─────────────────────────────┐
│  The internal forces of the girder│
│  are calculated, the bridge is   │
│           solved                 │
└─────────────────────────────┘
```

Figure 5.6 Algorithm for girder stiffened suspension structure – linking equations in fastenings on hangers [12]

Both algorithms require the monitoring of the converging process and, if needed, its manual correction, because a minor change of the cable's internal forces brings about major changes of displacements in the system, and the system becomes unstable while being solved, and instead of converging, it starts to oscillate between some unreal solutions, or is dispersed.

It became evident that it is reasonable to converge all linearly interdependent components into a uniform linear equation system, which thereafter will be dependent on the cable's internal force H. Thus, the solution is reduced to the search of such H, in the case of which, when placing the displacements calculated from the linear equation system into the expression linking the elongation of the cable and the displacements (5.16) and the H found in its solution equals the H used for compiling the linear equation system. As an algorithm, such a system could be described as follows:
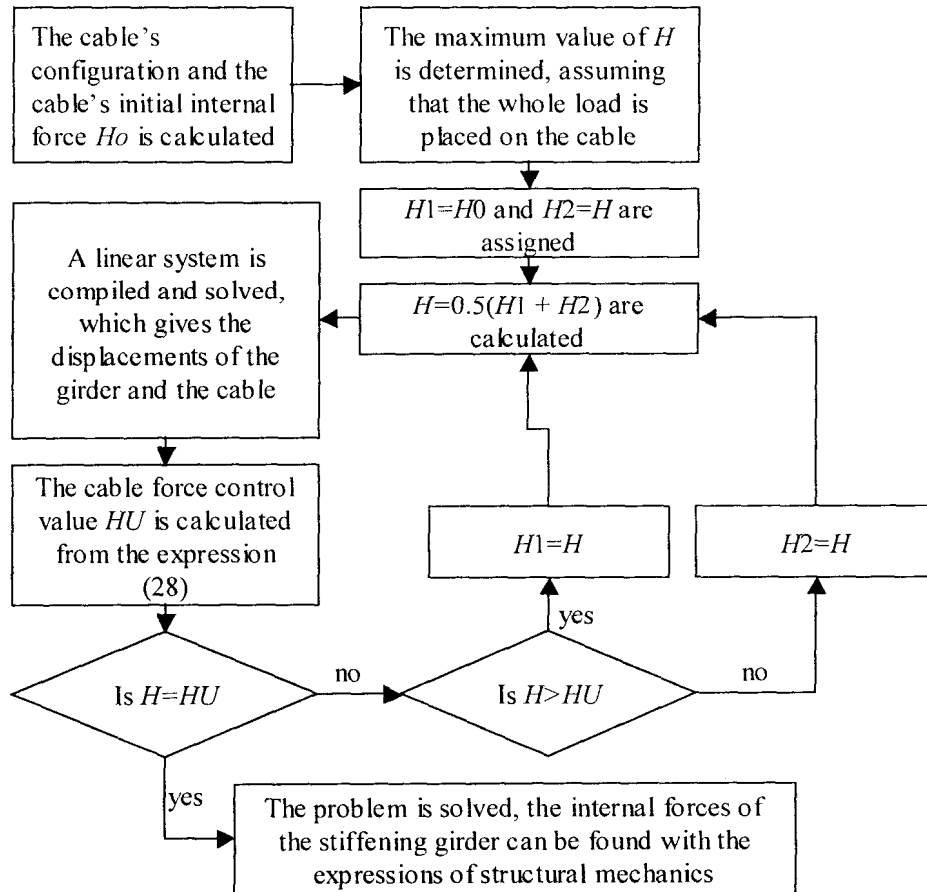
Figure 5.7 Algorithm for controlling the interactive process [12]

The matrix of the linear equation system of the corresponding system can be presented as follows:

$$
\begin{vmatrix}
A_{1,1} & A_{1,2} & 0 & \ldots & 0 & 0 & 0 & 0 & 0 & \ldots & 0 & 0 & 0 & 0 \\
A_{2,1} & A_{2,2} & A_{2,3} & \ldots & 0 & 0 & 0 & 0 & 0 & \ldots & 0 & 0 & 0 & 0 \\
0 & A_{3,2} & A_{3,3} & \ldots & 0 & 0 & 0 & 0 & 0 & \ldots & 0 & 0 & 0 & 0 \\
\ldots & \ldots & \ldots & \ldots & \ldots & \ldots & \ldots & \ldots & \ldots & \ldots & \ldots & \ldots & \ldots & \ldots \\
0 & 0 & 0 & \ldots & A_{n-1,n-1} & A_{n-1,n} & 0 & 0 & 0 & \ldots & 0 & 0 & 0 & 0 \\
0 & 0 & 0 & \ldots & A_{n,n-1} & A_{n,n} & 0 & 0 & 0 & \ldots & 0 & 0 & 0 & 0 \\
-1 & 0 & 0 & \ldots & 0 & 0 & B_{1,1} & B_{1,2} & B_{1,3} & \ldots & B_{1,n-1} & B_{1,n} & B_{1,n+1} & B_{1,n+2} \\
0 & -1 & 0 & \ldots & 0 & 0 & B_{2,1} & B_{2,2} & B_{2,3} & \ldots & B_{2,n-1} & B_{2,n} & B_{2,n+1} & B_{2,n+2} \\
0 & 0 & -1 & \ldots & 0 & 0 & B_{3,1} & B_{3,2} & B_{3,3} & \ldots & B_{3,n-1} & B_{3,n} & B_{3,n+1} & B_{3,n+2} \\
\ldots & \ldots & \ldots & \ldots & \ldots & \ldots & \ldots & \ldots & \ldots & \ldots & \ldots & \ldots & \ldots & \ldots \\
0 & 0 & 0 & \ldots & -1 & 0 & B_{n-1,1} & B_{n-1,2} & B_{n+1,3} & \ldots & B_{n-1,n-1} & B_{n-1,n} & B_{n-1,n+1} & B_{n-1,n+2} \\
0 & 0 & 0 & \ldots & 0 & -1 & B_{n,1} & B_{n,2} & B_{n+1,3} & \ldots & B_{n,n-1} & B_{n,n} & B_{n,n+1} & B_{n,n+2} \\
0 & 0 & 0 & \ldots & 0 & 0 & B_{n+1,1} & B_{n+1,2} & B_{n+1,3} & \ldots & B_{n+1,n-1} & B_{n+1,n} & B_{n+1,n+1} & B_{n+1,n+2} \\
0 & 0 & 0 & \ldots & 0 & 0 & D_1 & D_2 & D_3 & \ldots & D_{n-1} & D_n & 0 & D_{n+2}
\end{vmatrix}
\times
\begin{vmatrix}
w_1 \\ w_2 \\ w_3 \\ \ldots \\ w_{n-1} \\ w_n \\ F_1 \\ F_2 \\ F_3 \\ \ldots \\ F_{n-1} \\ F_n \\ \varphi_0 \\ V_A
\end{vmatrix}
=
\begin{vmatrix}
C_1 \\ C_2 \\ C_3 \\ \ldots \\ C_{n-1} \\ C_n \\ C_{F,1} \\ C_{F,2} \\ C_{F,3} \\ \ldots \\ C_{F,n-1} \\ C_{F,n} \\ C_{F,n+1} \\ C_D
\end{vmatrix}
\tag{5.24}
$$

The matrix components are the following: Further derived from the expression (5.10), we get

$$
H\left(\frac{a_i\left(w_{i-1}-w_i\right)}{a_i a_{i-1}}+\frac{a_{i-1}\left(w_{i+1}-w_i\right)}{a_i a_{i-1}}\right)=-H\left(\frac{a_i\left(z_{i-1}-z_i\right)}{a_i a_{i-1}}+\frac{a_{i-1}\left(z_{i+1}-z_i\right)}{a_i a_{i-1}}\right)-F
\tag{5.25}
$$

from here

$$
\begin{aligned}
H\left(a_i w_{i-1}-\left(a_{i-1}+a_i\right)w_i+a_{i-1}w_i\right)= \\
=-H\left(z_i w_{i-1}-\left(z_{i-1}+z_i\right)w_i+z_{i-1}w_i\right)-F_i a_{i-1}a_i
\end{aligned}
\tag{5.26}
$$

Thus, the matrix components $A_{i,j}$ and free term C_i can be expressed as follows:

$$
\begin{aligned}
&A_{i,i-1}=a_i H; \quad A_{i,i}=H\left(a_{i-1}+a_i\right); \quad A_{i,i+1}=a_{i-1}H; \\
&C_i=-H\left(z_i w_{i-1}-\left(z_{i-1}+z_i\right)w_i+z_{i-1}w_i\right)-F_i a_{i-1}a_i
\end{aligned}
\tag{5.27}
$$

The coefficients $B_{i,j}$ and $C_{F,i}$ have been derived from the universal equation of girder's elastic curve (5.22) and can be presented as follows:

If $i > j$ and $l \le i \le n$, then $B_{i,j}=\dfrac{\left(x_i-x_j\right)^3}{6E_B I_B}$, otherwise $B_{i,j}=0$.

$$
B_{i,n+1}=x_i; \quad B_{i,n+2}=\frac{x^3}{6EI}
\tag{5.28}
$$

The free term $C_{F,i}$ depends on the specific load situation of the bridge, and contains all these coefficients of the universal equation of the elastic curve, which do not contain the sought deformations and internal forces.

$$
\begin{aligned}
C_{F,i}=\sum_{k=1}^{s}F_k\frac{\left(x-b_k\right)^3}{6}\times H\left(x-b_k\right)+\sum_{l=1}^{t}p_l\frac{\left(x-c_l\right)^4}{24}\times H\left(x-c_l\right)- \\
-\sum_{l=1}^{t}p_l\frac{\left(x-d\right)^4}{24}\times H\left(x-d_l\right)
\end{aligned}
\tag{5.29}
$$

In the case of a bridge loaded with uniform loading p, the free term is in the following form:

$$C_{F,i} = \frac{px_i^4}{24E_B I_B} \qquad (5.30)$$

The coefficients of the last row of the matrix are derived from the equilibrium condition of the moments as related to the bridge's support B, and are presented as follows:

$$D_i = (l - x); D_{n+2} = l; \qquad (5.31)$$

And the free term depends on the loads placed on the bridge; in the case of a uniformly loaded bridge the term is

$$C_D = \frac{pl^2}{2} \qquad (5.32)$$

5.3.4. Combined suspension-cable-stayed systems

The calculation of combined systems can be divided into two groups. In the first case, the bridge is constructed as a cable-stayed bridge, because this simplifies the assembly, and after the installation of the hanger, the cables are dismantled. In such a situation, the bridge's dead weight must be calculated similarly to that of a cable-stayed bridge, and afterwards separately as a suspension bridge. When calculating a suspension bridge, the cable's initial internal force can no longer be found from the total dead weight of the cable and the stiffening girder, but only from the cable's dead weight, because after the dismantling of the cables, the stiffening girder, mounted as a cable-stayed bridge, does not load the cable freely any more, but is engaged together with it. This causes a difference in specifying the loads, as compared with the calculation of ordinary suspension bridge, because the girder's dead weight must now be included in the complementary weight, however other calculation principles remain. When receiving the traffic load, a bridge like this behaves analogously with a traditionally built suspension bridge of the same kind, but while building the bridge, during the assembly of the cable-stayed bridge, a bridge camber must be provided, which would balance the later deformations upon the removal of the cables.

In the other case, the cables installed during the assembly are maintained, and they will function as complementary stiffening elements. A construction working like this cannot be examined as a suspension or a cable-stayed bridge, but as a cooperation of different kinds of structures functioning in parallel.

5.3.5. The covered calculation model and basic equations

Examinig the combined system situation, where the stay cables are kept in place after the cable assembly, the discrete approach to the problem provides various solutions. First, the solution process depends on how the suspension cable is engaged with the cable-stayed bridge. If a complementary suspension cable is mounted to the existing cable-stayed bridge, then the behavior of the anchor cables of the cable-stayed bridge and of the anchor cables of the suspension

bridge must be differentiated during the calculations, and the combination action of them both must be considered while calculating the displacements of the pylon. The situation where the cable is mounted between the pylons and the anchor cable is already initially mounted with a greater cross-section, considering its later work with the cable, is easier to calculate. In such a case, the part considering the deformations of the anchor cables will be left out of the part describing the cable, the bridge can fully be considered as a cable-stayed bridge.

The general approach of all methods is similar to the discrete element methods of suspension bridges; but when with suspension bridges the hanger and the stiffening girder were taken as separate elements, then with the combined system, the hanger and the cable-stayed bridge can be examined separately. A system compiled like this can basically be solved in two ways.

First, two separate bridges can be solved parallel, seeking such a combination of internal forces of hangers, where the corresponding displacements of the cable-stayed bridge and the suspension cable would be equal. In addition to its dead weight and imposed load, the cable-stayed bridge will then also be loaded by the combination of the contact forces of the hangers.

In practice, such a method can be solved by using the cable discrete element method (5.1 ... 5.6), and, for the calculation of the cable-stayed bridge, either FEM or some other discrete method.

The calculation of the bridge can be divided into two stages. First, the initial condition of the bridge is solved, where the cable-stayed bridge is loaded with the stiffening girder's mounting-time dead weight, and the cable is loaded with the dead weights of the cable and the hangers. It is also possible to give the cable a complementary pre-stress by stressing the hangers, in such a case this must also be considered while determining the initial condition of the cablestayed bridge. The initial condition of the bridge without stressing the hangers is given in Figure 5.5.
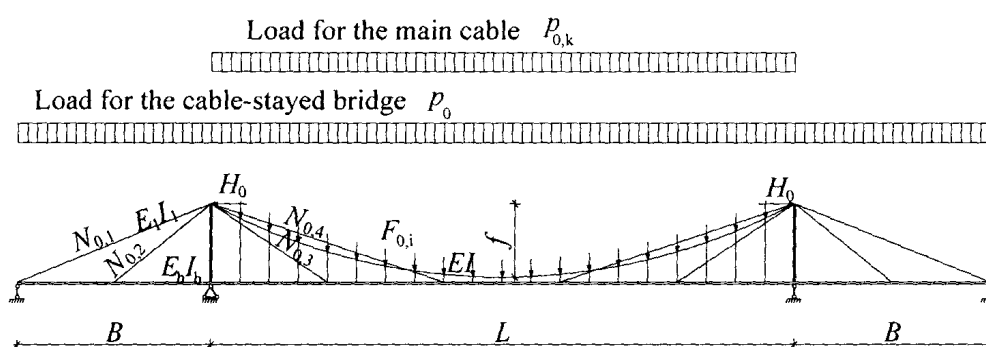
Figure 5.8 Initial condition of the combined system

In the second calculation situation, (Figure 5.8), in addition to the bridge's own dead weight, a complementary traffic load is also applied to the cable-stayed bridge, and the balancing influence of the cable in the fastening points of the hangers is described by the contact forces ΔF_i.

Load for the main cable $P_{0,k}$

Load for the cable-stayed bridge $p_0 + p_t$

H H

N_1 E_1 N_4 $F_i = \triangle F_i + F_{0,i}$ EI_b

N_2 $E_b I_b$ N_3

$\triangle F_i$

B L B
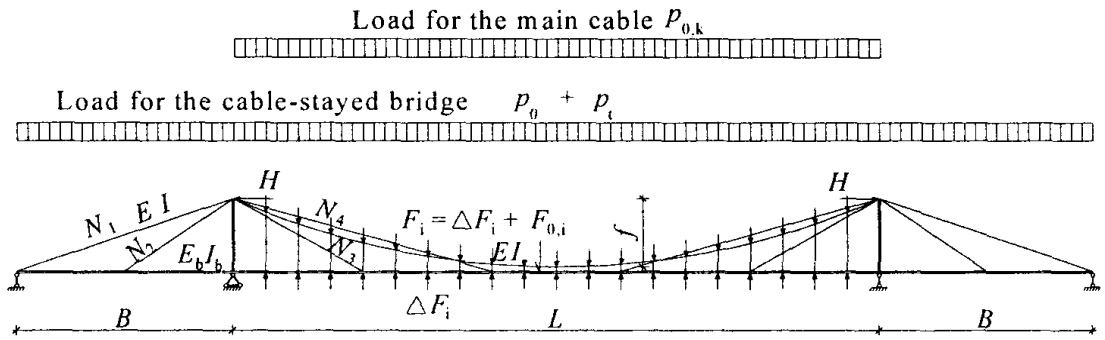
Figure 5.9 Bridge in the working state

Thus, the problem is solved, when we find such a combination of contact forces, where the corresponding displacements of the cable and the cable-stayed bridge are equal. The solution process is successive and can be presented as the following algorithm:

The cable-stayed bridge's initial internal forces in the stays, and the main cable's initial internal force *Ho* are calculated.

The initial contact forces are calculated, assuming that the cable has ~90% of the total load of the bridge.

Using the contact forces and loads on the bridge, the cable-stayed bridge is solved by FEM.

Using the contact forces, by way of discrete method, the displacements of the cable's nodal points are found.

The new displacements are calculated from the average of the displacements of the cable and the girder, and through the displacements, the new contact forces and the cable's internal force *H* are calculated.

If the displacements found equal the corresponding displacements of the cable

no

yes

The internal forces in the cable-stayed bridge are calculated, the bridge is solved.

Figure 5.10 Algorithm for solving hybrid cable stayed suspension bridge

Another way of solution is to use the formulas of the discrete element method of the cable-stayed bridge together with the discrete element method of the suspension bridge. The linear parts of both the cable-stayed and suspension bridges can be converged into a joint matrix, and analogously to the discrete

element method of cable-stayed bridges, the solution of the whole system depends on the finding of the sought cable force H. A problem like this is solved much faster than the first variant, because, in stead of a complex of nonlinear elements, this problem only has one non-linear component, the value of which influences the solution of the whole liner equation system, and the values of which can be sought within given limitations. The weakness of the method lies in the complexity of the matrix compiled, and the inevitable loss of calculation accuracy accompanying the solving of a great matrix [5.18].

5.4. Nonlinear finite element method [33,42]

5.4.1. General

5.4.2. Equations governing the problem

Let us consider a small sag cable (i.e. cable for which the angle between the tangent in any cable point and a straight line joining its ends is small) loaded with an arbitrary load in its plane. Let us consider an infinitesimal element in this cable – the described in the initial stage (first, assembly stage) by the load q0, temperature T0 and tension H0; the length of this element is equal to dso (Figure 5.11). Once the load is applied to the cable (second, final stage with the load q, temperature T and tension H), the length of an elementary cable section equals ds (Figure 5.12). Both stages together with loads in both planes (xy and xz) are presented also in Figure 2.
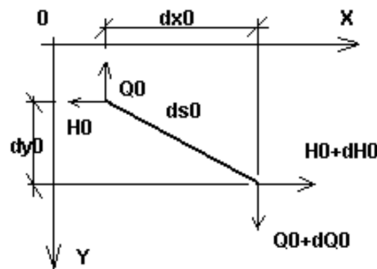
Figure 5.11 Infinitesimal element in the initial stage [33].
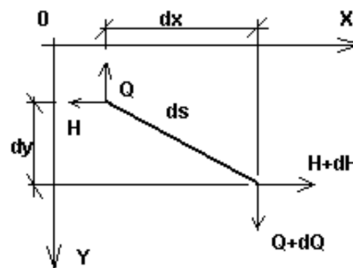
Figure 5.12 Infinitesimal element after applying the load [33].

Assuming a small cable sag value and taking into account that the total cable force must be tangent to the cable, one can assign the appropriate cable elongation as a function of static values only. Once the integration along the total cable length is done, the known formula for a cable with a small cable sag value will be obtained. The cable chord elongation value Δ can be derived from (5.33).
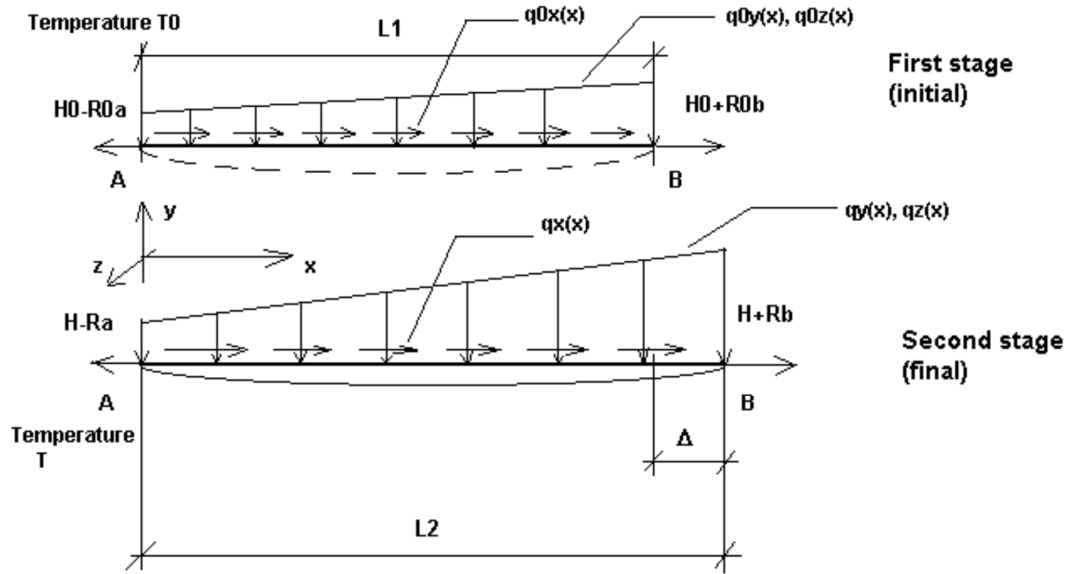
Figure 5.13 Integration along the total cable length

$$L2 - L1 = \Delta = \frac{Hl}{EA} - \frac{H0l}{EA} + \alpha \Delta Tl + \delta -$$

$$- \frac{1}{2} \left(\int_0^l \frac{[Qy(x)]^2 + [Qz(x)]^2}{[H + N(x)]^2} \, dx - \int_0^l \frac{\left[Q_y^0(x)\right]^2 + \left[Q_z^0(x)\right]^2}{[H0 + N0(x)]^2} \, dx \right), \qquad (5.33)$$

where:

A, B - beginning and end cable node,
EF   - cable tension rigidity (where: E - Young's modulus, F - cable cross-section area),
 a   - coefficient of thermal expansion,
l   - initial cable length (for an unloaded cable),
Δ   - distance change between the supports,
d   - initial, internal cable shortening/elongation (regulation),
ΔT   - change in temperature,
Q(x) - function of shear force as for the beam with pinned supports (according to indexes: in the Y- and Z-axis directions and for the initial and final stage, respectively) - schematic drawing below (Figure 5.14),
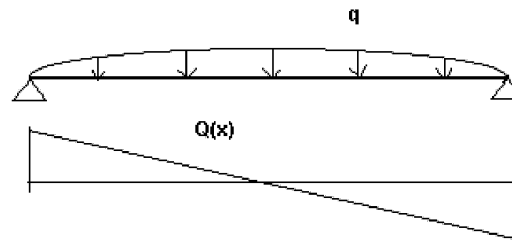
Figure 5.14 Function of shear force

N(x) - axial force function caused by the static load for a beam with fixed supports (during the initial or final stage) - schematic drawing below (Figure 5.15).
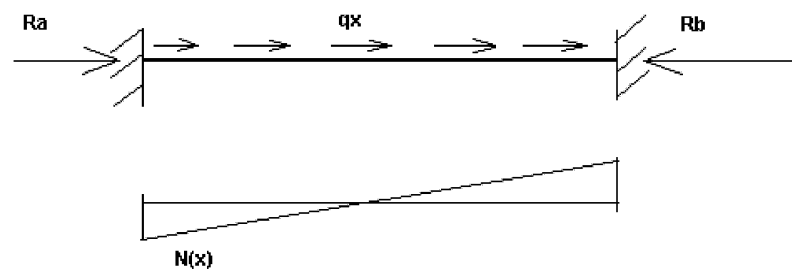
Figure 5.15 Function of axial force

5.4.3. Cables in Finite Element Method theory

Cable element theory in FEM is based on the general theory of cables with a small value of cable sag. According to this theory, cable rigidity is an implicit function of the following parameters: cable tension rigidity (EA), cable tension, cable support displacements, and transverse loading in both directions (p_y, p_z).

5.4.3.1. Cable equation for the assembly stage
Unloaded cable

$$q_{0x} = q_{0y} = q_{0z} = 0$$
$$H_0 = 0 \qquad\qquad (5.34)$$
$$T_0 = 0$$

For which the length is equal to:
$$L1 = 1$$
Cable anchored in the structure with all loads of the first (assembling) load case:

$$qx = qx^{(1)}$$
$$qy = qy^{(1)}$$
$$qz = qz^{(1)}$$
$$\Delta T = T^{(1)}$$

(5.35)

L2 – Distance between support nodes A and B of the deformed cable: L2= distance (A+U$_A$, B+U$_B$),

Where: U$_A$ – Displacement of the point A

U$_B$ – Displacement of the point B

Various situations for the first assembling load case are possible:

Force H is known (controlled)

$$H = \begin{cases} \sigma Ax \\ H \end{cases}$$

(5.36)

From the equation (5.33):

$$\Delta = \frac{Hl}{EA} + \alpha \Delta T + \delta - \int_0^1 \frac{Q_y^2(x) + Q_z^2(x)}{[H + N(x)]^2} dx$$

(5.37)

L value is the distance between the beginning and end node of the cable. From the equation (5.37) one can assign the initial cable elongation δ essential for obtaining the required force H:

$$\delta = \Delta - \frac{Hl}{EA} + \alpha \Delta T + \int_0^1 \frac{Q_y^2(x) + Q_z^2(x)}{[H + N(x)]^2} dx$$

(5.38)

Tension force H is unknown, then:

$$L2 = length\left(A + U_A^{(1)}, B + U_B^{(1)}\right)$$

(5.39)

Then, solving the equation according to the force H

$$L2 - L1 = \frac{Hl}{EA} + \alpha \Delta T + \delta - \int_0^1 \frac{Q_y^2 + Q_z^2}{[N(x) + H]^2} dx$$

(5.40)

And iterating through the system of equations, the final value of the assembling force is found.

It is equal to:

$$N(x) = \sqrt{[H + N(x)]^2 + Q_y^2 + Q_z^2}$$

(5.41)

If no nodal displacements are considered that is,

$$L2 = length(A, B)$$

(5.42)

Solving the equation (5.40) the initial value of the force required for the cable anchorage between supports is found.

5.4.3.2. Load cases after anchorage

After completing the structure analysis, results for cable elements are similar to those obtained for bar elements; however, some differences remain. The differences include:

- No shearing forces and moments can be obtained for cable elements,
- For cable elements either the simplified deformation (assigned as for the truss bar) or the exact deformation (described by the differential equation of the sag line) can be obtained
- Additional results for cable elements (as a result of the assembly stage):

Axial force (tensile) is calculated from the formula:

$$N = \sqrt{FX^2 + FY^2 + FZ^2} \tag{5.43}$$

Where:

N – force applied along the cable tangent

FX, FY, FZ – N force components projected on directions of successive axes of the local coordinates system

5.4.3.3. Cable equation during the cable's work in the structure

When an arbitrary case (i) is defined after the first assembling case, cable behaviour is obtained by solving the equation (5.33). Iteration of such an equation is run according to the following assumptions:

$$
\begin{aligned}
&H0 = H^{(1)} \\
&q0 = q^{(1)} \\
&\Delta T = T^{(i)} - T^{(1)} \\
&L1 = \text{length}\left(A + U_A^{(1)}, B + U_B^{(1)}\right) \\
&L2 = \text{length}\left(A + U_A^{(i)}, B + U_B^{(i)}\right) \\
&q = q^{(i)} + q^1
\end{aligned}
\tag{5.44}
$$

q – load from the first load case is automatically added to the load in the (i) case

Tension force H is treated as an unknown quantity.

5.4.4. Bar elements in the non-linear analysis

5.4.4.1. Preliminary remarks and assumptions

The following assumptions have been adopted for bar (beam) elements:

- Uniform formulation
- Uniform element allowing for material and/or geometrical non-linearity
- Standard displacement degrees of freedom at 2 extreme nodes

$$d = (u, \varphi) = \left[u_x, u_y, u_z, \varphi_x, \varphi_y, \varphi_z\right]^T \tag{5.45}$$

- There are 2 levels of geometrical non-linearity available: non-linearity (second order theory), and P-DELTA which is the most accurate theory possible with large displacements and rotations; this is an incremental approach with a geometry update.

- Assuming small displacements and absence of physical non-linearity for the limit, the results are identical as for standard linear elements
- Shear and torsion states are treated as linearly elastic and have to be uncoupled from axial forces and bending moments on the cross section level.
- All types of element loads are allowable (identically as for standard elements). However, it is assumed that nodal forces acting on a structure are determined at the beginning of the process. The changes in the transfer of element loads onto nodes resulting from geometrical or material non-linearity are ignored.

5.4.5. Geometry, sign convention for forces, displacements, stresses and strains
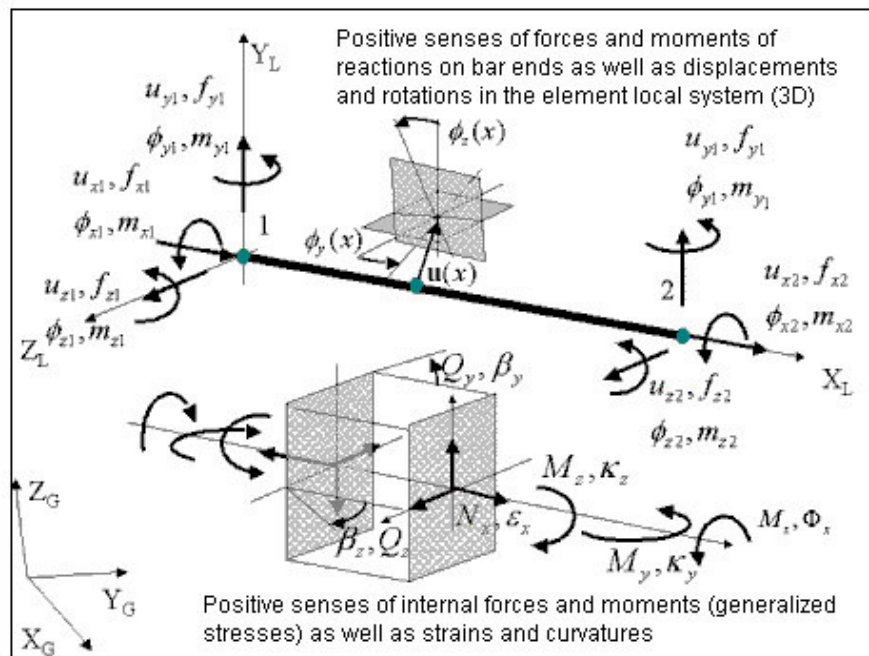
Figure 5.16 Geometry, sign convention for forces, displacements, stresses and strains

5.4.5.1. Basic kinematic relationships
In the element local system and in the geometrically linear range, the generalized strains E on the cross section level are as follows (symbol $(\bullet)_{,x}$ indicates calculation of the differential along the direction of the bar axis):

$$E = \left(\varepsilon_{0x}, \kappa_y, k_z, \beta_y, \beta_z, \varphi\right)^T \qquad (5.46)$$

where:
Axial strain in the bar axis: $\qquad \varepsilon_{0x} = u_{,x}$

Curvatures:
$$K_y = \phi_{y'x}$$
$$K_z = -\phi_{z'x}$$

Average angles (strain):
$$\beta_y = v_{'x} - \phi_{z'}$$
$$\beta_y = w_{'x} - \phi_y$$

Unit torsion angle:
$$\varphi = \phi_{x'x}$$

5.4.5.2. Displacement approximation

When there is a possibility to consider shear influence and consistence of results obtained for the linear element, physical shape functions considering shear influence have been implemented.

2D bars:

$$u(x) = Nu; \; N = \begin{bmatrix} h_1 & 0 & 0 & h_2 & h_2 & 0 \\ 0 & h_3 & h_4 & 0 & 0 & h_6 \\ 0 & h_3 & h_4 & 0 & 0 & h_6 \\ h_1 & 0 & 0 & h_3 & h_3 & 0 \\ 0 & h_1 & h_8 & 0 & 0 & h_{10} \\ 0 & h_1 & h_8 & 0 & 0 & h_{10} \end{bmatrix} \tag{5.47}$$

Table 5.1 Shape functions and their derivatives are expressed by the formulas

i	h_i	$h_{i,x}$
1	$1-\zeta$	$-1/L$
2	ζ	$1/L$
3	$\dfrac{1}{L(1+2\kappa)}\left[6\zeta - 6\zeta^2\right]$	$\dfrac{1}{L^2(1+2\kappa)}\left[6 - 12\zeta\right]$
4	$\dfrac{1}{1+2\kappa}\left[(1+2\kappa) - 2(2+\kappa)\zeta + 3\zeta^2\right]$	$\dfrac{1}{1+2\kappa}\left[-2(2+\kappa) + 6\zeta\right]$
5	$\dfrac{1}{L(1+2\kappa)}\left[-6\zeta + 6\zeta^2\right]$	$\dfrac{1}{L^2(1+2\kappa)}\left[-6 + 12\zeta\right]$
6	$\dfrac{1}{(1+2\kappa)}\left[-2(1-\kappa)\zeta + 3\zeta^2\right]$	$\dfrac{1}{L(1+2\kappa)}\left[-2(1-\kappa) + 6\zeta\right]$
7	$\dfrac{1}{(1+2\kappa)}\left[(1+2\kappa)\right]$	$\dfrac{1}{L(1+2\kappa)}\left[-2\kappa - 6\zeta + 6\zeta^2\right]$
8	$\dfrac{1}{(1+2\kappa)}\left[-1(1+\kappa)\zeta + (2+\kappa)\zeta^2 - \zeta^3\right]$	$\dfrac{1}{(1+2\kappa)}\left[-1(1+\kappa) + 2(2+\kappa)\zeta - 3\zeta^2\right]$
9	$\dfrac{1}{(1+2\kappa)}\left[2\kappa\zeta + 3\zeta^2 - 2\zeta^3\right]$	$\dfrac{1}{L(1+2\kappa)}\left[2\kappa + 6\zeta - 6\zeta^2\right]$
10	$\dfrac{L}{(1+2\kappa)}\left[\kappa\zeta + (1-\kappa)\zeta^2 - \zeta^3\right]$	$\dfrac{1}{(1+2\kappa)}\left[\kappa + 2(1-\kappa)\zeta - 3\zeta^2\right]$

where:

$$\xi = x / L$$

$$\kappa = \left\{ \frac{6EI_z}{k_y GAL^2}, \frac{6EI_y}{k_z GAL^2} \right\} \text{ for planes XY and XZ, respectively.} \tag{5.48}$$

5.4.6. Kinematic relationships for the matrix notation

When considering the influence of imposed strains

$$E^0 = \left\{ \varepsilon_0^{\Delta t}, \kappa_y^{\Delta t}, \kappa_z^{\Delta t} \right\} \tag{5.49}$$

Increment of generalized (sectional) strains:

$$\Delta E = B_L \Delta u_{Loc} - \Delta E^0 \tag{5.50}$$

$$\Delta u_{Loc} = T \Delta u_{Glo} \tag{5.51}$$

$$\varepsilon = \begin{bmatrix} \varepsilon_{0x} \\ \kappa_z \\ \beta_y \end{bmatrix} = \begin{bmatrix} h_{1,x} & 0 & 0 & h_{2,x} & 0 & 0 \\ 0 & -h_{3,x} & -h_{4,x} & 0 & -h_{5,x} & -h_{6,x} \\ 0 & h_3 - h_{7,x} & -h_{8,x} & 0 & h_5 - h_{9,x} & -h_{10,x} \end{bmatrix} \cdot \begin{bmatrix} u_1 \\ u_2 \end{bmatrix} \tag{5.52}$$

where:

$$u = \{u_1, u_2\} = \{u_{x1}, u_{y1}, \phi z1, u_{x2}, u_{y2}, \phi_{z2}\}^T \tag{5.53}$$

5.4.6.1. Strains at a point (layer)

Given the generalized strains $\{\varepsilon_{0x}, \kappa_y, \kappa_x\}$ of a cross section, the ε_{xl} strain or its increment $\Delta\varepsilon_{xl}$ at any point of the cross section l - of the coordinates yl, zl, is calculated as

$$\varepsilon_{xl} = \varepsilon_{0x} + \kappa_z y_l \tag{5.54}$$

$$\varepsilon_{xl} = v_l^t E; v = \{1, z_1, y_1\}^T \tag{5.55}$$

finally, strain increment in the layer:

$$\Delta\varepsilon_{xl} = v_l^T \left(\Delta E - \Delta E^0 \right) = v_l^T \left(B\Delta u - \Delta E^0 \right) \tag{5.56}$$

5.4.6.2. Geometrical non-linearity

The following configurations are taken into consideration:
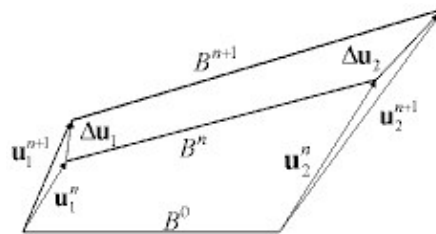
Figure 5.17 Explanation for configurations

B^0 - initial configuration

B^n - reference configuration (the last one for which equilibrium conditions are satisfied)
B^{n+1} - current configuration (iterated).

An entry point for the element formulation is the virtual work principle saved in the following form for displacement increments:

$$\int \tau_{ij}^n \delta \Delta \eta_{ij} dV + \int_V C_{ijkl} \Delta \varepsilon_{kl} \delta \Delta \varepsilon_{ij} dV = F^{n+1} - \int_V \tau_{ij}^n \delta \Delta e_{ij} dV, \forall \delta u \qquad (5.57)$$

where: $\Delta \varepsilon$ strain increment while moving B^n to B^{n+1}, Δe, $\Delta \eta$ constitute its parts, correspondingly: linear and non-linear with respect to the displacement increment Δu, whereas τ is a stress referring to the reference configuration and C_{ijkl} is a tensor of tangential elasticity modules.

5.4.6.3. Kinematic relations
Strain increments in the matrix notation:

$$\Delta E = \Delta e + \Delta \eta = B \Delta u_{Loc} + \frac{1}{2} g^T H_N g \qquad (5.58)$$

where:

$$g = \left\{ u,_x ; \upsilon,_x ; \omega,_x ; \phi_{x,x} ; \phi_{y,x} ; \phi_{z,x} \right\}^T \qquad (5.59)$$

then the displacement increment gradient $g = \Gamma \Delta u$

$$\Gamma = N,_x \qquad (5.60)$$

whereas

$$H_N = \begin{bmatrix} 0 & 0 & 0 \\ 0 & 1 & 0 \\ 0 & 0 & 0 \end{bmatrix} \qquad (5.61)$$

is a selection matrix.

5.4.6.4. Nodal force vector and element stiffness matrix

Algorithm on the element level

$$K_{Loc} = K_L + K_\sigma \qquad (5.62)$$

$$f^{n+1} = f_{ext}^{n+1} - \int B^T \sum\nolimits^{n+1} dx - K_\sigma^{n+1} u^{n+1} = f_{ext}^{n+1} - f_{int\,L}^{n+1} - g_{int\,NL}^{n+1} \qquad (5.63)$$

$$K_L = \int_0^L B^T DB dx \qquad (5.64)$$

$$K_s = \int_0^L \Gamma^T \left(NH_N \right) \Gamma dx \qquad (5.65)$$

The element geometry is not modified; the local-global transformation is performed with the use of initial transformation matrix ^0T

$$\Delta u_{Loc} = {}^0 T \Delta u_{Glo} \tag{5.66}$$

$$\Delta E = B \Delta u_{Loc} + \frac{1}{2} g^T H g - \Delta E^0 \tag{5.67}$$

$$\Sigma^{n+1} = \Sigma^{n+1}\left(\Sigma^n, \Delta E\right), \tag{5.68}$$

$$K_\sigma = K_\sigma\left(\Sigma^{n+1}\right), \tag{5.69}$$

$$f_{Loc}^{n+1} = f_{ext}^{n+1} - f_{int\,L}^{n+1} - f_{int\,NL}^{n+1} \tag{5.70}$$

$$f_{Glo} = {}^0 T^T f_{Loc} \tag{5.71}$$

$$K_{Loc} = K_L + K_\sigma \tag{5.72}$$

$$K_{Glo} = {}^0 T^T K_{Loc} {}^0 T \tag{5.73}$$

5.4.7. P-Delta option

It is a certain variant of bar description allowing for large displacements. The approach of the updated Lagrange description is applied here.
Nodal force vector and element stiffness matrix

$$K_{Loc} = K_L + K_\sigma \tag{5.74}$$

$$f^{n+1} = f_{ext}^{n+1} - \int B^T \Sigma^{n+1} dx = f_{ext}^{n+1} - f_{int}^{n+1} \tag{5.75}$$

$$K_L = \int_0^{L^o} B^T D B \, dx \tag{5.76}$$

$$K_s = \int_0^{L^o} \Gamma^T \left(\Sigma^{n+1}\right) \Gamma \, dx \tag{5.77}$$

$$\underline{\Sigma} = \begin{bmatrix} N & M_y & 0 \\ M_y & N & 0 \\ 0 & 0 & 0 \end{bmatrix} \tag{5.78}$$

One can also notice that in the cable equation (5.33), as opposed to traditional solutions applied to cable calculations, axial force can vary along the cable's length (in denominators of both integration functions in equation (5.33), the following functional components exist: $[H+N(x)]^2$ and $[H0+N0(x)]^2$). It allows for more accurate results.

5.4.8. Solving the system

Non-linear analysis consists of incremental application of loads. In calculations, loads are not considered at a time, but are gradually increased and solutions to successive equilibrium states are performed. Non-linear behaviour in current case of a structure results in a non-linear force–deformation relation in the whole structure (geometric non-linearity). Geometric non-linearity considers the following effects for the whole structure.
  – Non-linear analysis - takes account of the second-order effects, such as changing the stiffness of the element under the influence of the stress

state in the element. At the same time, this analysis considers generation of moments resulting from the action of vertical forces at the nodes displaced horizontally.

– P-delta analysis - takes account of the third-order effects, such as the additional lateral rigidity and stresses resulting from deformation. This effect considers additional forces arising in a deformed structure such as a beam with fixed supports on both ends, loaded by a vertical load, longitudinal forces arise and the deflection decreases.

Using geometric non-linearity takes the actual higher-order effects into consideration and often has effect on improving the convergence of the calculation process for a structure including non-linear elements. Incremental or arc-length methods solve a system of non-linear equations. In the incremental method, the right-hand load vector is divided into n equal increments. A consecutive load increment is applied to the structure once the state of equilibrium for the previous increment is achieved. The norm of unbalanced forces is specified for each step, allowing for monitoring of the structure force-deformation relations. The arc-length method of displacement steering should be applied when the incremental algorithms of solving equations by force steering are not convergent. An example of the non-linear process within the incremental method is shown in the Figure 5.18. Values used for non-linear calculations are displayed.
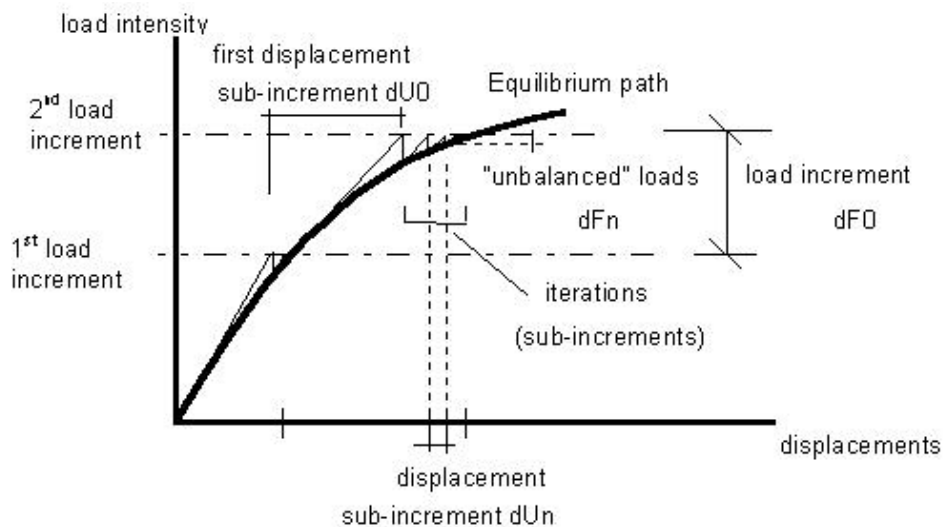
Figure 5.18 Example of the non-linear process

There are three available algorithms for solving a non-linear problem, set the following parameters of non-linear analysis.
For the Initial stress method:
– Matrix K not actualized after each subdivision
– Matrix K not actualized after each iteration
For the Modified Newton
– Matrix K not actualized after each subdivision

For the Modified Newton-Raphson method:
  – Matrix K actualized after each iteration
For Full Newton
  – Matrix K not actualized after each subdivision
Raphson method
  – Matrix K actualized after each iteration

The algorithm of the Broyden-Fletcher-Goldforb-Shanno (BFGS) procedure modifies the stiffness matrix during calculations. In certain cases, the use of the line search algorithm may improve the convergence of the method.

In general, the quickest way to get the solution of the problem is to apply the Initial Stress method, while the calculations take the longest time when the user decides to select Full Newton-Raphson method. However, the greatest probability of obtaining convergence of a method in the case of Full Newton-Raphson, while the probability is the smallest in the case of Initial Stress method.

The convergence of the process is checked and the iteration process is stopped once the state of equilibrium is achieved. Displacement increments dUn and unbalanced forces are essentially zero (sufficiently small in comparison with the tolerance parameters for both values). The iteration process is stopped in the case of divergence. Lack of convergence can be interpreted either as the numerical effect of structure overloads or as a result of numerical process instability (such as when the load is divided into a small number of intervals). In such cases, the number of load increments can be increased, which usually helps the process to converge.

Parameters which influence the course of non-linear calculations.
  – Load increment number is used when dividing a load into smaller segments. For complex structures where the impact of non-linear effects is considerable, calculations may not converge if the analysis for the value of a load is applied in one step. The number of load increments influences the number of calculation iterations. The greater the number of increments, the greater the probability for the calculations to reach the point of convergence.
  – Maximum iteration number in each load increment is used to control the calculation process during one load increment.
  – Allowable increment length reduction number (modification) defines how many times the number of load increments can be changed when calculations do not reach convergence (refer to the increment length reduction factor below).
  – Increment length reduction factor is used to modify the required number of load increments. This is the conditional option, used only when calculations do not reach convergence for the currently defined parameters. If convergence is not achieved, the size of load increment is reduced (depending on the value of the coefficient) and calculations continue. This is repeated until convergence is achieved or the iteration process exceeds the allowable number of step length reductions.

Parameters which influence the arc-length method parameters.
Load increment number

  – Maximum iteration number for one increment.
  – Maximum load factor λ_{max} - The maximum value of the load parameter.
  – Node number, degree of freedom - Specify the number of a node located on a structure roof and displacement direction, respectively.
  – Maximum displacement for selected degree of freedom D_{max} - The maximum value of a displacement at a selected node.

The Arc-length method is applied during non-linear pushover analysis. It is strongly recommended when non-linear structure attributes are defined in a structure model.

5.4.9. Practical remarks on calculations of cable structures

Practical consideration regarding calculations of cable structures are as follows:

1. Definition of initial tension forces in cables should be well thought-out. Values of tension forces or stresses specified in a cable definition indicate exactly the values required by the algorithm in the assembly load case within the appropriate cable (measured along its chord). This requirement provides for finding the necessary cable length. If tension forces implemented in an isostatic structure are not balanced, then the equilibrium cannot be reached.

It is often the case that the user defines the tension force of a cable smaller than the load (e.g. dead weight) acting on it; in such cases it is evident that no physical solution to this model exists. A similar problem concerns the static model presented in the drawing below.

The model presented may exist as a model of a whole structure or be part of a larger structure. If the definition of a cable assigns casual values of the tension forces of the assembly to cables nos. 1, 2 and 3, then most probably it will be impossible to fulfill the equilibrium conditions for the horizontal direction (the total of horizontal components of tension forces from all the three cables would have to be equal or close to zero). Therefore, the calculation process for this structure will not be convergent or the calculation errors will occur. Such errors are typical of abnormally large displacements and rotation angles of structure nodes (to fulfill the equilibrium conditions, abnormally large rotation angles are defined in the structure, which most often results in exceeding the domain of the functions: acos, asin or root).

Thus, in the initial stage of calculations it is more favourable to define cables by specifying the cable length instead of tension forces. Only after becoming familiar with approximate values of tension forces, the user may determine values of tension forces for reasonable values of cable length, keeping in mind that the equilibrium conditions should be fulfilled at least approximately in nodes similar to those in the model shown in the drawing above.

A similar situation takes place for collinear chains of cables to whom the same values of the tension force are ascribed; the analysis will not be convergent, since tension forces cannot be alike in all the cables due to the cable sag.
.
2. Cables show no bending stiffness; for collinear cable chains or cable nets it should be remembered that they have no stiffness in the perpendicular direction, if additionally, the third-order non-linear effects (P-delta), i.e. the effect of geometry (shape) modification on the structure stiffness, are not taken into account.

3. Since cable elements cause strong non-linearity of the system, in some cases the user should:
·   define a higher number of load increments (>10),
·   apply the "Full Newton-Raphson" algorithm (which means that the K stiffness matrix should be updated after each load increment and sub-increment).

However, the above parameters should not always be set. In some cases, when solution convergence is achieved even in one load increment, the simplest algorithm ("Initial Stress") can be used.

4. If cables are defined by specifying their length and loads are applied to a structure, and as a result, some cables will not work (will not carry any forces), then the analysis of a cable structure may reach no convergence. To avoid this, the self-weight load should be applied to all cables in the assembly load case. It reflects the actual situation, since real structures do not include cables which do not carry tension, there is always a slight tension resulting from the cable dead weight.
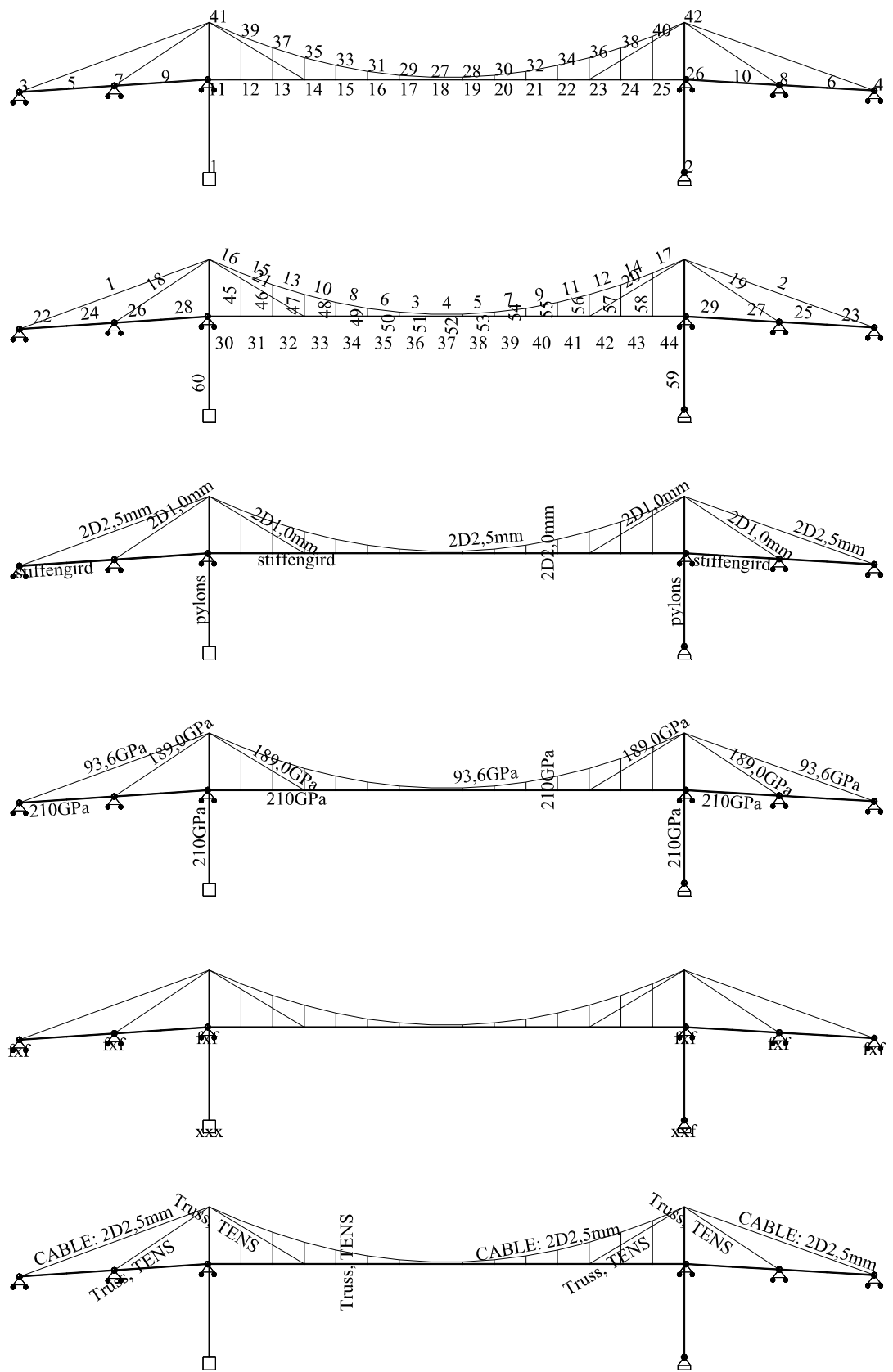
Figure 5.19 Main parameters of the FEM model.

6. Comparison of experimental results and static analysis

6.1. Construction stage

6.1.1. Vertical displacements

Figure 6.1 shows a comparison of vertical displacements for a construction stage. It corresponds exactly to a case when the stiffening girder is assembled as a whole and the structure starts working as a cable-stayed structure. It is not correct when the stiffening girder is assembled traditionally for a cable-stay bridge – starting from the pylons, installing details of the stiffening girder by adding cable-stays, but it provides also an estimation for cases when the stiffening girder is assembled step by step. Though the comparison enables us to verify analysis methods – we can use the chosen analysis methods also for a construction stage. Still, in the scale chosen it is complicated to model the installation of the stiffening girder.

In fact, theoretical and experimental results are in an acceptable compliance. In a maximum case, the difference is 17%. The overall tendency that experimental values are greater than the calculated ones is comprehensible. This effect can be explained in terms of the additional deformation of details.

Also, the effect of the deflection graph being unsymmetrical for a symmetrical load can be explained by an unequal deflection of details and unsymmetrical support conditions.

For horizontal displacements of anchor nodes, the coincidence is much better.
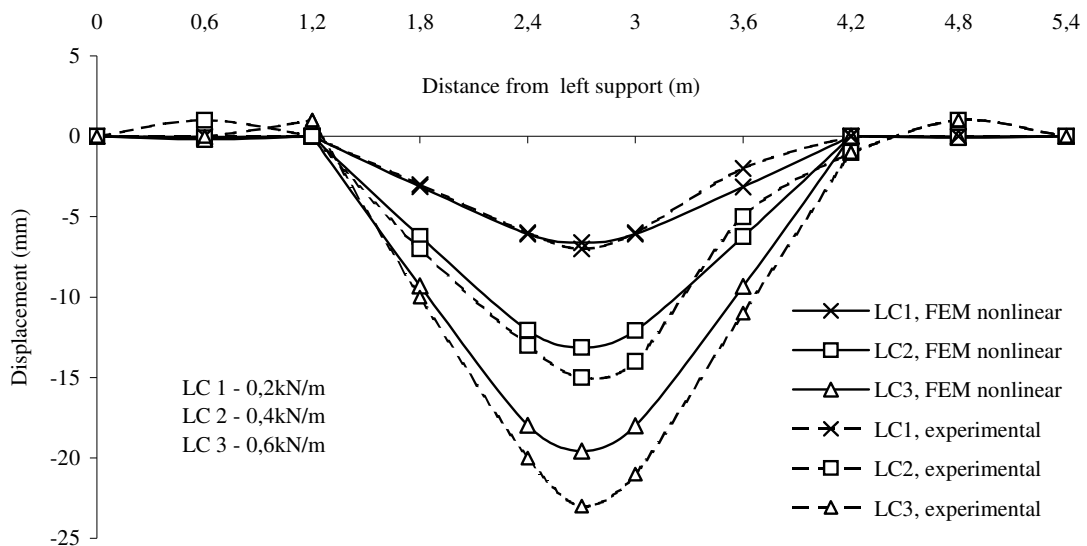
Figure 6.1 Comparison of vertical displacements for combined cable-stayed suspension bridge (under the action of dead weight).

6.1.2. Horizontal displacements of pylons

Figure 6.2 shows the horizontal displacements of pylons for the same construction stage and loadings.

As a result of the examination of horizontal displacements of the pylons, we may draw a conclusion that overall behaviour is in coincidence. However, in the current case, it must be pointed out that the method used for pylon measurements has marked disadvantages: first, the thread that was attached to the top of the pylon unfortunately had friction against the measurement scale which was situated at the support; second, although a minimum unit for scale was in the same calibre as the measured values, it caused remarkable occasional mistakes in testing. As shown in the graph, this trend was acceptable.
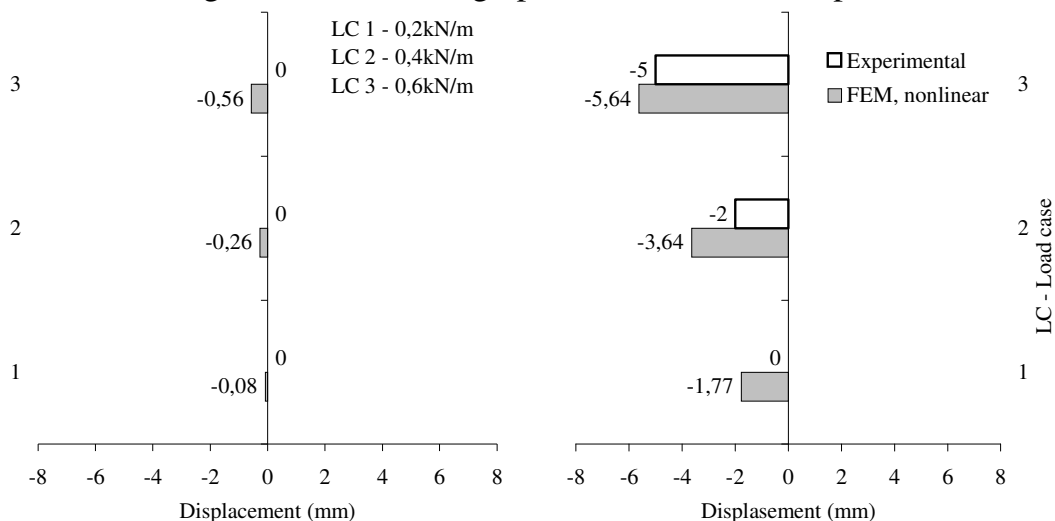
Figure 6.2 Comparison of horizontal displacements at the top of pylons for the combined cable-stayed suspension bridge (under the action of dead weight).

6.1.3. Horizontal displacements of anchors

Figure 6.3 presents the horizontal displacements of anchor nodes for the same construction stage. For anchor nodes the coincidence of comparison is much more fulfilling because of a better measuring solution. Still, the influence of node deformation is smaller than for the vertical displacements.
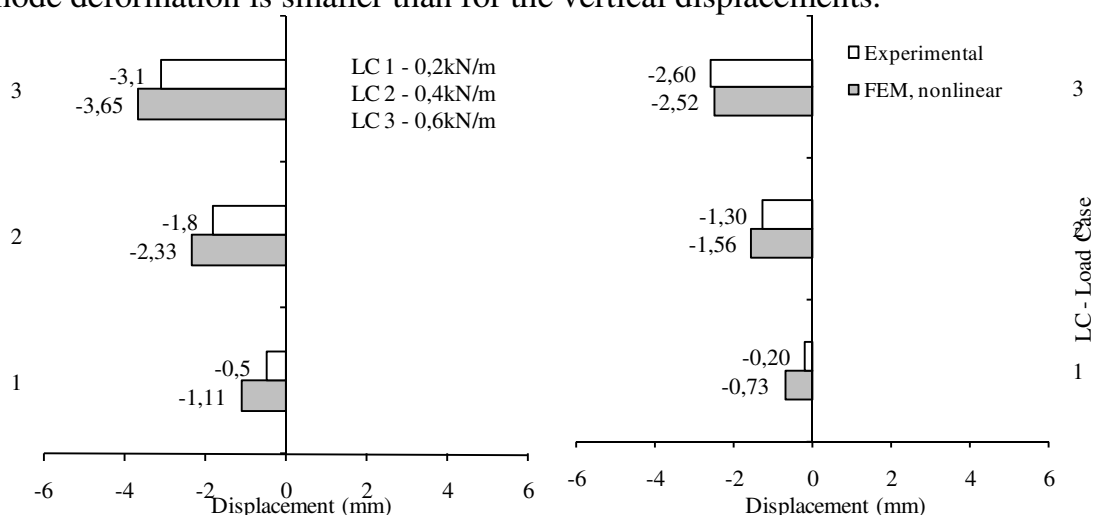
Figure 6.3 Comparison of horizontal displacements at anchor nodes for the combined cable-stayed suspension bridge (under the action of dead weight)

6.1.4. Final stage

6.1.5. Vertical displacements

Below experimental results and comparisons under the action of a uniformly distributed traffic load are presented. For the current case the stiffening girder is made of timber board. Further, a steel stiffening girder with correct stiffening and bending characteristics is used.

Only deflections from traffic loads are presented, some of the deformation and measuring errors will be assembled and we can see some improvement in compatibility. For greater values, the measuring error is relatively smaller than for smaller values.
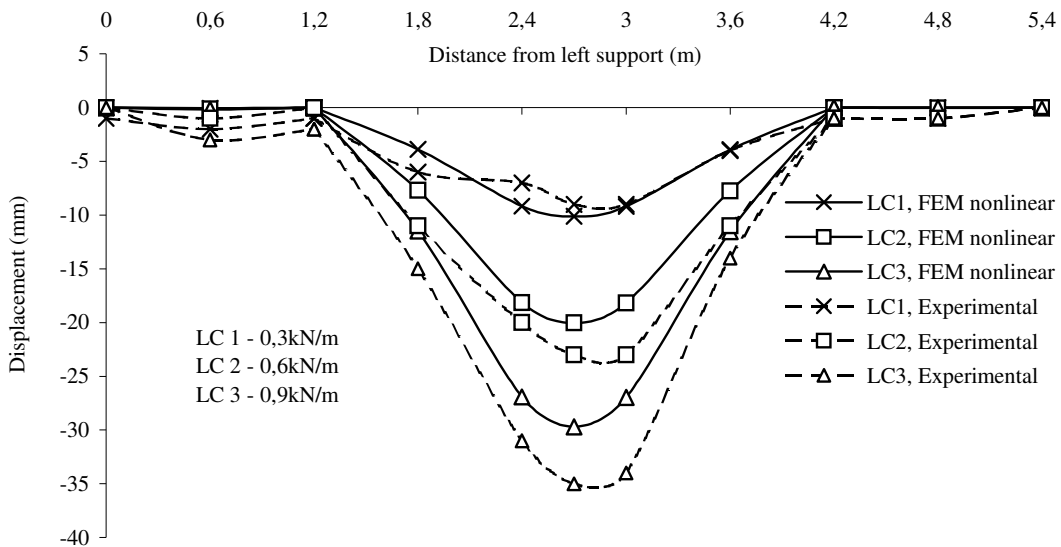
Figure 6.4 Comparison of vertical displacements for the combined cable-stayed suspension bridge (under the action of traffic load)

6.1.6. Horizontal displacements of anchors
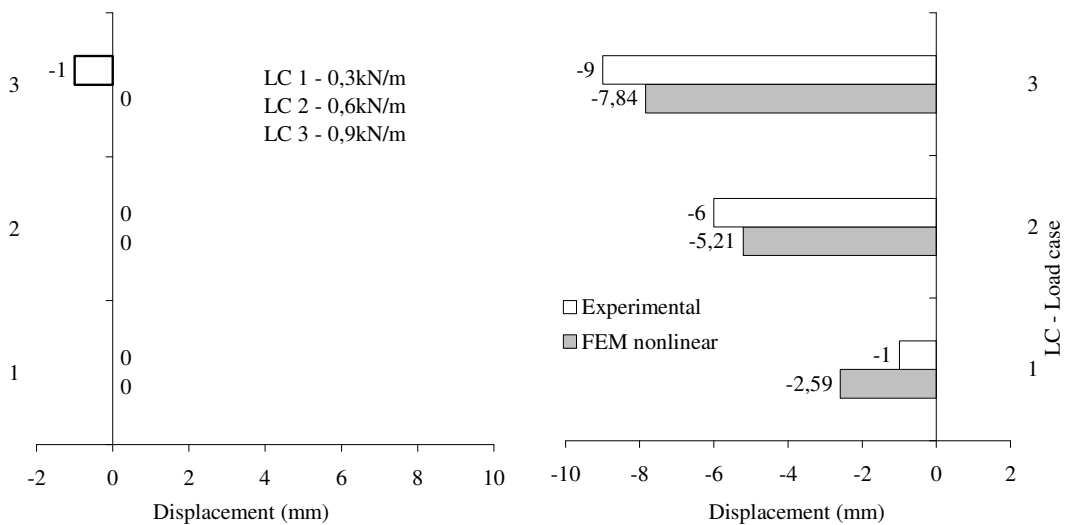
Figure 6.5 Comparison of horizontal displacements at the top of pylons for the combined cable-stayed suspension bridge (under the action of traffic load).

Figure 6.5 presents horizontal displacements at the top of pylons and Figure 6.6 shows those for anchor nodes. Overall estimations can be made similarly to vertical displacements – coincidence is very suitable for both displacement graphs. Only uniformly distributed load cases were tested. A model in which the timber stiffening girder did not comply with buckling characteristics was tested, as described above. Therefore, the stiffening girder was replaced with a steel stiffening girder in compliance to assume the goals established.
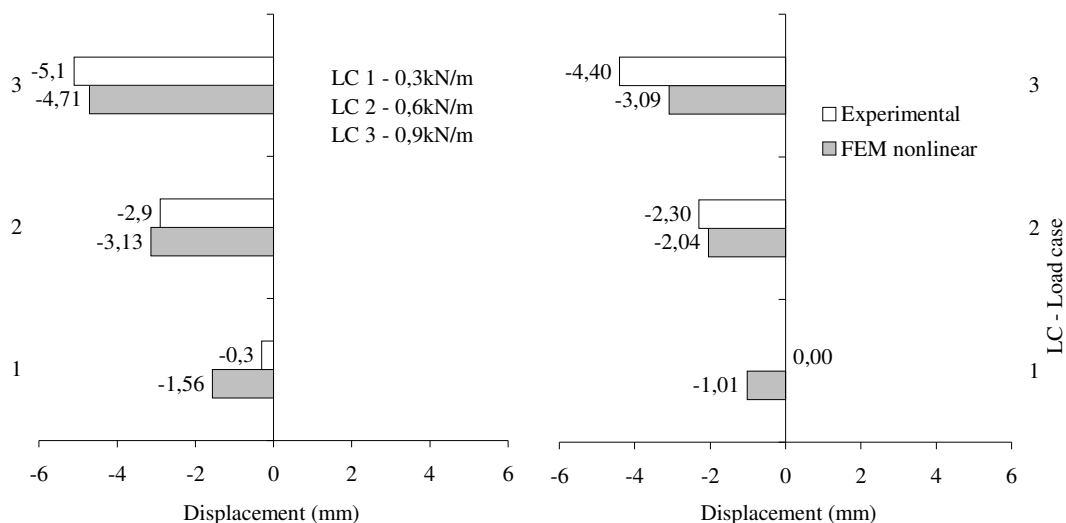
Figure 6.6. Comparison of horizontal displacements at anchor nodes for the combined cable-stayed suspension bridge (under the action of traffic-load)

6.1.7. Final stage – improved model

6.1.8. Vertical displacements

One of the main goals in the experimental investigation was to ensure the stability of the stiffening girder if the solution for the stiffening girder was changed. A timber board was changed to the symmetrically placed steel angles to model improved axial and bending stiffness. In advance, it should be mentioned that with a timber stiffening girder the modelling of some details was slightly better. Deformation of details was smaller or even missing. This effect can be explained by the fact that friction and local pressure works with some metal details compressed against timber. Both, one direction movement and back and forth movement in the details appears less observable. In the case of a timber board stiffening girder, no sign of buckling was noticed, even when the load values were greater than the design ones.

The model of the steel stiffening girder was in exact compliance with the initial structure – correct results for buckling effects.

In the improved model, uniform and half-span asymmetrical and narrow intensity load cases with different load values were studied. The influence of the tandem was not modelled in the experimental investigation. The influence of the tandem is examined in detail in Section 9.4.1.

Overall coincidence may be considered favourable, especially in uniformly distributed cases and cases which preceded the maximum load. Deformation of details extremely expressed in cases of maximum uniformly distributed loads when the difference between the experimental and the theoretical values is 15%. Also, this load causes a constant gap for some measuring points. It is well illustrated in Figure 6.15 where at the end of the experiment, vertical displacements without the traffic load were measured. We can see gapped measurements which are also unsymmetrical.

Cases of unsymmetrical load distribution with 1/5 of the span length intensively loaded result in an effect where part of the stiffening girder near the load is inclined to negative deformation. This effect is characteristic of the stiffening girder as a bended beam in the elastic ground, where the cable work is an elastic support. Also, in this case the effect of the backlash of details should be mentioned. However, taking into account that the difference is 5 ... 6%, we may be satisfied with the compatibility of the results.
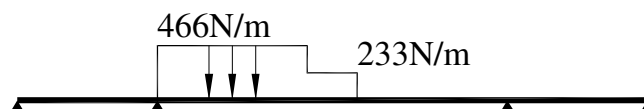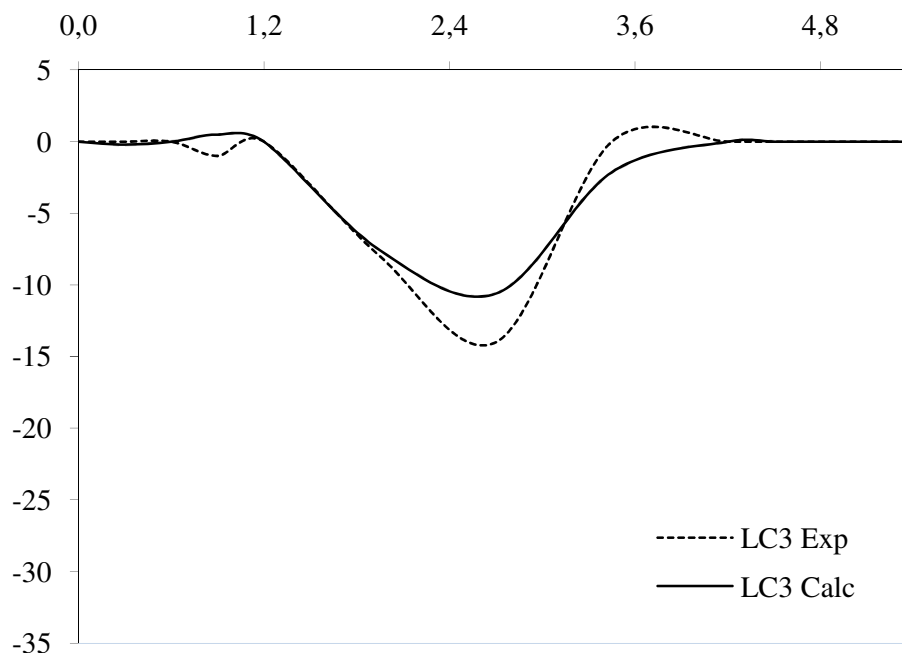
Figure 6.7 Vertical displacements LC-3.
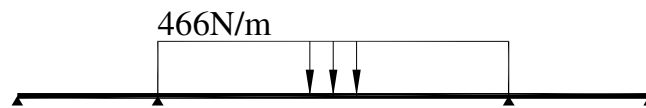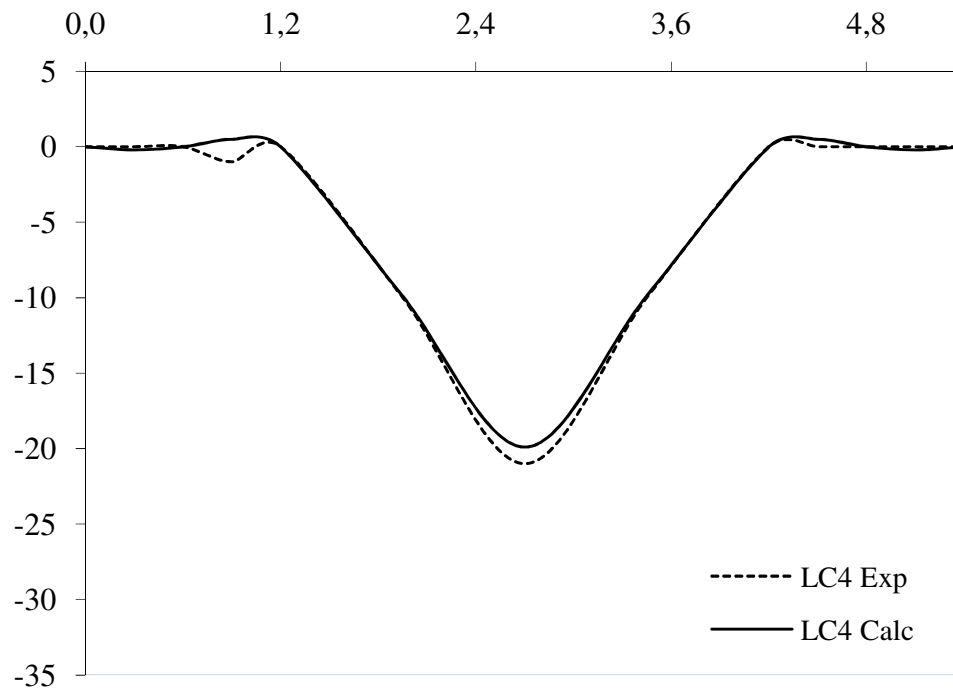
Figure 6.8 Vertical displacements LC-4.
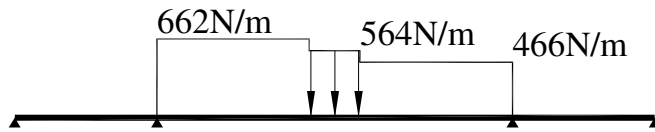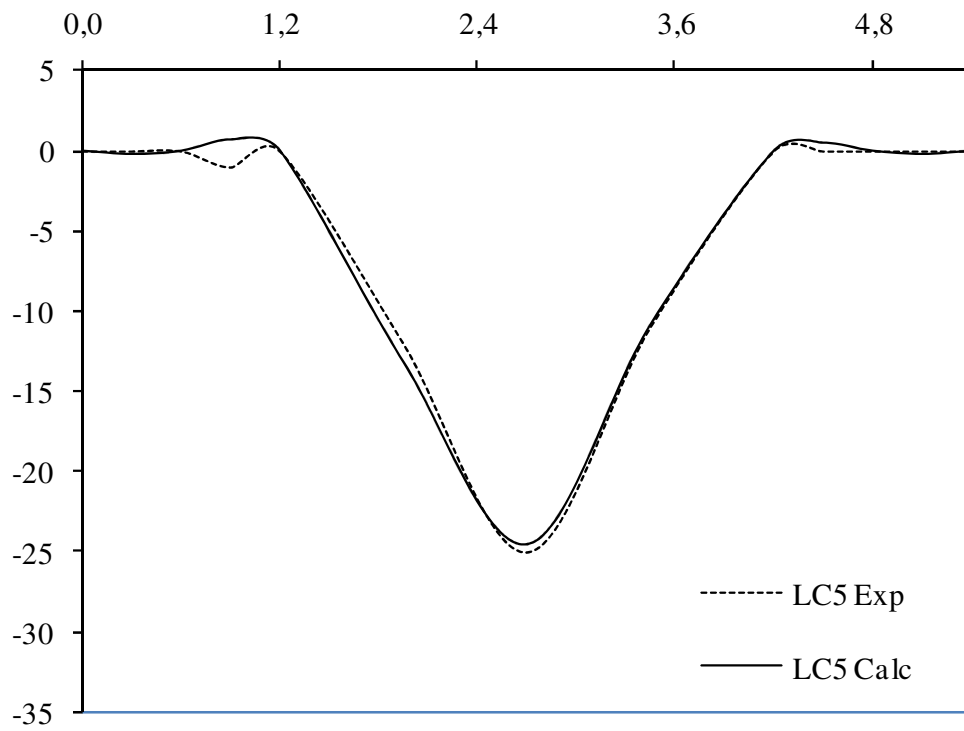
Figure 6.9 Vertical displacements LC-5.
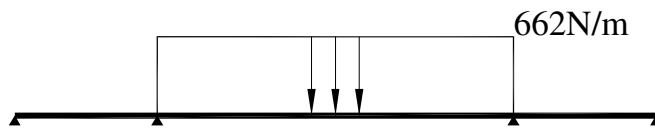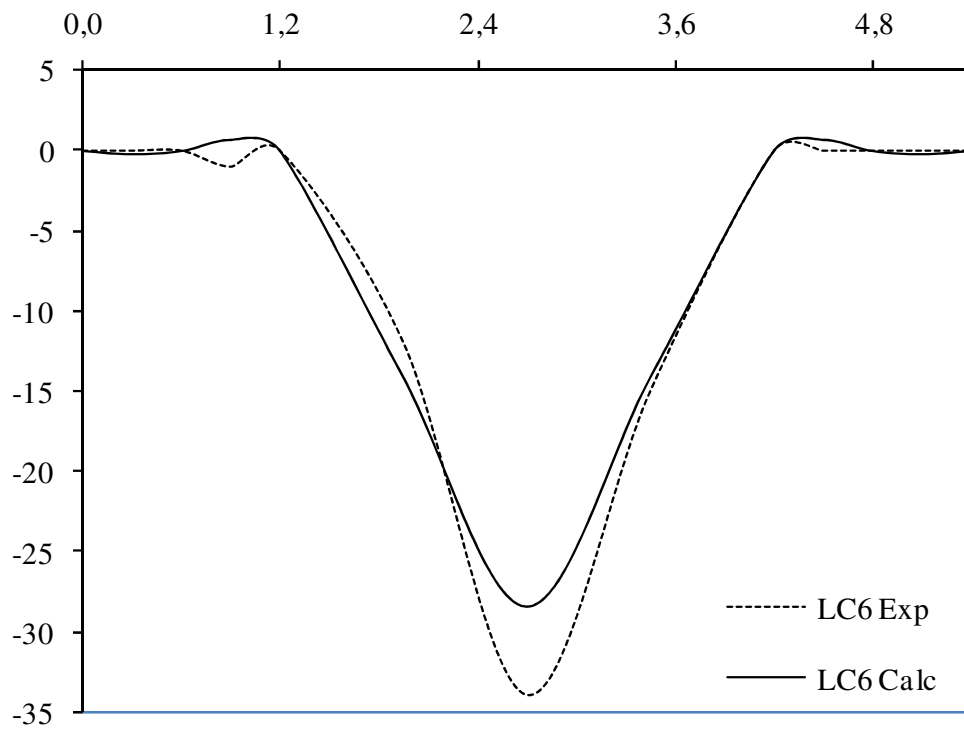
Figure 6.10 Vertical displacements LC-6.
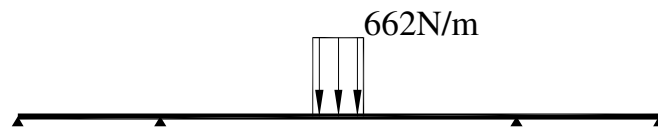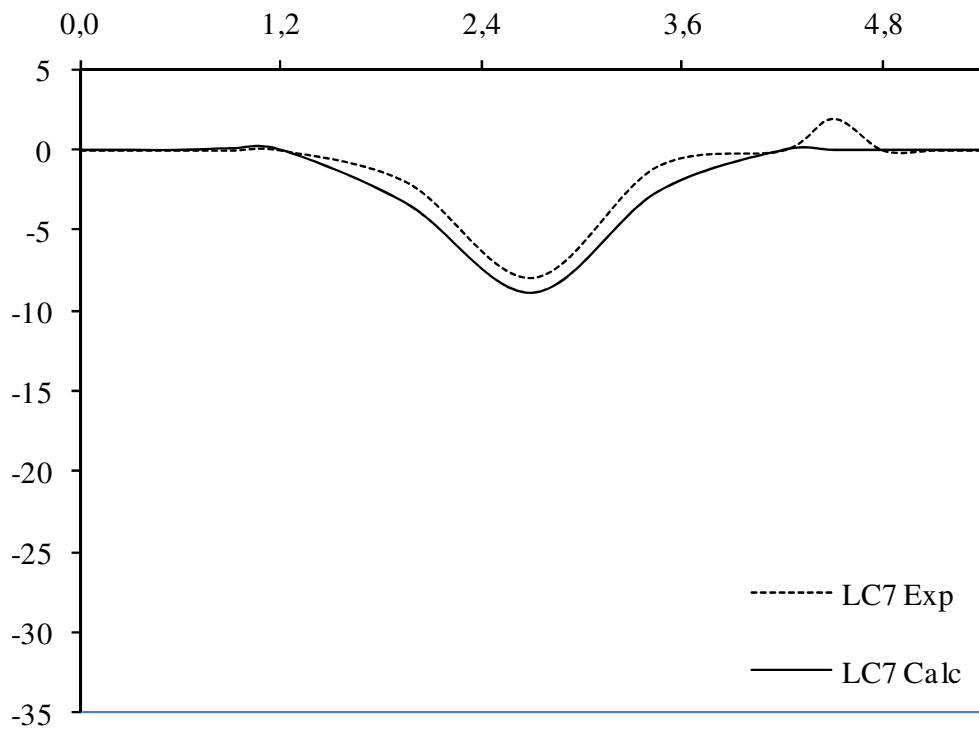
Figure 6.11 Vertical displacements LC-7.
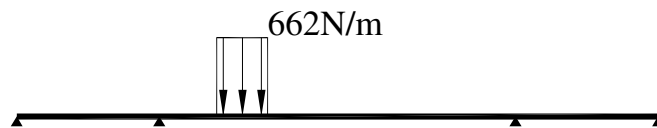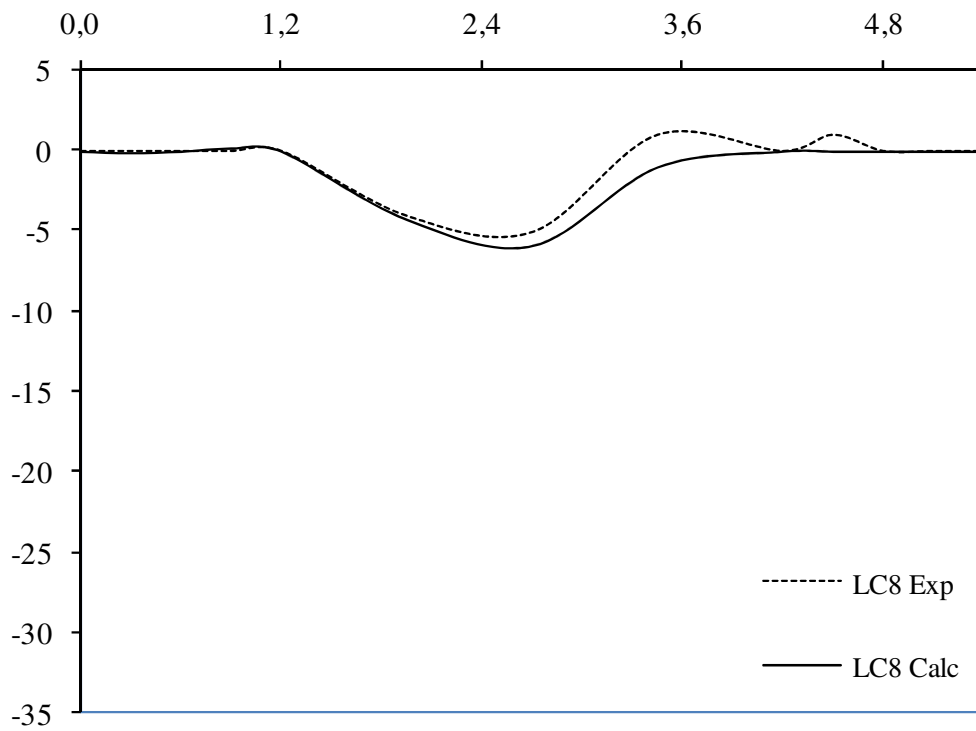
Figure 6.12 Vertical displacements LC-8.
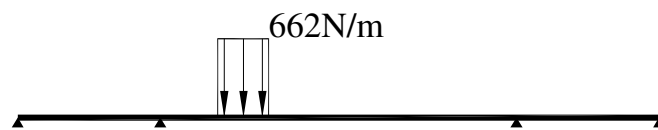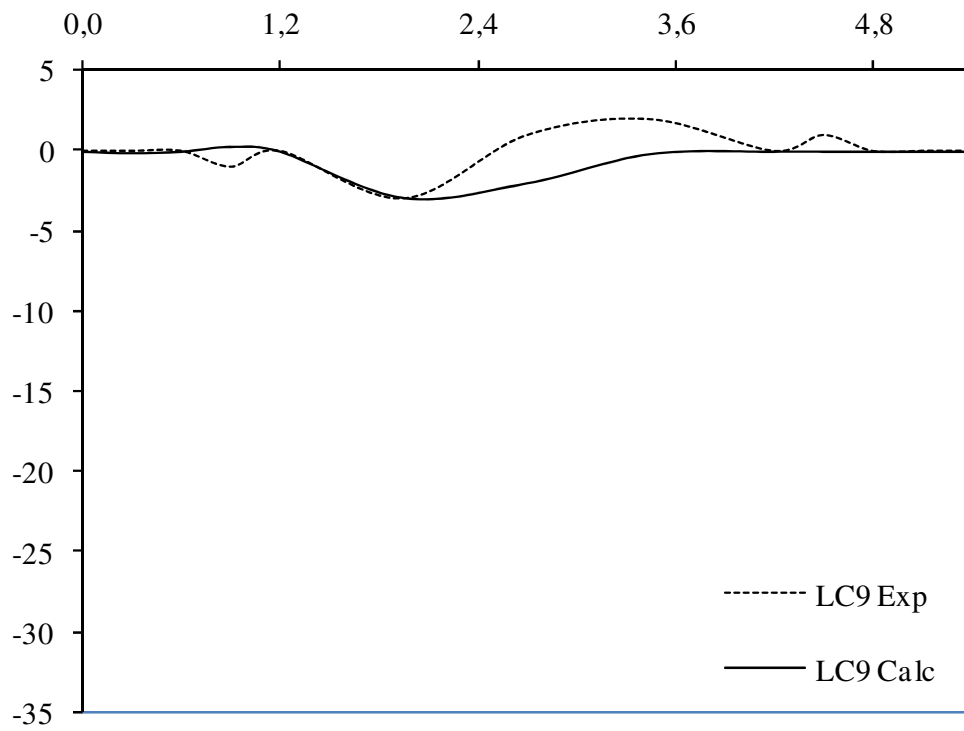
Figure 6.13 Vertical displacements LC-9.
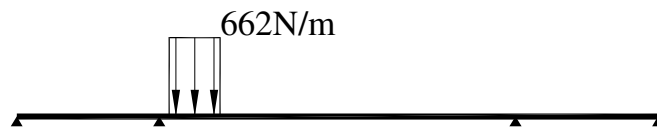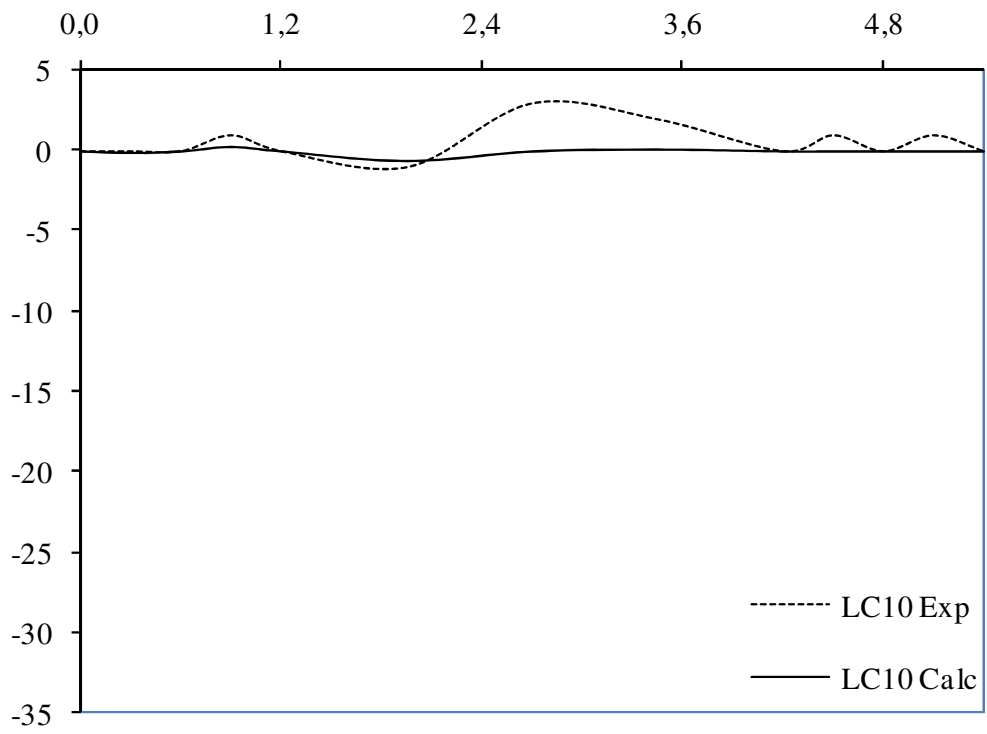
Figure 6.14 Vertical displacements LC-10.
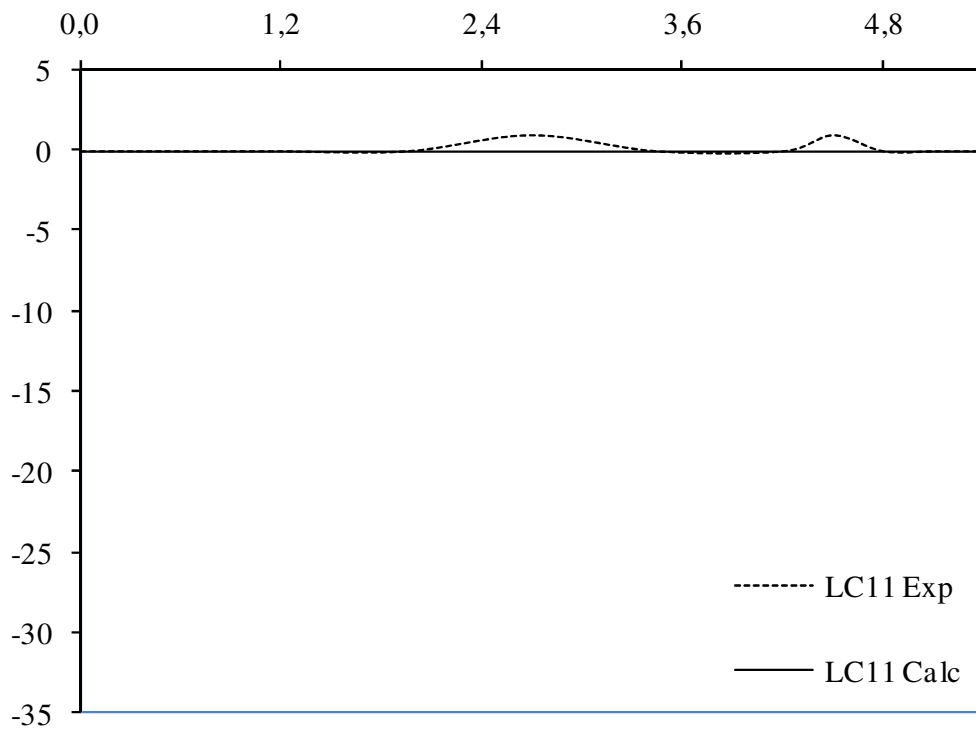
Figure 6.15 Vertical displacements LC-11.

6.1.9. Horizontal displacements of anchors

Figure 6.16 shows horizontal displacements for anchor supports and Figure 6.17 presents those for pylons.. Load values and distribution cases are the same as above. Based on the comparison of horizontal displacements, we can suppose that maximum loading resulted in the compliance of the fixed support of the left pylon and this gap in the figures resulted in all subsequent cases – but overall effects of acting are described correctly. The solution for the fixed support of the left pylon, the leg between with little stiffness support plate (see Figure 4.14) was unfortunate.

The stiffening girder of the improved model is a steel beam modelled by two steel angles and horizontal brace members between them. Brace members are fixed to the steel angles with a bolt and a screw. At the top of brace members and in the flange of the angle, holes with a diameter greater than bolts are found. This solution can cause an effect in which local buckling and deformation can cause no described shortening of the stiffening girder.
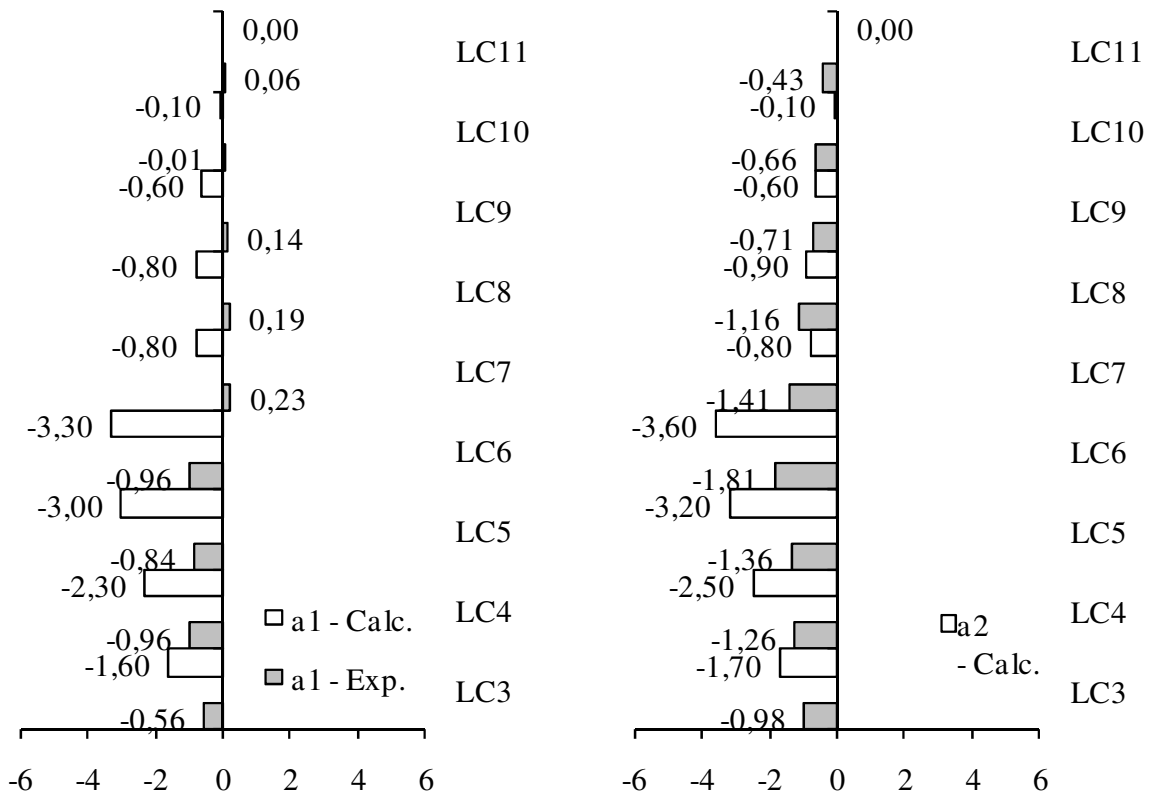
Figure 6.16 Horizontal displacements of the left and the right anchor.

6.1.10. Horizontal displacements of pylons
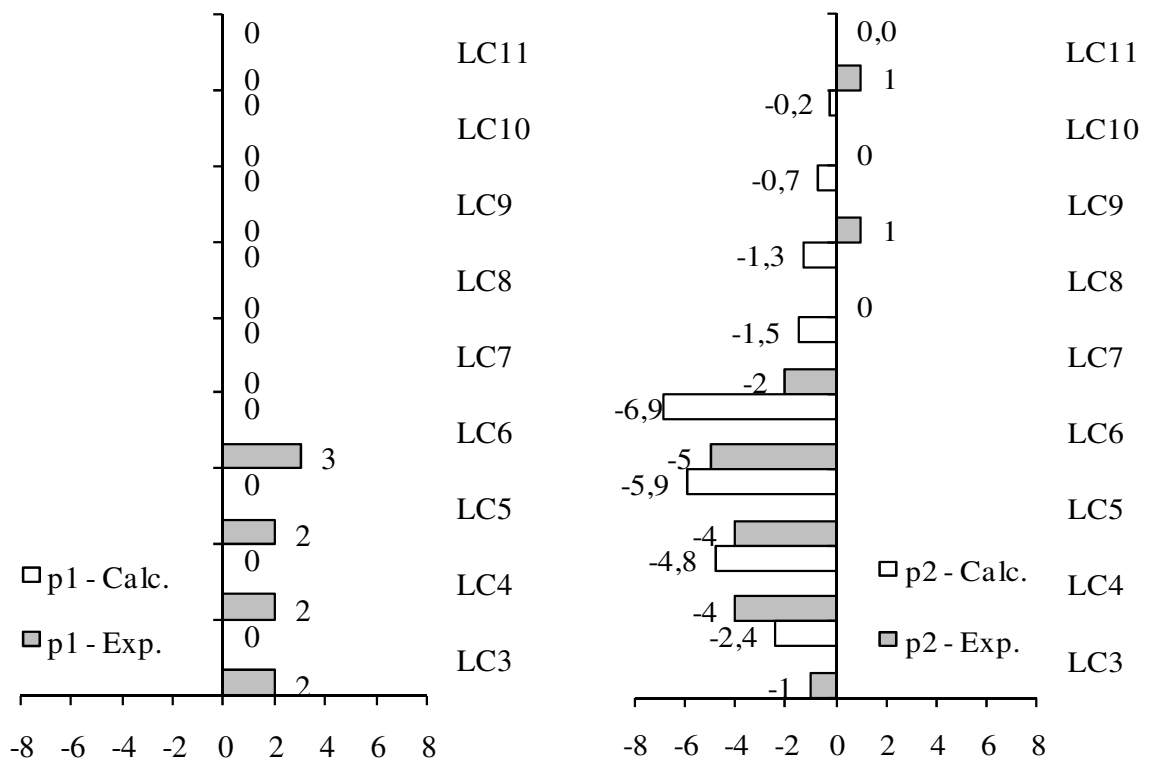
Figure 6.17 Horizontal displacements at the top of the left and the right pylon.

7. Buckling of stiffening girder

One of the main goals of experimental investigation was ensuring the buckling capacity of stiffening girder. As described above for structure self-anchored scheme was chosen. All geometrical and stiffness parameters for stiffening girder was modelled to accord to the actual structure.

Modelling geometrical and stiffness characteristics for stiffening girder is obvious and clear comparing the support conditions for buckling. Describing supports for different buckling modes is much more complicated and much more opened for failing. In addition questions like predicted acting and realisation of presupposed supports arise. Despite the fact that loads to supports from pre-buckling shape of structures geometry may appear marginal, supports bearing capacity and stiffness should be ensured.

Experimental testing of the bridge structure showed no risk for buckling of stiffening girder and also no hint like pre-buckled deformed shape. Theoretical analysis supports this result firmly. Analysis shows that total uniformly distributed load can be increased 4,2 times or traffic load 7,6 times – see Figure 7.1. Figure 7.1 shows dependence of buckling load factor on the uniformly distributed traffic load. For predicting buckling the buckling load factor must obtain value less than 1,0 – see Table 7.1 for detail explanation. Buckling load factors for all load cases tested in experimental research are presented in Table 7.2.
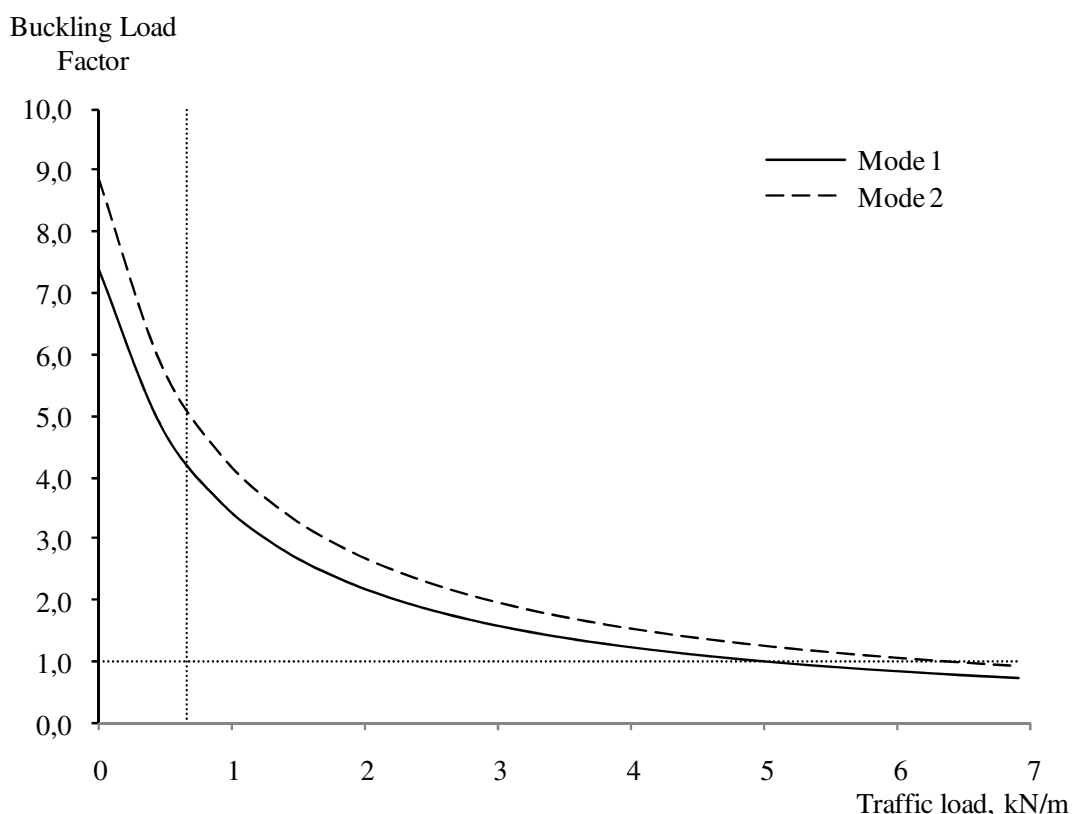
Figure 7.1 Dependence of buckling load factor on the uniformly distributed traffic load

Table 7.1 Interpretation of buckling load factor

Buckling will occur at	
	Buckling Load Factor × Actual Load = Critical Buckling Load
$1 < BLF$:	Buckling not predicted
	The applied loads are less than the estimated critical loads. Buckling is not expected.
$0 < BLF < 1$:	Buckling predicted
	The applied loads exceed the estimated critical loads. Buckling is expected.
$BLF = 1$:	Buckling predicted
	The applied loads are exactly equal to the estimated critical loads. Buckling is expected.
$BLF = -1$:	Buckling not predicted
	The model is in compression and buckling is not expected. However, buckling will be expected if you if you multiply all loads by the negative BLF. For example, if you apply a tensile force on a bar, the BLF should be negative.
$-1 < BLF < 0$:	Buckling not predicted
	Buckling is predicted if you reverse all loads.
$BLF < -1$:	Buckling not predicted
	Buckling is not expected even if you reverse all loads.

In Figure 7.2, Figure 7.3 and Figure 7.4 three different shapes of buckling modes are presented. In Figure 7.2 the most predictable in plane buckling mode, in Figure 7.3 second most predictable in plane buckling mode. Figure 7.4 illustrates most predictable out of plane buckling mode. Before out of plane buckling occurs there are various additional predictable in plane modes. Exactly this buckling modes accord to the load case LC 6 used in experimental research, see Figure 6.10.

From the Table 7.2 it is clearly seen that out of plane buckling is remarkably less predictable. Buckling load factor for "first" out of plane mode is 12 times less predictable than "first" in plane mode. Of course only in plane vertical load

was taken into account in buckling analysis. It is clear that this buckling load factor will decrease when out of plane loads will be added to the scheme.

Should be remarked that scheme used in this thesis has advantages for out of plane buckling modes which is caused by aspect that side spans have multiple supports which decreases the effective buckling length for centre span.

Table 7.2 Buckling load factors for investigated load cases

Load Case Nr.	Buckling load factors		
	Mode 1	Mode 2	Mode 3
LC3	6,0	7,1	
LC4	4,9	5,9	
LC5	4,5	5,5	
LC6	4,2	5,1	50,3
LC7	6,2	7,6	
LC8	6,5	7,9	
LC9	7,1	8,3	
LC10	7,4	8,7	

* For load mode 3 and all other load cases the factor is > than 50,3.
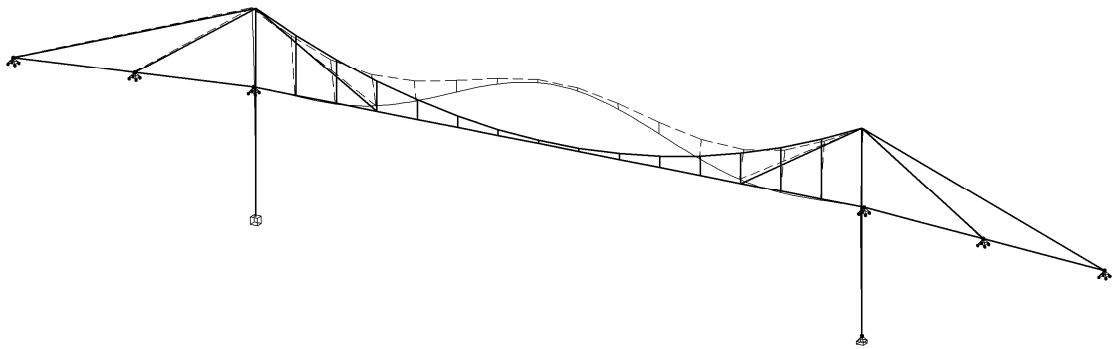
Figure 7.2 Buckling mode 1
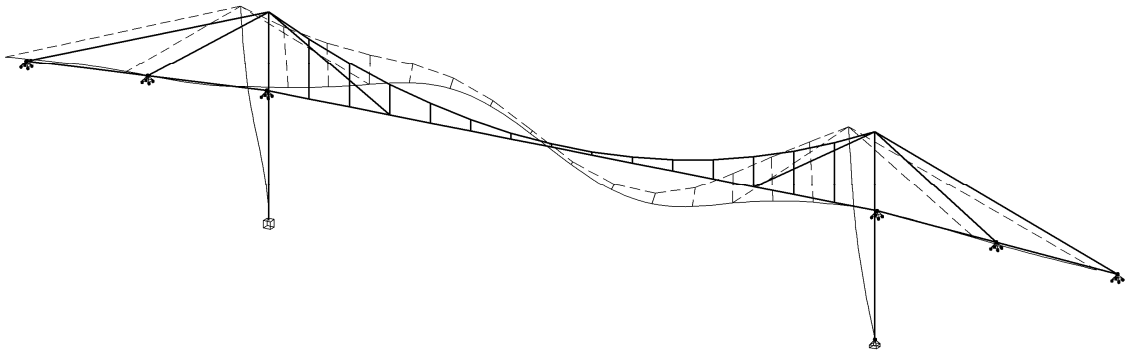
Figure 7.3 Buckling mode 2
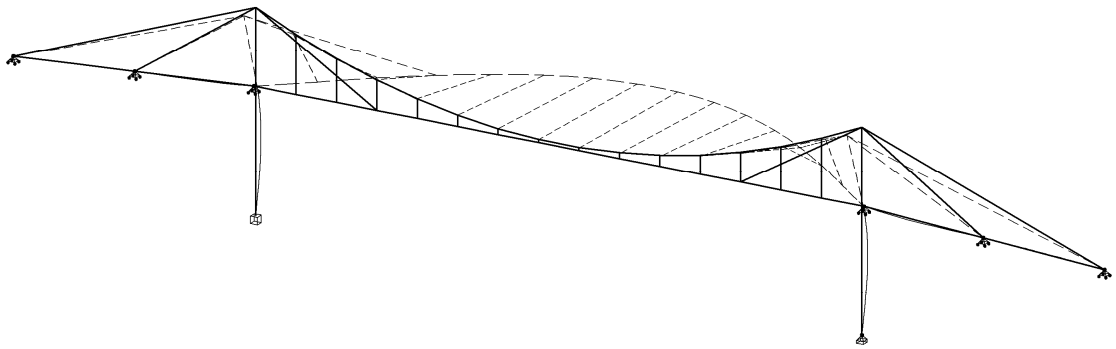
Figure 7.4 Buckling mode 3

8.   Theoretical research

In this section influence of main parameters, like geometrical and stiffness relations, to the structural behaviour are presented. At the end of the section main inner-force and stress distributions for maximum tested case are presented. All of these parameter values are presented taking into account serviceability limit state requirements. Choosing scheme and its parameters aspects of ultimate limit state characteristics should be considered also.

Influence of parameters were investigated independently when the combined effect can be supposed.

8.1.   Deformations

The first essential geometrical parameter, height of pylon for current scheme is effectual to choose between 0,1 ... 0,15 of the span length – consequential from Figure 8.1, Figure 8.2 and Figure 8.3. In our experimental model it was 0,127.
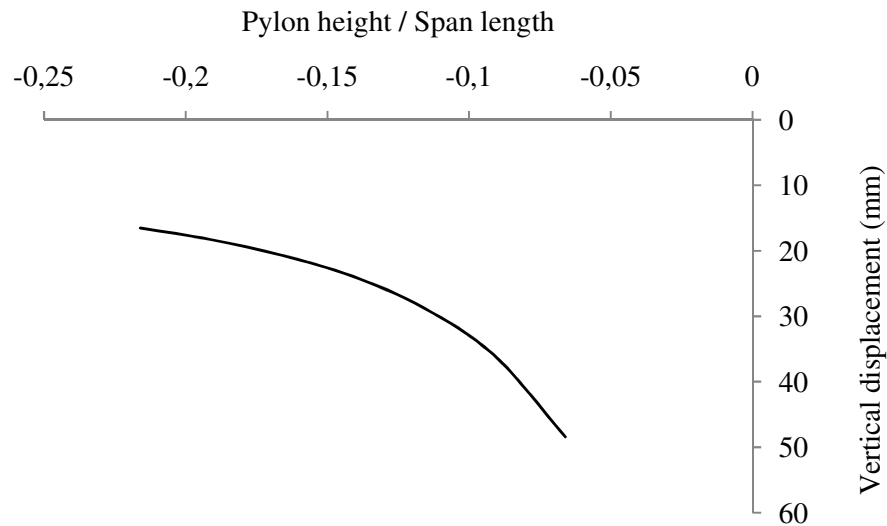
Figure 8.1 Dependence of the vertical deflection on the pylon height.
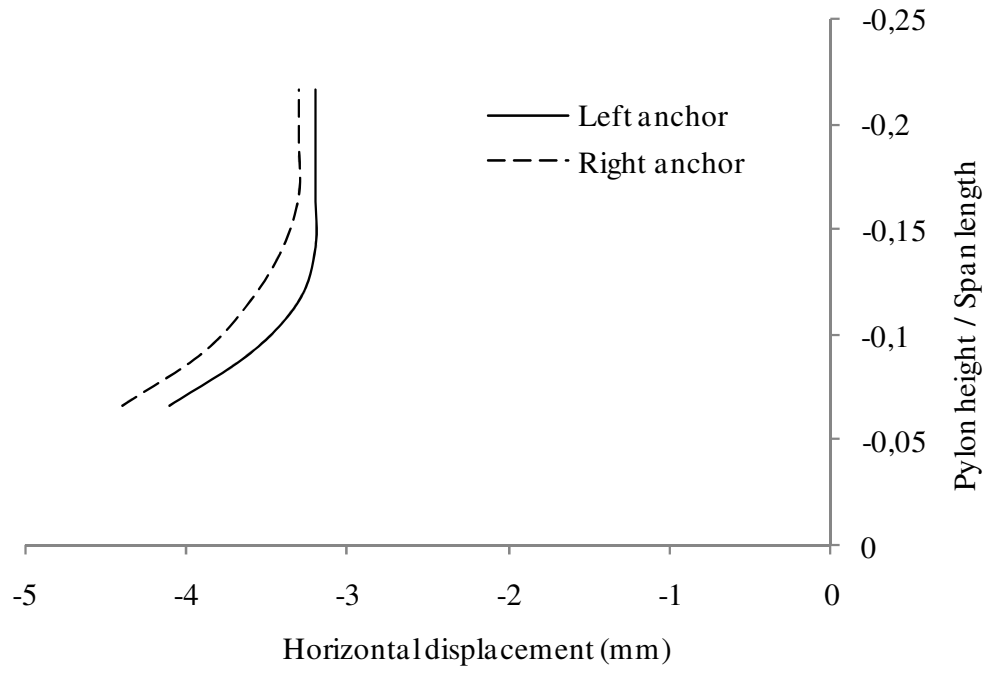
Figure 8.2 Dependence of the anchor horizontal displacement on the pylon height.
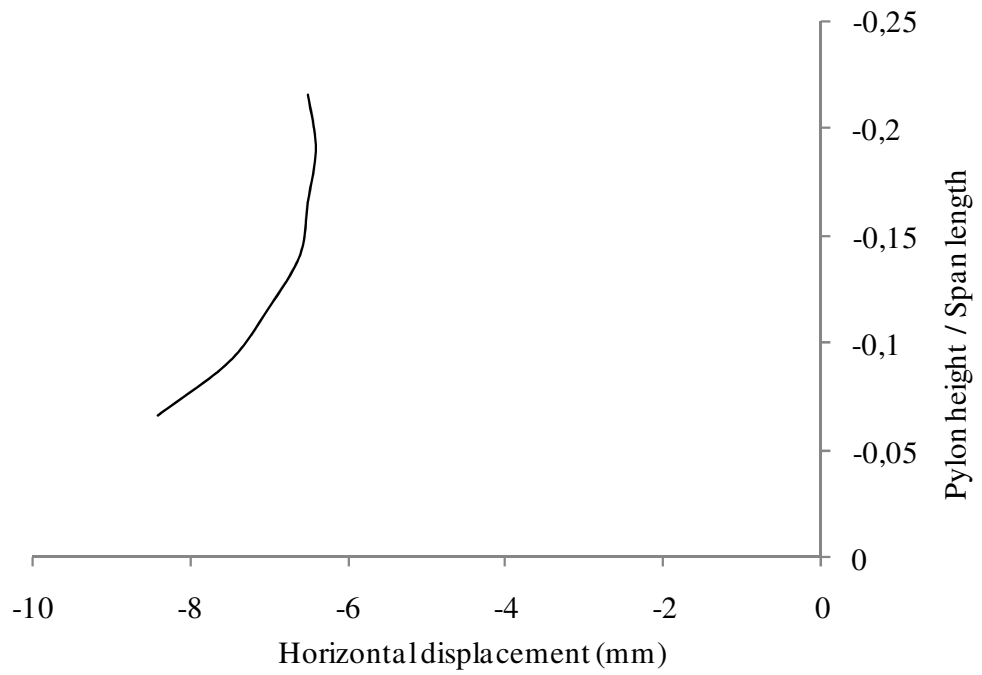
Figure 8.3 Dependence of the right pylon horizontal displacement on the pylon height.

For scheme under investigation, side spans length should be 0,2 ... 0,4 of central span – see Figure 8.4, Figure 8.5 and Figure 8.6. In our experimental model realation of side and central span was 0,40.

Side span / Middle span
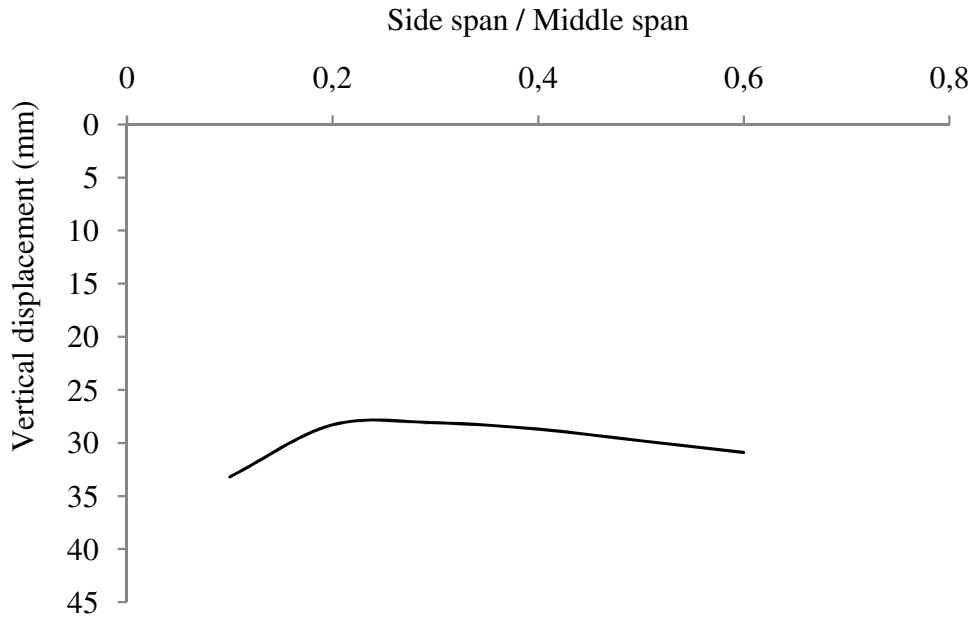
Figure 8.4 Dependence of the vertical displacement on the length of side span.
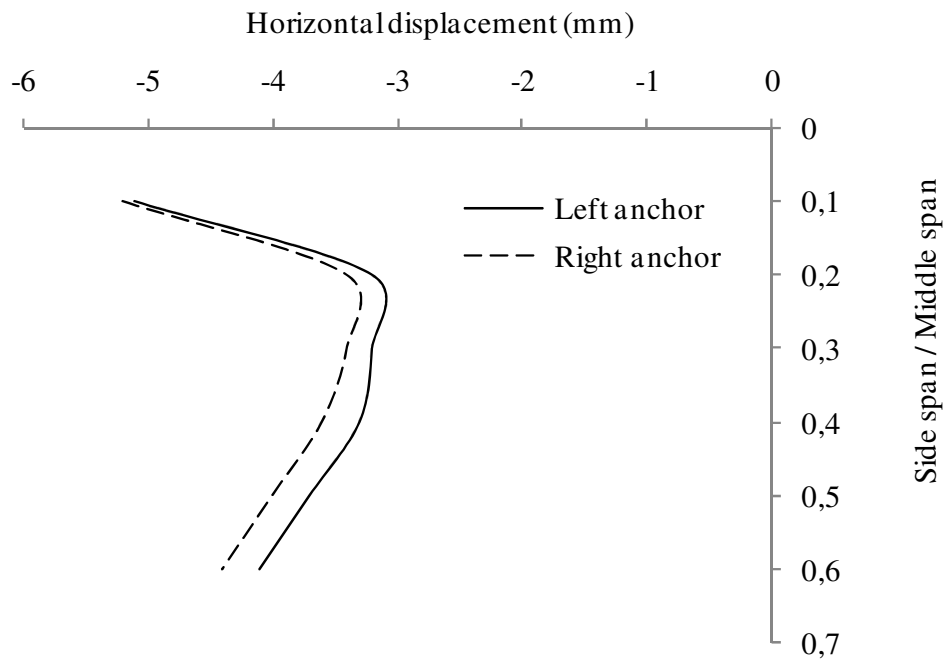
Figure 8.5 Dependence of the anchor horizontal displacement on the length of the side span.
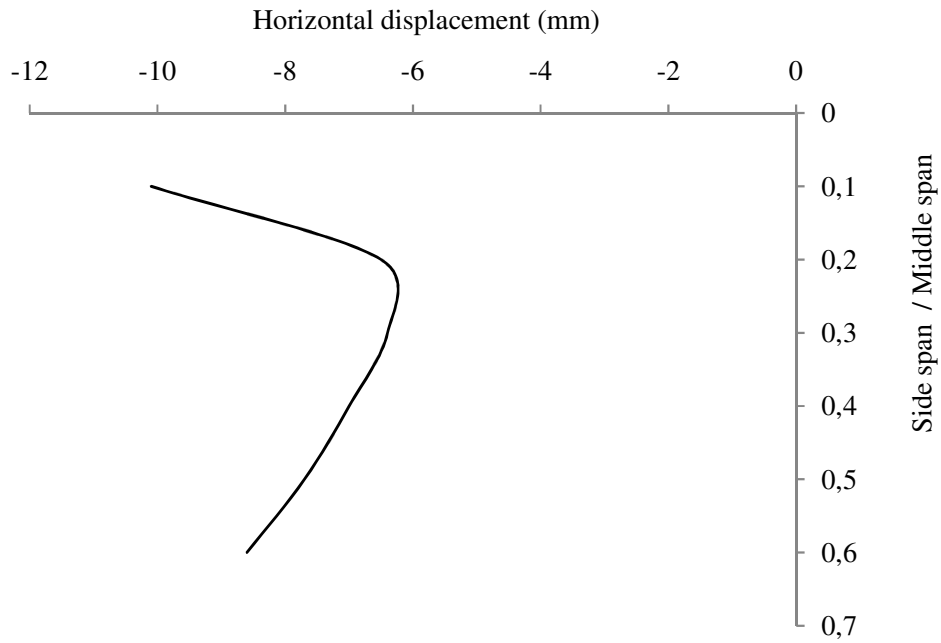
Figure 8.6 Dependence of the right pylon horizontal displacement on the length of the side span.

In case of one cable-stay in the middle span or for resultant of cable stays reaction, optimal range for fixing cable stay to the stiffening girder is 0,3 ... 0,37 of the span length – consequential from Figure 8.7. Figures for horizontal displacement, Figure 8.8 and Figure 8.9, showed optimal range 0,26 ... 0,33 but the influence himself is marginal.
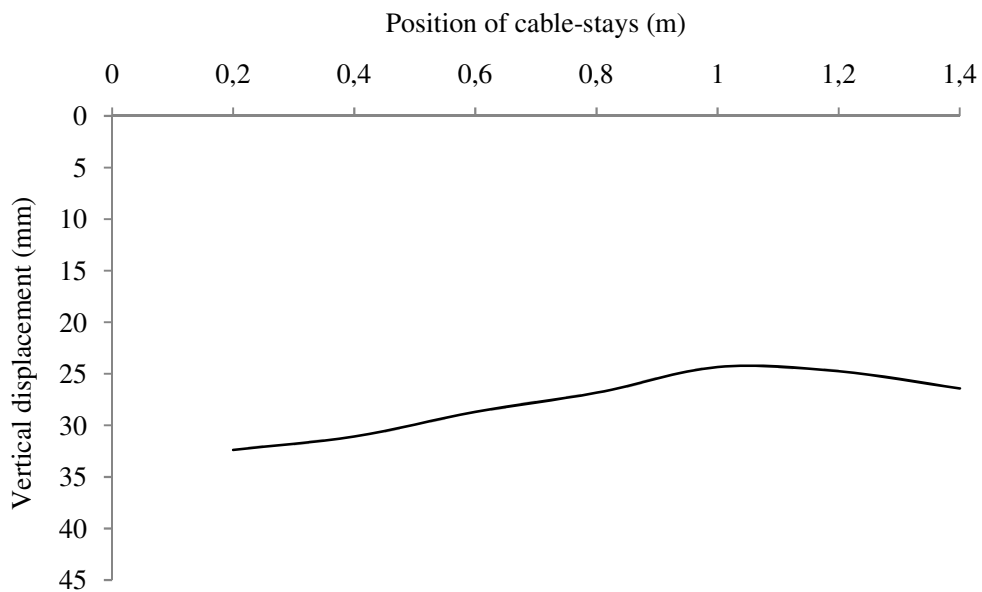
Figure 8.7 Dependence of the vertical displacement on the position of the cable-stay.
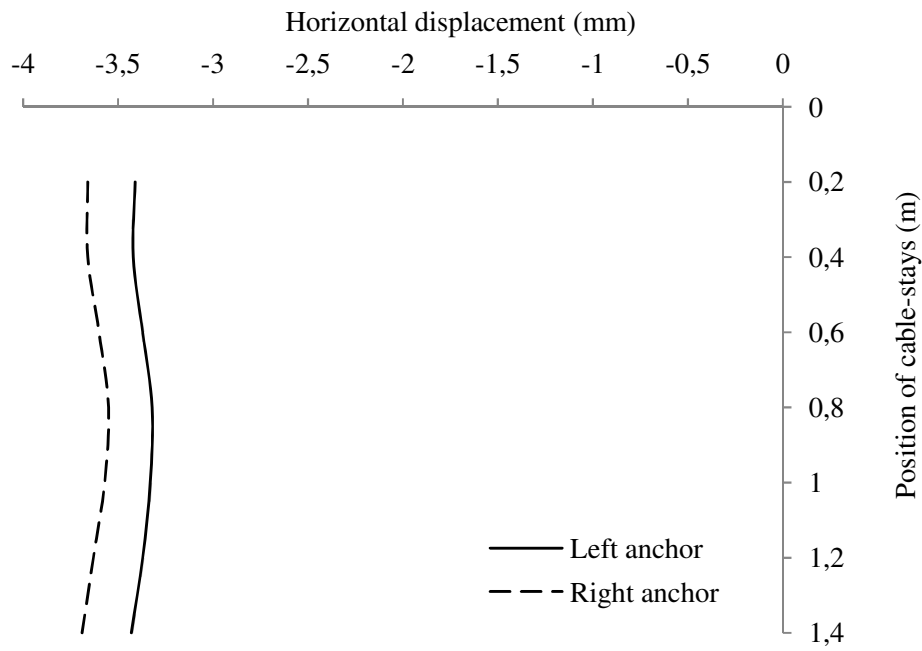
Figure 8.8 Dependence of the horizontal displacement of the anchor on the position of the cable-stay.
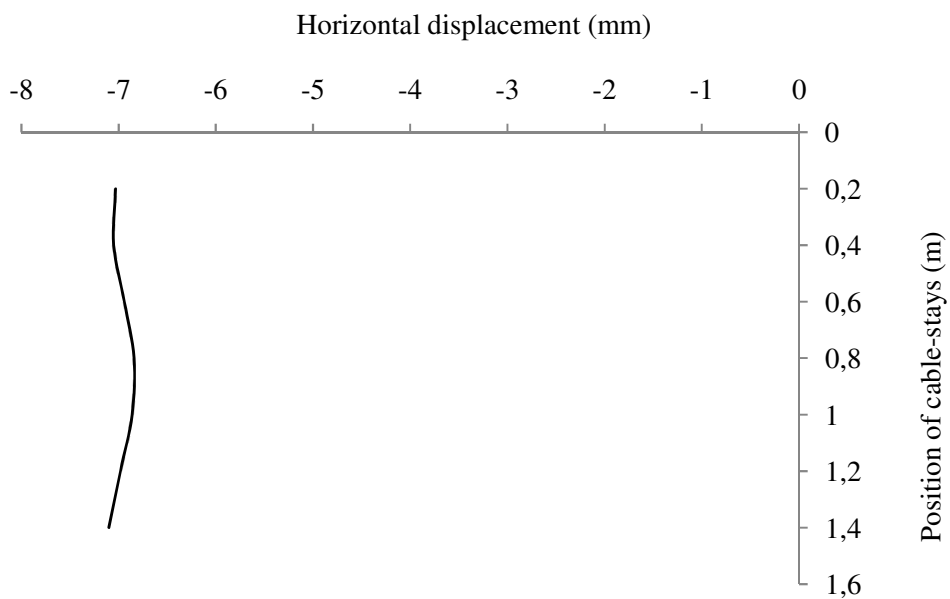
Figure 8.9 Dependence of the horizontal displacement of the right pylon on the position of the cable-stay.

From Figure 8.10, Figure 8.11 and Figure 8.12 we can see that for deflection existence of cable stays even if they have small stiffness is the main factor - if the capacity of cable stay is ensured. Adding stiffness to cable stay has intense effect up to value 60% of carrying cables axial stiffness.

Sectional area of cable-stays (cm²)
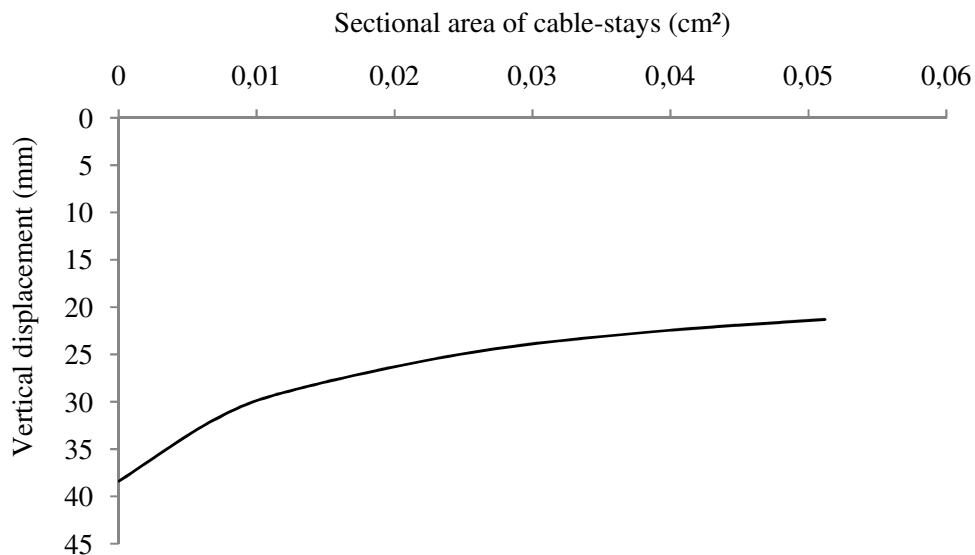
Figure 8.10 Dependence of the vertical displacement on the sectional area of the cable-stay.
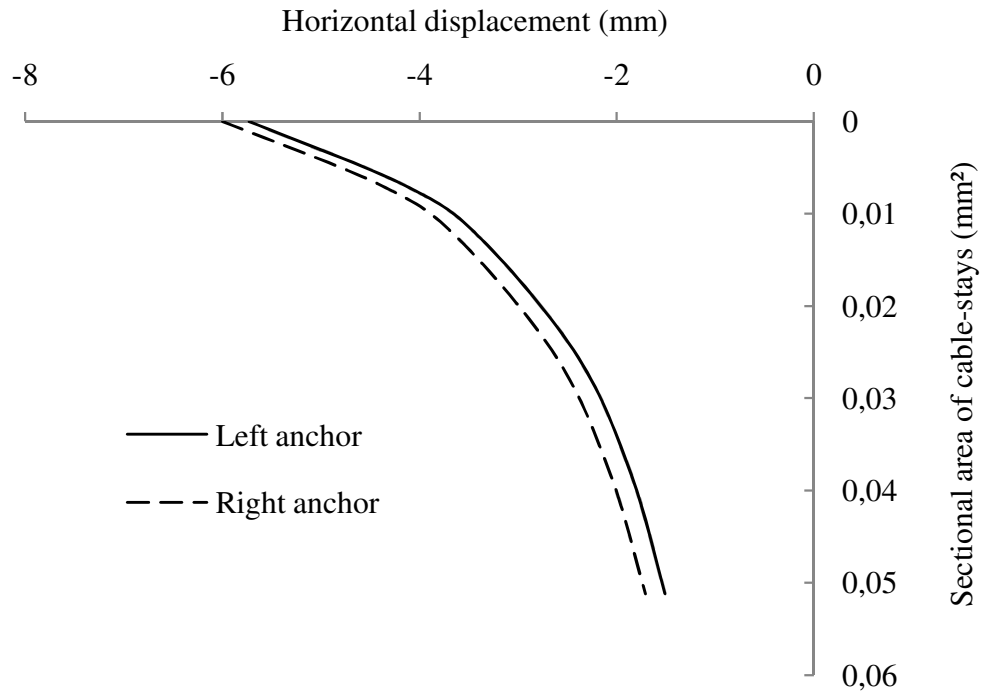
Figure 8.11 Dependence of the anchor horizontal displacement on the sectional area of the cable-stay.
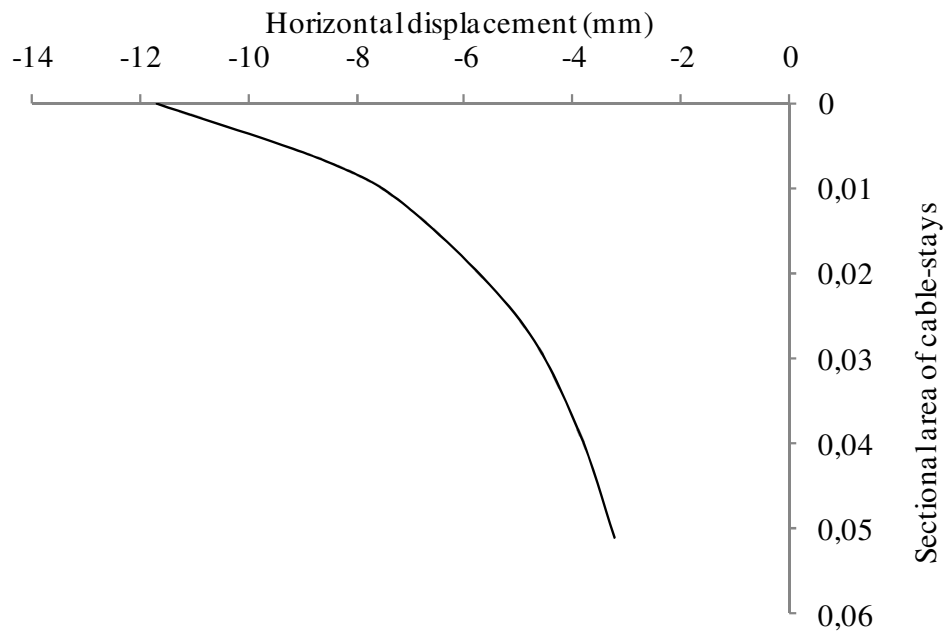
Figure 8.12 Dependence of the right pylon horizontal displacement on the sectional area of the cable-stay.

8.2. Essential estimation to the calculation methods

In current scheme almost linear acting of anchor span causes excessive influence to the nonlinear acting of the carrying cable in the centre span. Additional horizontal displacement in direction to the central span results in increasing of the vertical displacements. This scheme is not the expressive way to show benefits of nonlinear approach.

As we can see from Figure 8.13 difference for nonlinear analysis methods regarding the linear one is 8 ... 14% in case of symmetrical uniformly distributed loading. Comparison in the Figure 8.13 shows that for combined cable stayed scheme and when uniformly distributed load is dominant in first steps of design linear analysis is effective to use. Choosing between the different nonlinear approaches in real design less laborious should be used.

Advantages of different nonlinear solutions in general should be analysed and discussed additionally. In this type of analysis computational errors in forming the equations and solving them should kept in mind.
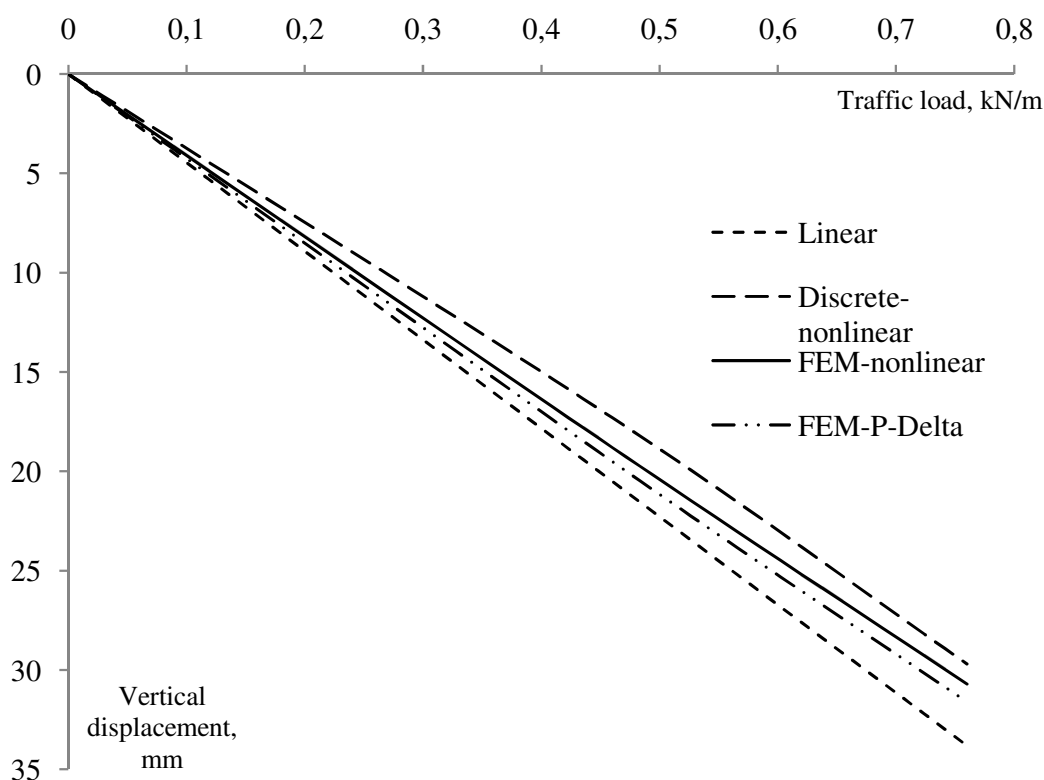
Figure 8.13 Vertical displacement under the action of uniformly distributed symmetrical load for different analysis methods.

8.3. Inner forces

Below for experimental-model inner-force and stress distributions are illustrated. Stress and inner-force graphs are also presented for uniformly distributed load with maximal value – load case number 6 (LC-6) in experimental research.

In Figure 8.14 stress for cable stays, carrying cables and hangers are presented. If only tension member's axial stress take a design criterion then sectional area of cable stay should be increased and sectional area of carrying cable should be decreased.

Figure 8.15 illustrates normal stress in stiffening girder from bending moment and axial force. Figure 8.16 presents shear force and Figure 8.17 bending moment in stiffening girder.

Taking into account only inner forces of stiffening girder for current scheme, geometry of cable stays should be adjusted to support stiffening girder in central part of the span. In this case distribution of inner forces is more favourable – minimum and maximum values for bending moment will be about the same.
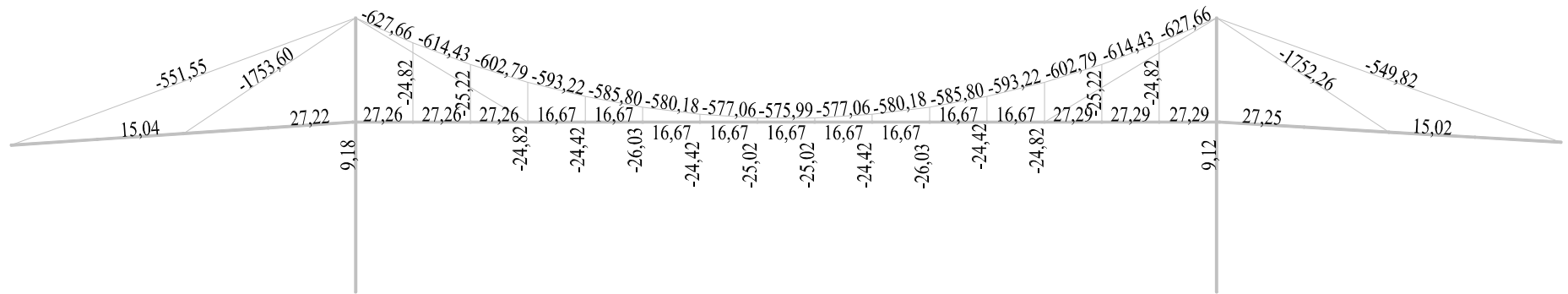
Figure 8.14 Stresses caused only by axial forces.
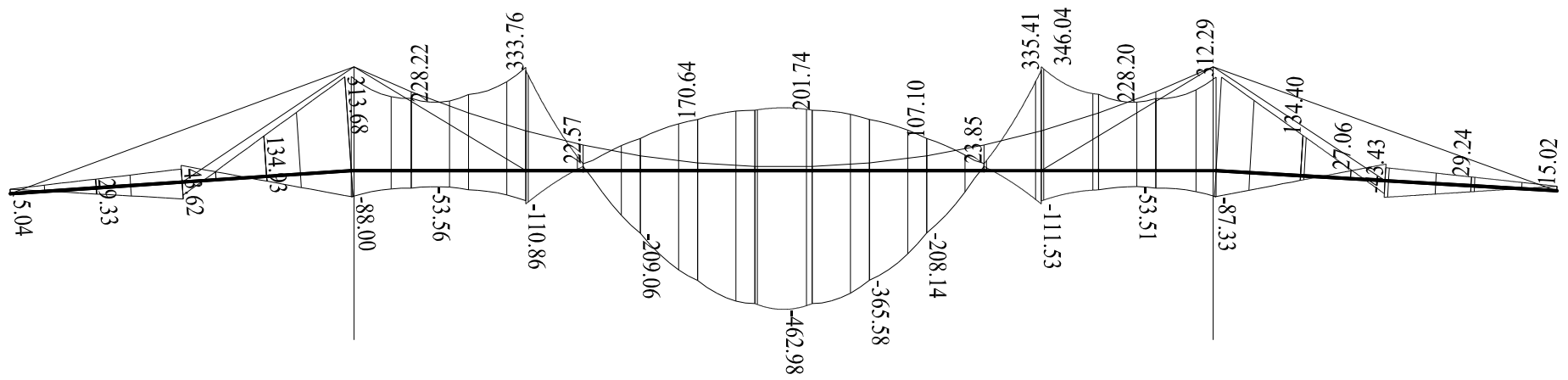
Figure 8.15 Normal stress in the stiffening girder caused by normal forces and the bending moment.
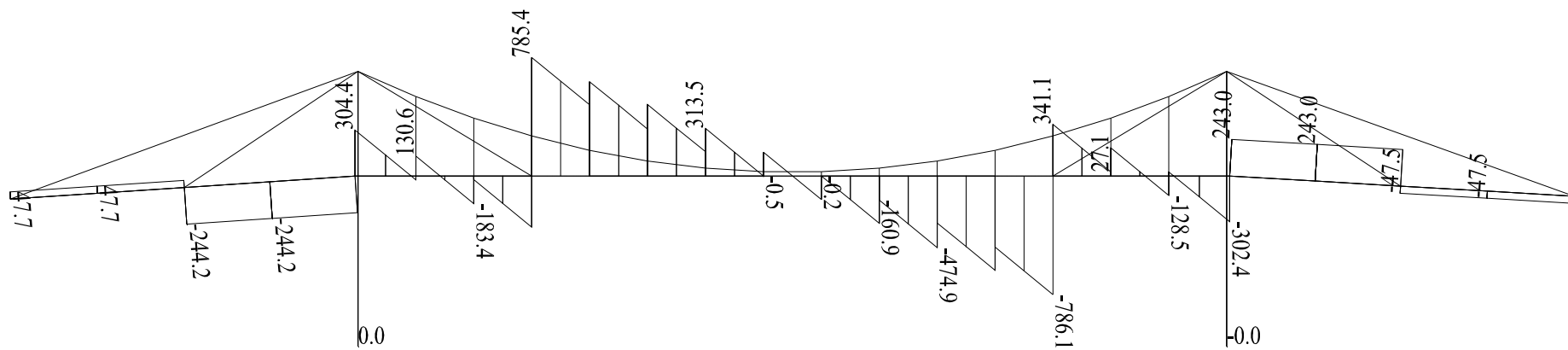
Figure 8.16 Shear forces of the stiffening girder.
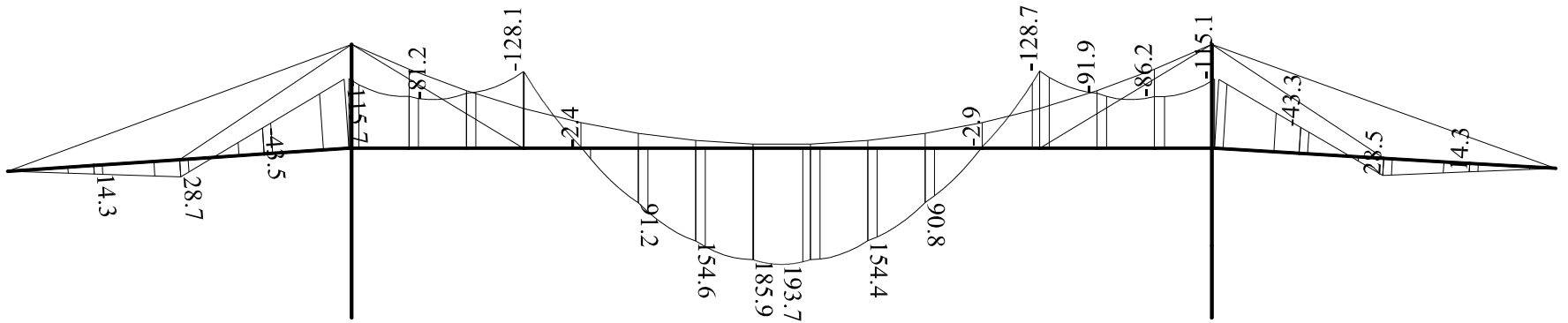
Figure 8.17 Bending moments of the stiffening girder.

9. Discussion

9.1. General

This thesis can be regarded as one stage for further research, especially for the case of the fixed-link solution. The thesis provides main guidelines for static analysis and points out weaknesses that should be avoided later on. Therefore, combined scheme, the most complicated scheme for the suspension bridge that was justified is causal. Further work for the fixed-link will concentrate on a very different sphere of research.

1. Traffic load values and distributions that take into account local conditions, alternative transportations and their future developments;
2. wind load measurements and possible critical areas for final expatiation as well as in the construction stage;
3. construction solutions for local conditions;
4. ecological influences and requirements for future navigability;
5. detailed geological and geotechnical research.

9.2. Scheme

The structural scheme for the thesis was chosen in view of greater generalisation. Taking this scheme as a navigable span for the fixed link, local conditions and span length that prefer self-anchored solutions because of construction of outer supports are laborious and expensive.

More studies have been reported on traditional suspension and cable-stayed bridge than on combined schemes. For that reason combined scheme is most informative to investigate and gives knowledge also for suspension structures and cable stayed structures.

One of the prospective structural schemes for combined scheme is combining the stiffening girders material and section also.

Using self anchored scheme is effective in final stage but it causes remarkable difficulties and expenses for design and construction in construction stage. Also probability for failures increases remarkably when non-traditional scheme will be used in real design.

Combined schemes have useful and irreplaceable usage in reinforcing and stiffening the existing structures. Adding cable stays to the suspension structures also gives opportunity to adjust displacements and inner forces.

9.3. Parameters

General research can give guidelines and correlations for geometric, stiffness and loading parameters but to ensure final estimations for choosing a scheme and its parameters for every bridge – solid research should be conducted for traffic load actions.

The thesis showed that if model parameters are scaled exactly to the original bridge structure, the diameter of carrying cables can be decreased and the diameter of cable stays should be increased.

For a stiffening girder, the bridge geometry and stiffness should be adjusted to equalize the positive and negative bending moments.

Buckling analysis showed that ensuring the general stability of stiffening girder is not the dominant factor and parameters for stiffening girder taking into account other aspects as dominant ones is possible. Later on the buckling should be checked. Greater load values and distributions are useful to provide that the stability of a stiffening girder is ensured with sufficient structural safety.

9.4. Loading effects

9.4.1. Influence of tandem

In Figure 9.1, Figure 9.3 and Figure 9.5 the deflections and inner forces of the stiffening girder under the action of correct Load model 1 (Eurocode). Load model consists of a uniformly distributed vertical load and tandem loads in lanes. The legend shows the position for the tandem from the left anchor, graph "without" shows the deflection or the inner force without the tandem. Figure 9.2, Figure 9.4 and Figure 9.6 describe the influence of the tandem without a uniformly distributed load. For the influence of deflection, 11% is the most unfavourable position, for bending moments - 8% and for shear forces - 10%.

Figure 9.7 shows the influence of the tandem on the horizontal displacements. Tandem moves from the left pylon to the right one in the middle span. Naturally they have maximum values if the tandem is acting in the middle range of the span. If for the right pylon displacement maximal value is achieved exactly in central position, then for anchor supports the most unfavourable position is in 0.37× middle span length distance from the left pylon. This asymmetric effect is caused by the asymmetrical description of pylons support, for the left pylon fixed and for the left pylon pinned support was used.
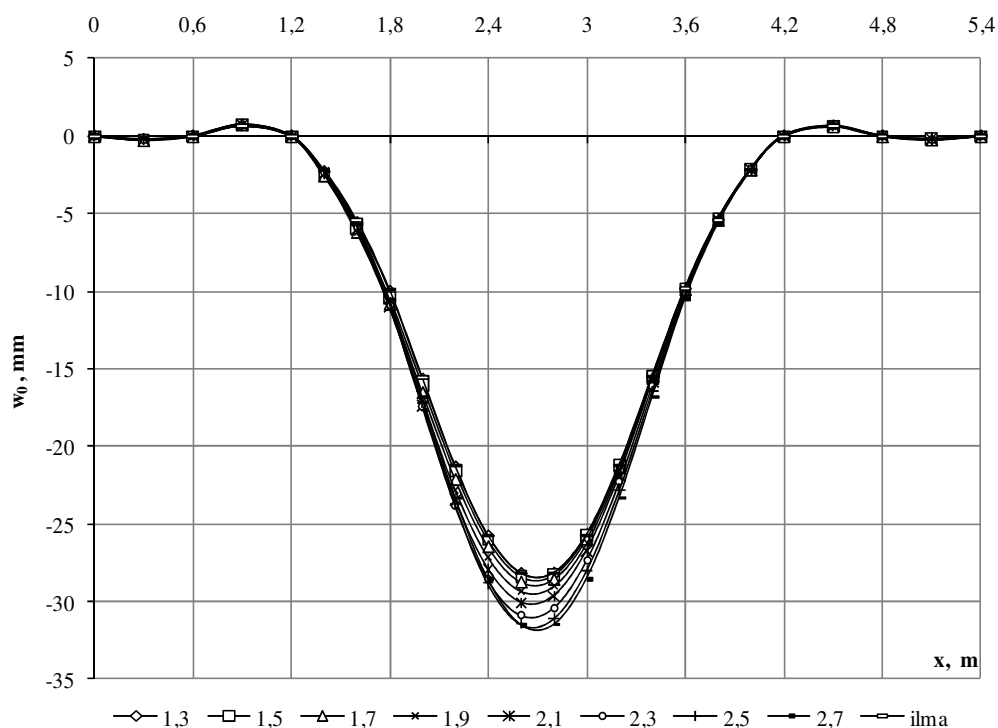
Figure 9.1 Deflection of the stiffening girder.
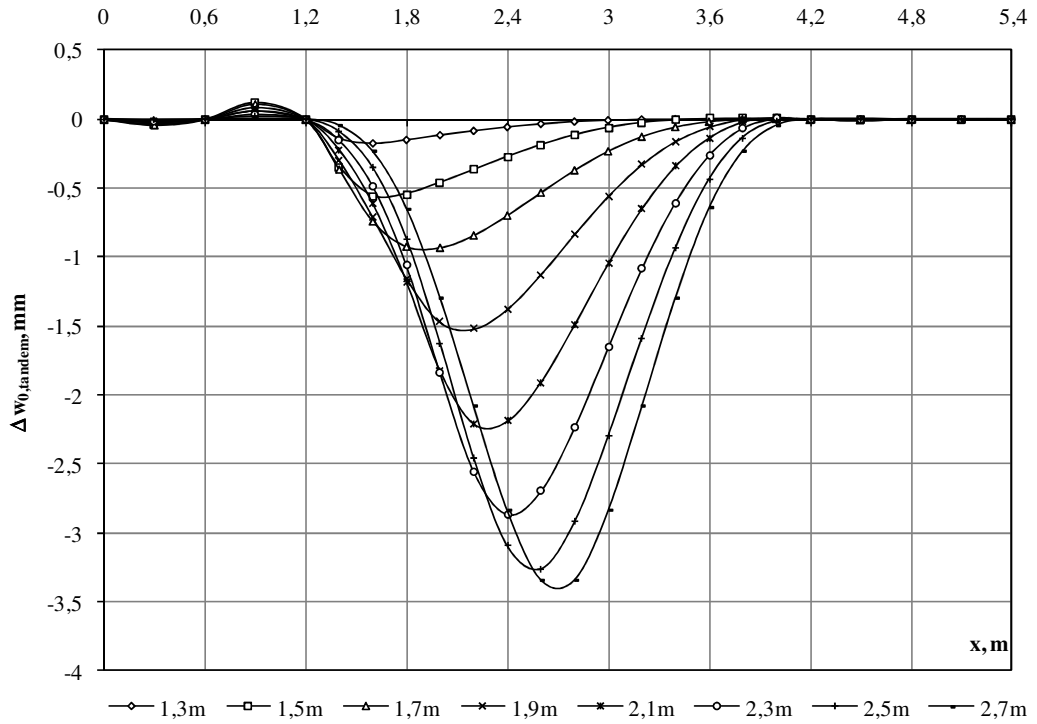
Figure 9.2 Differences in deflections.
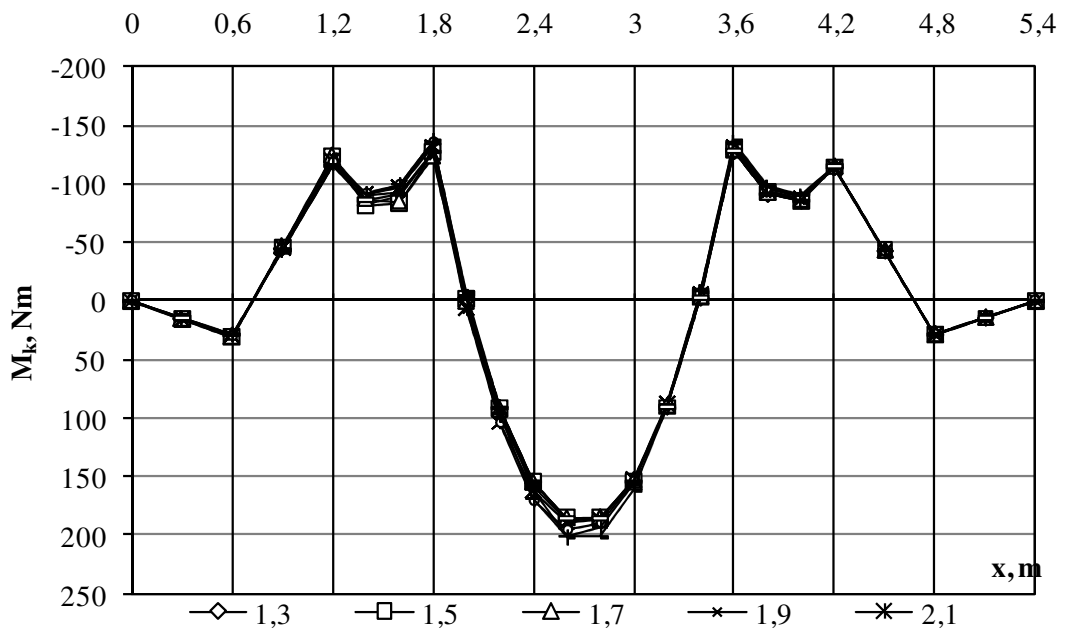
Figure 9.3 Bending moments of the stiffening girder.
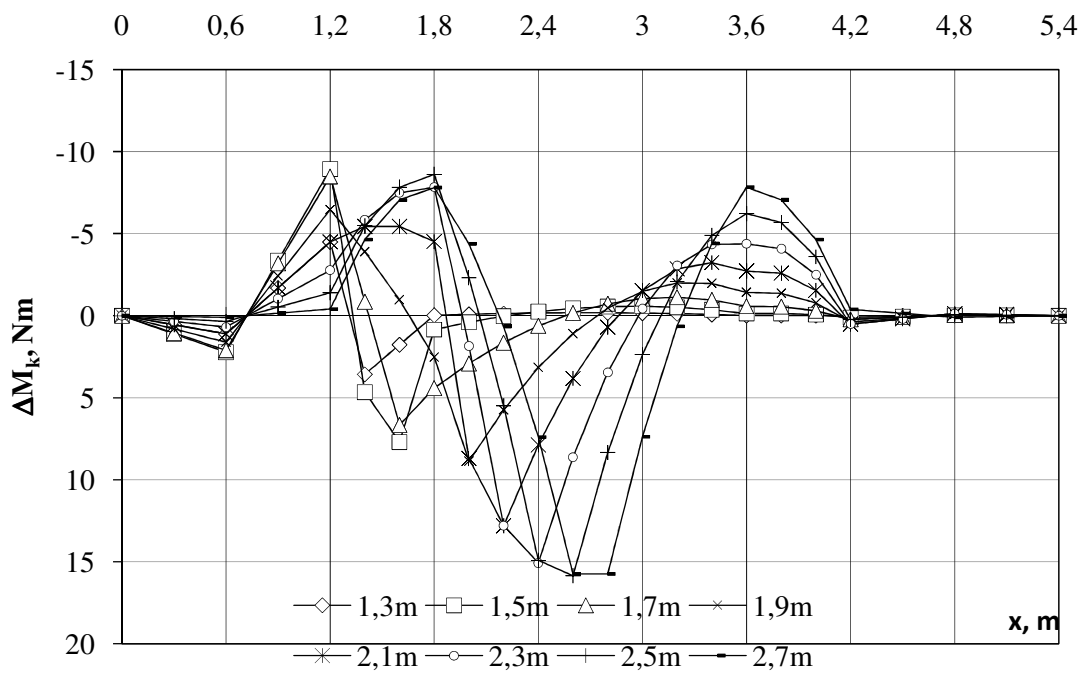
Figure 9.4 Differences in the bending moment of the stiffening girder.
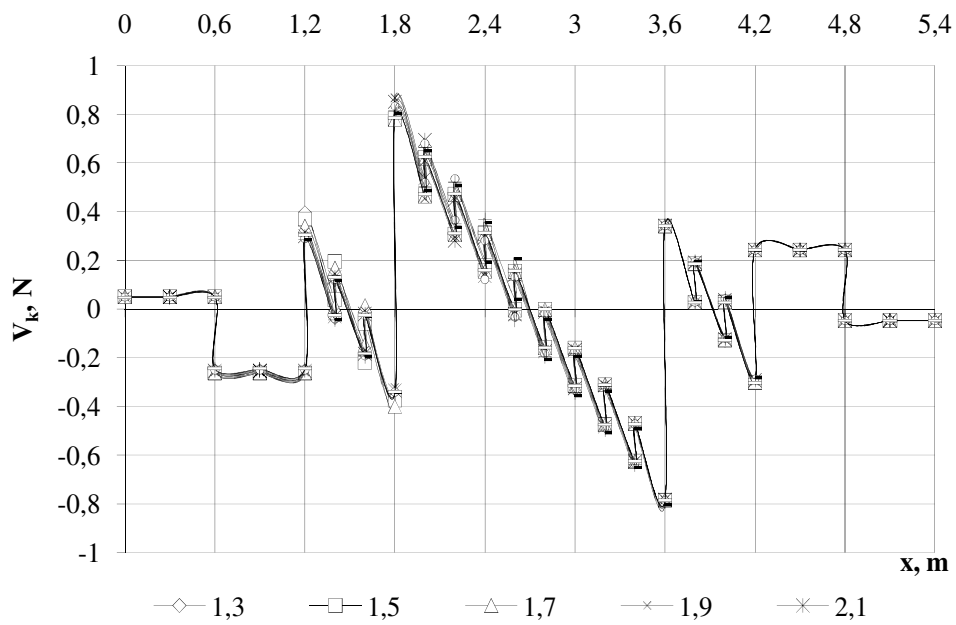
Figure 9.5 Shear forces of the stiffening girder.
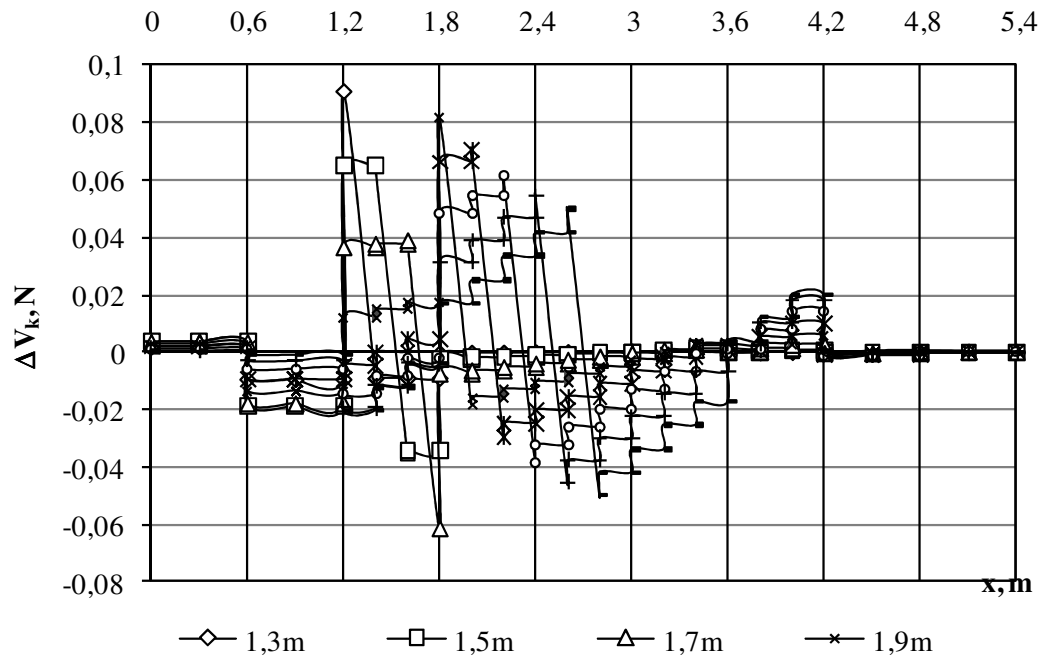
Figure 9.6 Differences in shear forces.
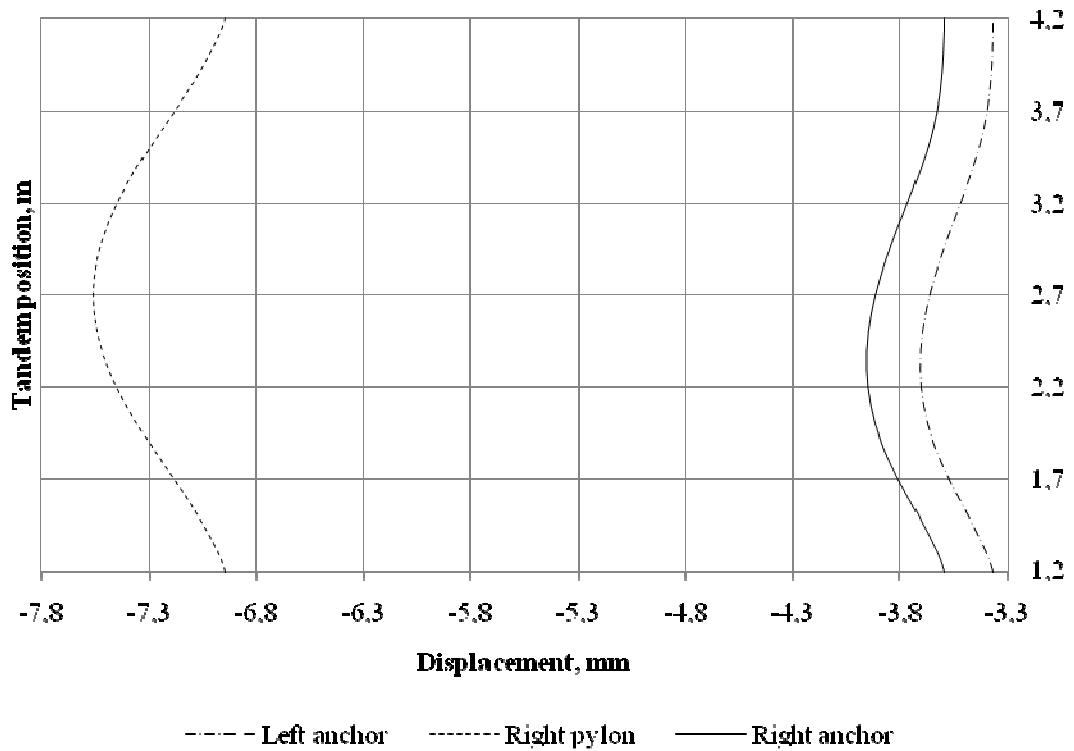
Figure 9.7 Influence of the tandem on the horizontal displacements.

10. Conclusions and further research

10.1. Conclusions

10.1.1. Literature

In view of recent developments, such as significant improvements in design methods, opportunities are open to design structures where local conditions are analyzed in detail. Developments in the design and analysis based on the flexibility of design standards indicate to the importance of preliminary research work in terms of geological and loading aspects. To illustrate the need for detailed guidelines comparison of Eurocode general guidelines and National Application of Finnish Standard shows 1,8 time advantage to Finnish Standard NA. Studies of this structure as one of the possible solutions for a fixed link reveal a need for detailed research work.

Since a suspension bridge and a cable-stayed structure are quite traditional, research interests have been addressed to the combined systems. Additional advantages of this system emerge especially when the geometry and the material for a stiffening girder are also combined – reinforced concrete for the cable-stayed system and steel for the suspension part of the structure.

This thesis provides valuable information and experimental data required for checking and ensuring the stability of the stiffening girder.

Studies through observations for the solution of the fixed link in the following areas were conducted: geology of the site, traffic load characteristics and prognosis, possible transport alternatives, maintenance of the road surface, and wind characteristics.

10.1.2. Modelling

Solution of fastenings is critical in modelling, especially because the scale of the fastenings is not adequate, which can have a negative effect.

Critical area is also selection and testing of stiffness and detailing of cables. Cables highly elastic and non-twisting should naturally be preferred in general. If scaling on the original structure deformation is critical, then scaling on the sectional area and stiffness should be reached.

In the studied case, the difference in stiffness test result for carrying cable was 17%. But in the cable-stay it was only 1%, which in this context is an extremely good result acceptable. The advantage of this effect is that it is predictable.

Another critical area is detailing of the cables. Details which are acting for friction or scotch should be preferred. Details with reverse bending and one-sided bolt joints should be avoided. The disadvantage of the details is the negative effect, i.e. the degree and direction are not predictable. Since the scale of the details in the model is non-adequate, this makes it difficult to see the overall effect.

Determination of loading parameters taking into account local traffic conditions is essential at the very first stage of planning the bridge.

Because of the specific relation of the traffic load and self-weight, structural behaviour of a traditional self-anchored suspension bridge in non-uniform load

distribution cases is unsuitable. In the present case, the relation of the traffic load and the self-weight is greater than it would commonly be. This value is caused by the narrowness of the bridge deck and therefore a hybrid cable-stayed suspension bridge is used. The geometry of a traditional suspension bridge (span length and height of pylons) was used, but the structural scheme was complemented to benefit the structural behaviour of the bridge.

The continual calculation method is useful to analyze the influence of different geometrical, stiffness and loading parameters for a traditional suspension bridge. The influence of the parameters can be determined with little modifications. In the final design, the discrete model should be used to reach an exact solution.

The main advantage of the hybrid suspension-cable-stayed structure lies in the simplification of the construction process of the self-anchored bridge (preliminary supporting of the stiffening girder before anchoring the main cables). An improvement of the structural behaviour in the conditions of one-side loading of the bridge may be also mentioned.

10.1.3. Testing

For the goal set, the loading system was appropriate – the overall acting of the structure is described with a sufficient degree of accuracy. The preliminary analysis chosen was adequate and the stability of the stiffening girder is ensured for this type of the structure. The technique used to measure vertical displacements from the stiffening girder to the suspended thread was suitable because of sufficient accuracy and convenience. Horizontal displacements of the model for the outer structure design near the model with the calliper was successful.

Horizontal displacements were measured with a hanging thread and a ruler at the support. To ensure exact readings from the ruler, the thread was in some cases too close to the ruler and friction obstructed free movement of the thread. Readings from the ruler are estimated from the ruler when the values are in the same dimension calibre as the divisions in the ruler. Certainly an overall tendency is reflected. Methods for description of analysis and design of structural acting are presented.

10.1.4. Comparison of results

Comparison of experimental and calculated results shows good agreement. However, solutions for some fastenings had drawbacks, causing a permanent gap in experimental results.

Overall coincidence for stiffening girder deflections is fair, For maximal uniformly distributed load difference being 15%. For horizontal displacements, the coincidence had many more unfavourable values but the overall dependence can be clearly seen.

During the experiment, the maximum load caused local deformation of some details which resulted in a gap for comparison to follow the load cases.

As mentioned before, measuring on horizontal displacements for the pylon was not successful. Also, for anchor supports, a steel stiffening girder was made by a steel bars with bolt joints where slight local deformation curvatures occur and

the curvature of the stiffening girder influences the projection length of the stiffening girder and horizontal displacements are not predictable in full-degree. Experimental investigations showed that there is no risk of buckling of the stiffening girder despite of its slenderness and little stiffness in bending. Also there was no hint like pre-buckled shape of the stiffening girder.

Buckling analysis confirmed this result. Most predictable buckling mode showed buckling load factor 4,2 – the total vertical load can be increased 4,2 times before the buckling becomes predictable.

In experimental investigation the model was not loaded to the buckling limit and therefore comparison with the buckling analysis cannot be carried trough in full degree.

10.1.5. Theoretical research

In theoretical research influence of geometrical and stiffness relations to the structural behaviour are presented.

For scheme in this thesis under investigation these suggestions can be pointed out:
- height of the pylon is effective to choose 0,1 ... 0,15 on the spans length
- side spans length is recommended to choose 0,2 ... 0,4 of the central span
- optimal range for fixing cable stay to the stiffening girder is 0,3 ... 0,37 of the span length
- existence of the cable stays even if they have small stiffness is the main factor if the capacity of the cable stay is ensured, adding stiffness to the cable stay has intense effect up to value 60% of the carrying cables axial stiffness.

For current scheme different analysis methods were compared. The comparison showed effectiveness of nonlinear approach in general concerning the linear, but comparing the different for various nonlinear analysis the variety range differs 6%. In real design less laborious should be used. Advantages of different nonlinear solutions in general should be analysed and discussed additionally. Although in this type of analysis computational errors in forming the equations and solving them should be kept in mind.

10.2. Further research

In the future it is essential to investigate cases of extreme load distribution under the action of concentrated loads, ship collision and other risk effects.

Particular attention should be paid to wind effects: static pressure, dynamic (oscillatory) effect and buffering.

11. References

1. Kulbach, V. A system of nondimensional parameters for evaluation of different cable System. Proceedings of 5th International Conference Modern Building Materials, Structures and Techniques, Vilnius 1997, p.194-199
2. Kulbach, V. Statical analysis of girder- or cable-stiffened suspension structures. Proceedings of the Estonian Academy of Sciences. Engineering. No. 1, 1995, p.2-19
3. Kulbach, V. Half-span loading of cable structures. Journal of Constructional Steel Research, No. 49, 1999, p. 167-180.
4. Kulbach, V. Design of different suspension bridges. Proceedings of The Conference Eurosteel '99, CVUT, p.395-398
5. Kulbach, V., Talvik I. Bridge structures for the fixed link Saaremaa. Strait Crossings 2001. Balkema Lisse, 2001,p.221-226
6. Kulbach, V. Cable Structures-Design and Static Analysis, Tallinn: Estonian Academy Publichers, 2007.
7. Kulbach, V., Talvik I. Analysis of self-anchored bridge in Estonia. Proceedings IABSE Conference Soul 2001. Cable Supported bridges – Challenging Technical Limits IABSE Reports, Vol. 84. Soul, 2001, p.170-171 (full text on the CD-ROM)
8. Kulbach, V., Kivi E. Experimental investigation of the Saaremaa suspension bridge model. Proceedings Estonian Academy of Sciences, No. 8. Tallinn, 2002, p. 114-120.
9. Kulbach, V., Kivi, E. Analysis and design of suspension structures with (Syrja, 2003)yielding supports. In International Syposium on Lightweight Structures in Civil Engineering. Warsaw, 2005, p. 145-151.

10. Kulbach, V., Idnurm, S. and Idnurm, J. Discrete and continuous modelling of suspension bridges. Proceedings of the Estonian Academy of Sciences, No. 8. Tallinn, 2002, p. 121-133.

11. Kulbach, V., Idnurm S., Idnurm, J. Static analysis of suspension bridges loaded by concentrated forces. Journal of Structural Mechanics, Helsinki, Vol 34, 2000,2 3-14.

12. Idnurm, J. Discrete Analysis of Cable-Supported Bridges. Tallinn University of Technology, Tallinn, 2004.

13. Kulbach, V., Kivi, E. Analysis and design of suspension structures with yielding supports. Lightweight structures in Civil Engineering. Contemporary problems. Warsaw, 2005, p.145 – 151.

14. Kulbach, V., Aare, J. Metal Structures II. Tallinn, Valgus, 1970 (in Estonian)

15. Kulbach, V. Static behaviour of straight cables under primary and secondary cross loading. Proceedings Estonian Academy of Sciences. 1990, no 39, p.278-281.

16. Aare, J., Kulbach, V. Accurate and approximate analysis of static behaviour of suspension bridges. Journal of Structural Mechanics (Helsinki) 1984, No17 (3), p. 1-12

17. Kulbach, V., Continual analysis of suspension bridges. In 4th Euromech Solid Mechanics Conference, Book of Abstracts. Metz, 2000, p. 634-635.

18. Kulbach, V. A universal approach to analysis and design of different cable structures. In System-Based Vision for Strategic and Creative Design, Swets & Zeitlinger, Lisse, 2003, p. 951-956.

19. Pre-stressed Suspension Structures. Special Issue of Proceedings Estonian Academy of Sciences, Engineering, no 8, 2002.

20. Tärno, I. Effects of contour Ellipticity upon structural behaviour of hyparform suspended roofs. Royal Institute of Technology, Stockholm, 1998.

21. Chen, W-F., Dyan, L. Bridge Engineering Handbook, 1999

22. Bangash, M.Y.H Suspension and Cable-Stayed Bridges. Prototype Bridge Structures. Thomas Telford Publishing, London 1999

23. Karavajczyk, E. Finite element simulations of integral bridge behaviour. Stockholm, Royal Institute of Technology, 2001

24. Karoumi, R. Response of cable-stayed and suspension bridges to moving load vechicles. Stockholm, Royal Institute of Technology, 1998

25. Tibert, G. Numerical analyses of cable roof structures, Royal Institute of Technology, 1999.

26. Syrjä, R. Vertical traffic loads on bridges according to Eurocodes. Helsinki, Helsinki University of Technology, 2003.

27. Jouzapaitis A., Norkus, A. Calculation of cable total displacements considering complex conditions, Vilnius, Vilnius Gediminas Technical University, Foundations of civil and environmental engineering No.6, 2005.

28. Ermopoulus J.Ch., Vlakinos A.S., Wang Y.-C. Stability analysis of cable stayed bridges, Computers & Structures, Vol. 44, No 5, 1992, p.1083-1089

29. Ochsendorf J. A. and Billington D.P. Self-Anchored suspension bridges, ASCE Journal of Bridge Engineering, Vol.4. No 3.1999, p.151-156

30. Cable Supported Bridges – Challenging Technical Limit. IABSE Reports, Vol 84, 2001.

31. N.J. Cable Supported Bridges, Second edition. J. Wiley & Sons, New York, 1997.

32. Kulbach, V., Idnurm S., Parts A. Comparison of technical and economical aspects of fixed link Saaremaa, Tallinn University of Technology

33. Autodesk Robot Structural Analysis Professional - User Manual, Autodesk Incorporated, 2009

34. prEN 1991-2. Actions on structures – Traffic loads on bridges. Brussels, 2002.

35. EVS-EN 1991-2/NA:2007 Actions on structures - Part 2: Traffic loads on bridges. NATIONAL ANNEX

36. Siltojen kuormat. Helsinki, Tiel, 1999 (in Finnish)

37. Hoffman J.D., Methods for Engineers and Scientists. Marcel Dekker Inc., New York, 2001.

38. Kudo H., Shioi Y., Hasegawa A., Suzuki N. Tsugaru Strait Bridge and Nagisa Bridge – Combining a Suspension & Cable-Stayed Bridge and Steel & Prestressed Concrete Bridge. 4th International Conference on Current and Future Trends in Bridge Design. Thomas Telford, London, 2005, p.67-75.

39. True H., The dynamics of vehicles on road and on Tracks: Proceedings of IAVSD Symposiums

40. O'Connor C., Show P.A. Bridge loads. Spon Press, London, 2000.

41. Troitsky M.S. Planning and design of bridges. John Wiley & Sons Inc, 1994.

42. Zienkiewicz O.C., Taylor R.L. The finite element method for solid and structural mechanics. Elsevier Ltd, Oxford, 2005.

43. Ryall M.J., Parke G.A.R., Harding J.E. The manual of bridge engineering Ed.2. Thomas Telford Ltd, London, 2000.

44. Takemura H., Ohura T., Onushi M., Tanabe T. A Study on a hybrid system of cable stayed prestressed concrete bridge and steel suspension bridge. Strait Crossings 2001. Krokeborg (ed), Swets & Zeitlinger Publichers, Lisse, 2001.

45. Tärno Ü. Model testing of structural space structures (Ehituslike ruumstruktuuride mudelkatsetused). Tallinn University of Technology, Tallinn, 2003.

46. Varum H., Cardoso R.J.S. A Geometrical non-linear model for cable systems analysis. International Conference on Textile Composites and Inflatable Structures – Structural Membranes 2005. E. Onãte and B. Kropin (Ed) CIMNE, Stuttgart, 2005.

47. Grigorjeva T., Juozapaitis A., Kamaitis Z. Finite element Analysis of the static behaviour of suspension bridges with flexible and rigid cables. 9th International Conference of Modern Building Materials, Structures and Techniques. Vilnius Gediminas Technical University, Vilnius, 2007.

48. SolidWorks 2007 Help, Dassault Systemes SolidWorks Corporation, 2007,

12. List of Figures

13. Curriculum Vitae

1. Personal data
Name	Egon Kivi
Date and place of birth	13.02.78 Tartu

2. Contact information
Address	Ehitajate tee 45-71
Phone	52 58 639
E-mail	egon@ekib.ee

3. Education history

Educational institution	Graduation date	Education
Tallinn Uniniversity of Technology	2002	MSc
Tallinn Uniniversity of Technology	2000	BSc

4. Language competence/skills (fluent/good/excellent/advanced; intermediate/average, fundamentals/ basic skills)

Language	Level
Estonian	native
English	average
Russian	basic skills

5. Professional Employment

Period	Organisation	Position
2006 -	E. Kivi Inseneribüroo OÜ	engineer
2004 - 2006	MSP Projekt OÜ	engineer
2002 - 2004	Inseneribüroo Märt Mõttus	engineer

6. Scientific work

Kivi, Egon; Kulbach, Valdek (2007). Control of dimensioning and investigation of the bridge for crossing a strait in Estonia. In: IABSE Symposium Weimar 2007: Improving Infrastructure Worldwide: Rapport: Weimar (Germany), Sept 19-21, 2007. IABSE, 2007, (93), 8 pp.

Kivi, E; Kulbach, V. (2006). Preliminary design and analysis of the bridge for a strait crossing in Estonia. In: V International Conference "The Metalwork in civil engineering": V International Conference "The Metalwork in civil engineering", Kiev 2006. Kiev:, 2006, 75 - 80.

Kulbach, Valdek; Kivi, Egon (2005). Analysis and design of suspension structures with yelding supports. Lightweight Structures in Civil Engineering, Contemporary problems. International Colloquium of IASS Polish Chapter. XI LSCE - 1995-2005 (145 - 151). Warsaw : Wydawnictwo Naukowe

Kivi, Egon (2004). Experimental investigation of the Saaremaa suspension bridge model. In: Modern Buildings Materials, Structures and Techniques: 8th

International Conference Modern Buildings Materials, Structures and Techniques May 19–22, 2004, Vilnius, Lithuania. Vilnius: Technika, 2004, (1; 1), 247 - 248.

7. Defended theses

2002, Tallinn University of Technology, MSc thesis "Structural behaviour of suspension structure with loaded anchor cables – theoretical and experimental research" (in Estonian)

14. Elulookirjeldus

1. Isikuandmed
     Ees- ja perekonnanimi   Egon Kivi
     Sünniaeg ja –koht   13.02.78 Tartu
     Kodakondsus   eesti
2. Kontaktandmed
     Aadress   Ehitjate tee 45-71
     Telefon   52 58 639
     E-posti aadress   egon@ekib.ee

3. Hariduskäik

Õppeasutus	Lõpetamise aeg	Haridus
Tallinna Tehnikaülikool	2002	MSc
Tallinna Tehnikaülikool	2000	BSc

4. Keelteoskus (alg-, kesk- või kõrgtase)

Keel	Tase
Eesti	emakeel
Inglise	kesk
Vene	alg

5. Teenistuskäik

Töötamise aeg	Ülikooli, teadusasutuse või muu organisatsiooni nimetus	Ametikoht
2006 -	E.Kivi Inseneribüroo OÜ	insener
2004 - 2006	MSP Projekt OÜ	insener
2002 - 2004	Inseneribüroo Märt Mõttus OÜ	insener

6. Teadustegevus

Kivi, Egon; Kulbach, Valdek (2007). Control of dimensioning and investigation of the bridge for crossing a strait in Estonia. In: IABSE Symposium Weimar 2007: Improving Infrastructure Worldwide: Rapport: Weimar (Germany), Sept 19-21, 2007. IABSE, 2007, (93), 8 pp.

Kivi, E; Kulbach, V. (2006). Preliminary design and analysis of the bridge for a strait crossing in Estonia. In: V International Conference "The Metalwork in civil engineering": V International Conference "The Metalwork in civil engineering", Kiev 2006. Kiev:, 2006, 75 - 80.

Kulbach, Valdek;Kivi, Egon (2005). Analysis and design of suspension structures with yelding supports. Lightweight Structures in Civil

Engineering, Contemporary problems. International Colloquium of IASS Polish Chapter. XI LSCE - 1995-2005 (145 - 151). Warsaw : Wydawnictwo Naukowe

Kivi, Egon (2004). Experimental investigation of the Saaremaa suspension bridge model. In: Modern Buildings Materials, Structures and Techniques: 8th International Conference Modern Buildings Materials, Structures and Techniques May 19–22, 2004, Vilnius, Lithuania. Vilnius: Technika, 2004, (1; 1), 247 - 248.

7. Kaitstud lõputööd

2002, Tallinna Tehnikaülikool, Magistritöö "Koormatud ankruvantidega rippkonstruktsiooni töö teoreetilis eksperimentaalne uurimine"